UNIVERSIDAD AUTÓNOMA DE MADRID
Departamento de Bioquímica

In vitro analysis of Src family kinases in the metastatic process of MDA-MB-231 cell line

María Pilar Sánchez Bailón

Madrid, 2014

Departamento de Bioquímica
Facultad de Medicina
UNIVERSIDAD AUTÓNOMA DE MADRID

In vitro analysis of Src family kinases in the metastatic process of MDA-MB-231 cell line

Memoria presentada para optar al grado de Doctor con Mención Internacional por:

María Pilar Sánchez Bailón
Licenciada en Bioquímica y Biología

Directores de Tesis:
Dr. Jorge Martín Pérez
Dra. Annarica Calcabrini

INSTITUTO DE INVESTIGACIONES BIOMÉDICAS “ALBERTO SOLS”

A mi familia

ACKNOWLEDGEMENTS

En primer lugar quiero agradecer esta tesis al Dr. Jorge Martín Pérez, por permitirme formar parte de su grupo y por darme la oportunidad de poder llevar a cabo este proyecto. Gracias por tu apoyo, confianza, dedicación y disponibilidad durante estos años. A la Dra. Annarica Calcabrini, porque me ayudó mucho en mis inicios y lo ha seguido haciendo durante todo este tiempo. Gracias por tu paciencia y por poner un poco de optimismo. Gracias a ambos por todo lo que me habéis enseñado y no dudéis que si he llegado hasta aquí ha sido porque habéis sabido transmitirme vuestro entusiasmo por la ciencia, muchas gracias a los dos por ello.

I would like to thank Professor Kay-Uwe Wagner to allow me to be part of his group and made me feel as another member of his lab. It was a rewarding professional experience and I had a good time in the lab. I want to thank Dr. Kazuhito Sakamoto, Dr. Jeffrey W. Schmidt, Barbara L. Wehde, Nirakar Rajbhandari, and specially Aleata A. Triplett, for helping me and making my stay in Omaha more pleasant.

I would also like to thank Dr.Gabriela Dontu to give me the opportunity to be part of her group. I could learn valuable techniques, very useful for my career.

Al Profesor Javier León Serrano por las colaboraciones que hemos tenido en este tiempo y que, sin duda, han dado sus frutos.

Y ahora va mi agradecimiento a todos los que forman y han formado parte del laboratorio 0.2. Siempre he dicho que los agradecimientos ocuparían gran parte de mi tesis por toda la gente que ha pasado por el laboratorio y que ha contribuido a crear un buen ambiente en el lab. Voy a ir hacia atrás en el tiempo tratando de no olvidar a nadie. Para empezar, voy a agradecer a mi compañero de laboratorio, Víctor, con el cual he pasado estos últimos años y he compartido muchas horas y experimentos. Y al resto de componentes de mi actual grupo: Irma, María, Sandra G., Sandra M., Vero y Camille; sobre todo, porque me han estado escuchando mis quejas en estos últimos meses, y por las divertidas conversaciones y anécdotas a la hora de comer, gracias María aprendimos mucho portugués. Un año antes también fuimos familia numerosa con Alba, Cristina, Minerva y Cecilia y poco tiempo antes de marcharme a Omaha llegó Rocío; compartimos menos tiempo pero también fue agradable. Siguiendo hacia atrás en el tiempo pasaron por el laboratorio Bea, Maribel, María y Celia. Fue una temporada muy divertida (y también con mucho trabajo), con Bea contándonos todo tipo de historias y su excesiva confianza inicial, con Maribel su buena fe y su “ea”, con María, su energía matutina y su géiser de sample buffer y Celia con su “sí, yo entiendo”. Y ya llegamos a la época en que se incorporó Víctor, por entonces llamado padawan por Natalia, la cual también me puso un mote (mejor no mencionarlo) y dio bastante vida al laboratorio y al centro organizando sus certámenes de pinchos. Aquel verano también estuvieron Elena y Szymon. Se dieron entretenidas situaciones y

equívocos por el idioma, que siempre da mucho juego. El año anterior estuvo Izabela, con la que pude practicar “mi inglés” y con la que cogí bastante confianza. Y ya finalmente las primeras incorporaciones, Lourdes y Dani; los cuales sufrieron mi escasa paciencia inicial. Gracias Dani, aunque me hacías pensar demasiado, fuiste un gran compañero. Gracias a todos, ya que de una forma u otra habéis formado parte de esta tesis y me habéis hecho más agradable este camino, sin vosotros no hubiera sido lo mismo.

Al resto de compañeros del iib Cris, Alberto, Irene, Yenny, Isa, Laura, Sole, Raquel, María y Jose (1.3.1), Lucía, Diego… con los que he compartido comidas, charlas, horas de cultivo o de microscopio.

A la gente que conocí en las estancias; a Bea, Monti y Fara, con las que compartí muy buenos ratos en Londres. A Álvaro, Juliet y José Ramón con los que descubrí y experimenté la vida “omaheña”.

A Iñaki y Laura, compañeros del máster y después amigos; a Iñaki por haber sido un gran apoyo en Madrid y a Laura por nuestras quedadas esporádicas.

A mis amigos de facultad, porque ahí se inició nuestro camino científico durante esos años de carrera; después de muchas horas de clases y prácticas con unos buenos compañeros y amigos. A Rocío porque me aporta mucho como persona, a Carmen por estar pendiente de mí, a Raúl, Ana y Abe por apoyarme y estar ahí.

A Vero y María por escucharme y porque sé que siempre puedo contar con vosotras.

A las que fueron mis compañeras de piso al principio de llegar aquí, Laura y Miren; por escucharme y ayudarme en mis primeros años en Madrid y a las que conocí después, Elena e Iciar.

Finalmente a toda mi familia, y en especial a mis padres por haberme apoyado en todo momento, por animarme a estudiar y por haberme transmitido vuestra capacidad de esfuerzo. A mi tía por escucharme y ayudarme. Y a mis hermanos, al que quiere mandarme al otro lado del mundo para ir a visitarme, y al que dice que soy la eterna estudiante. Gracias también, por haberme visitado en mis estancias, es algo de agradecer cuando estás fuera de casa. Gracias a todos, porque sin vosotros, seguro que no hubiera sido posible.

INDEX

INDEX OF FIGURES AND TABLES

FIGURES

TABLES

ABSTRACT / RESUMEN

Breast cancer is the leading cause of cancer death of women in developed countries. In particular, triple-negative breast cancer is highly aggressive with reduced therapeutic options since lacks well-defined molecular targets and is very heterogeneous. It is defined by the absence of Estrogen receptor (ER), Progesterone receptor (PR), as well as, Human epidermal growth factor receptor 2 (HER2) and constitutes 10 – 20% of all breast cancer. Besides, it has been described that Src family kinases (SFKs) are involved in the development of human cancers, including breast cancer. Increases in SFKs activity is correlated with the progression of malignancy. Overexpression of c-Src or aberrant activation has been identified in various human cancers. Src is an essential component of several signalling pathways that regulate proliferation, survival, angiogenesis and metastasis.

This Doctoral Thesis is focused on unrevealing the mechanisms that depend on SFKs catalytic activity or on c-Src that lead to metastasis of the triple-negative/basal-like breast cancer cell line, MDA-MB-231. To accomplish this objective we have used three complementary approaches: inhibition of SFKs catalytic activity by using three selective inhibitors, Dasatinib, PP2 and SU6656; conditional expression of shRNA-c-Src or conditional expression of dominant-negative Src (SrcDN; K295M/Y527F).

We found that SFKs catalytic activity controlled cell proliferation at G1-S phase transition by regulating $p27^{Kip1}$ and c-Myc expressions, by using Dasatinib and PP2. In contrast, SU6656 provoked polyploid cells, a SFKs-independent effect caused by concomitant inhibition of Aurora B kinase. Furthermore, SFKs inhibition and c-Src depletion reduced cell migration and invasion capabilities of MDA-MB-231 cells by reducing phosphorylation of Src substrates, Y925-Fak, p130CAS, Y118-paxillin and Y14-caveolin 1, required for focal adhesion turnover and cell motility. The expression of SrcDN showed an additional pathway, through Akt activation, involved in cell migration and invasion. Besides, c-Src modulated the secretion of proteins involved in breast cancer progression and metastasis, including Cyr61, IGFBP4 and CTGF. We found a new exosomal protein, Cyr61, which regulated invasion and transendothelial migration, important for extravasation of tumour cells. Furthermore, c-Src modulated the survival of MDA-MB-231 cells in anchorage-independent conditions, as well as, was required to maintain the breast cancer stem/progenitor cell subpopulation by regulating the expression of pluripotency-associated transcription factors Oct3/4, Nanog and Sox2.

El cáncer de mama es la principal causa de muerte por cáncer en mujeres de países desarrollados. Concretamente, el cáncer de mama triple negativo es muy agresivo con reducidas opciones terapéuticas, ya que, carece de dianas moleculares claramente definidas y es muy heterogéneo. Se caracteriza por la ausencia de receptor de estrógeno (ER), receptor de progesterona (PR), así como, del receptor del factor de crecimiento epidérmico humano 2 (HER2) y constituye entre un 10-20% de todos los cánceres de mama. Además, se ha descrito que la familia de proteínas tirosina quinasa de Src (SFKs) está implicada en el desarrollo de cánceres humanos, incluido el cáncer de mama. La sobreexpresión de c-Src o la activación anormal se han identificado en varios cánceres humanos. Src es un componente esencial de varias vías de señalización que regulan proliferación, supervivencia, angiogénesis y metástasis.

Esta Tesis Doctoral se centra en desentrañar los mecanismos que dependen de la actividad catalítica de SFKs o de c-Src y que conducen a la metástasis de la línea celular de cáncer de mama triple negativa de tipo basal, MDA-MB-231. Para lograr este objetivo hemos usado tres aproximaciones complementarias: inhibición de la actividad catalítica de SFKs utilizando tres inhibidores selectivos, Dasatinib, PP2 y SU6656, expresión condicional de shRNA-c-Src o expresión condicional de Src dominante negativo (SrcDN; K295M/Y527F).

Nosotros encontramos que la actividad catalítica de las SFKs controla la proliferación celular en la transición G1-S mediante la regulación de la expresión de $p27^{Kip1}$ y c-Myc, usando Dasatinib y PP2. En cambio, SU6656 provocó poliploidía celular, un efecto independiente de las SFKs causado por la inhibición simultánea de Aurora quinasa B. Además, la inhibición de las SFKs así como el silenciamiento de c-Src redujeron la capacidad migratoria e invasiva de las células MDA-MB-231 mediante la disminución de la fosforilación de los sustratos de Src, Y925-Fak, p130CAS, Y118-paxilina and Y14-caveolina 1, necesaria para el recambio de las adhesiones focales y la motilidad celular. La expresión de SrcDN mostró una vía adicional, mediada por la activación de Akt, implicada en la migración e invasividad celular. Además, c-Src moduló la secreción de proteínas implicadas en la progresión y metástasis del cáncer de mama, incluyendo Cyr61, IGFBP4 y CTGF. Encontramos una nueva proteína exosomal, Cyr61, que reguló la invasión y la migración transendotelial, importante para la extravasación de las células tumorales. Además, c-Src moduló la supervivencia de las células MDA-MB-231 en condiciones de independencia de anclaje y era necesaria para el mantenimiento de la subpoblación de células troncales/progenitoras de cáncer de mama, a través de la regulación de la expresión de los factores de transcripción asociados a pluripotencia Oct3/4, Nanog y Sox2.

ABBREVIATIONS

Abi1	Abl-interactor 1
ADH	atypical ductal hyperplasia
AMPK	Protein kinase, AMP-activated, alpha 1 catalytic subunit
B2M	Beta-2-microglobulin
BRSK2	BR serine/threonine kinase 2
CaMKK*α*	Calcium/calmodulin-dependent protein kinase kinase 1, alpha
CaMKK*β*	Calcium/calmodulin-dependent protein kinase kinase 2, beta
CCL21	Chemokine (C-C motif) ligand 21
CCR7	Chemokine (C-C motif) receptor 7
Cdc42	Cell division cycle 42
Cdk1	Cyclin-dependent kinase 1
Cdk2	Cyclin-dependent kinase 2
Chk	Csk-homologous kinase
CHK2	Checkpoint kinase 2
CK1δ	Casein kinase 1, delta
CML	chronic myeloid leukaemia
CSCs	cancer stem cells
CSK	c-Src tyrosine kinase
Ct	threshold cycle
CTGF	CCN2, conective tissue growth factor
CXCL12	Chemokine (C-X-C motif) ligand 12
CXCR1	Chemokine (C-X-C motif) receptor 1
CXCR2	Chemokine (C-X-C motif) receptor 2
CXCR4	Chemokine (C-X-C motif) receptor 4
Cyr61	CCN1, Cysteine-rich protein 61
DCIS	ductal carcinoma *in situ*
DN	dominant negative
Doxy	doxycycline
ECM	extracellular matrix
EGF	Epidermal growth factor
EGFR	Epidermal growth factor receptor
Eph-A2	Ephrin type-A receptor 2
ER	Estrogen receptor
ERK2	Extracellular signal-regulated kinase 2
Fak	Focal adhesión kinase
FDR	false discovery rate
FGF	Fibroblast growth factor

FGFR	Fibroblast growth factor receptor
FGFR1	Fibroblast growth factor receptor 1
GH	Growth hormone
Grb7	Growth factor receptor-bound protein 7
GSEA	Gene Set Enrichment Analysis
GSK3β	Glycogen synthase kinase 3 beta
HER2	ERBB2, human epidermal growth factor receptor 2
HFBA	heptafluorobutyric acid
HIST1H4A	Histone H4
HIST2H2BF	Histone H2B type 2F
HIST2H3A	Histone H3.2
HNSCC	head and neck squamous cell carcinoma
HSP90α	Heat shock protein 90 alpha
HUVEC	human umbilical vein endothelial cells
Id1	Inhibitor of differentiation protein 1
IDC	invasive ductal carcinoma
IGF1	Insulin-like growth factor 1
IGF1R	Insulin-like growth factor 1 receptor
IGFBP4	Insulin-like growth factor binding protein 4
JNK	c-JUN amino terminal kinase
LCIS	lobular carcinoma *in situ*
Limma	linear models for microarray data
MAPK	Mitogen-activated protein kinase
MLCK	Myosin light-chain kinase
MMP-2	Matrix metalloprotrease 2
MMP-7	Matrix metalloprotrease 7
MMP-9	Matrix metalloprotrease 9
MMPs	Matrix metalloproteases
MMTS	methyl methanethiosulfonate
MMTV	mouse mammary tumour virus
MST2	Mammalian STE20-like protein kinase 2
MTT	3-(4,5-dimethylthiazol-2-yl)-2,5-diphenyl tetrazolium bromide
Nek2	NIMA-related kinase 2
NSCLC	non-small cell lung carcinoma
p130CAS	Crk-associated substrate
$p27^{Kip1}$	Cyclin-dependent kinase inhibitor 1B
PAPP-A	Pregnancy-associated plasma protein-A

PARP	Poly(ADP-ribose) polymerase
PDGF	Platelet-derived growth factor
PDGFR	Platelet-derived growth factor receptor
PDGFRβ	Platelet-derived growth factor receptor, beta polypeptide
PI3K	Phosphatidylinositol-4,5-bisphosphate 3-kinase
Plk1	Pole-like kinase 1
PR	Progesterone receptor
PRLR	Prolactin receptor
PTEN	Phosphatase and tensin homolog
PTP1B	Protein-tyrosine phosphatase 1B
PTPα	Protein tyrosine phosphatase-α
PyVmT	polyomavirus middle T antigen
qRT-PCR	quantitative real time-polymerase chain reaction
Rac1	Ras-related C3 botulinum toxin substrate 1
RIP2	Receptor-interacting serine-threonine kinase 2
ROCK	Rho kinase
RSV	Rous sarcoma virus
SD	standard deviation
SFE	sphere forming efficiency
SFKs	Src family kinases
SH2	Src homology 2
SH3	Src homology 3
SHP1	SH2-containing tyrosine phosphatase 1
SHP2	SH2-containing tyrosine phosphatase 2
SOD2	Manganese superoxide dismutase
SRPK1	SRSF protein kinase 1
SRS	Src-responsive signature
STAT	Signal transducer and activator of transcription
TBP	TATA-box binding protein
TBST	tris-buffered saline tween
TCEP	tris(2-carboxyethyl)phosphine
TDLU	terminal duct lobular unit
TetR	Tetracycline repressor
TKT	Transketolase
TNBC	triple-negative breast cancer
TRITC	tetramethylrhodamine
VEGFR	Vascular endothelial growth factor receptor

INTRODUCTION

1. BREAST CANCER

Breast cancer is a heterogeneous group of diseases characterized by loss of growth control, and disrupted tissue organization and differentiation (22).

1.1. Mammary gland structure and development

Mammary glands are secretory organs composed of distinct cell types: epithelial cells, adipocytes, infiltrated vascular endothelial cells, fibroblasts and immune cells. The inactive adult mammary gland is composed of 15 to 20 irregular lobes separated by connective tissue. The lobes radiate from the nipple and are further subdivided into several lobules termed terminal duct lobular units (TDLUs), the basic units of the mammary gland (85). The ductal epithelium is a bilayered structure that comprises two main cell types: basal and luminal. The outer layer of the gland consists of contractile myoepithelial basal cells and a small population of stem cells, which supply the different cell types. The inner layer is composed of secretory luminal epithelial cells (120) (Figure 1).

The mammary gland development occurs through three main stages: embryogenesis, puberty and adulthood; undergoing major changes during pregnancy and reaching its full developmental potential during the lactation phase. At the end of embryogenesis a rudimentary ductal system is generated by cues from mesenchyme. The mammary gland remains relatively quiescent until puberty. During puberty ductal morphogenesis occurs under the influence of hormones, including Growth hormone (GH), estrogen and Insulin-like growth factor-1 (IGF1), as well as, growth factors such as Epidermal growth factors (EGFs) and Fibroblast growth factors (FGFs). In the adulthood the gland undergoes mild proliferation and differentiation regulated by progesterone, as well as minor involution during the murine oestrus cycles; similar changes occurs in humans during the menstrual cycles. During pregnancy, progesterone together with prolactin provoke an extensive side-branching, making more complex TDLU structure, that finally forms secretory acinar structure. Prolactin stimulation continues to generate lactational competence of the mammary gland. The absence of suckling signals provokes the mammary gland involution, characterized by the apoptosis of acini cells and remodelling of lobular-alveolar structures. Matrix metalloproteases (MMPs) participate in this remodelling by degrading components of basement membrane and extracellular matrix (ECM) (76,120).

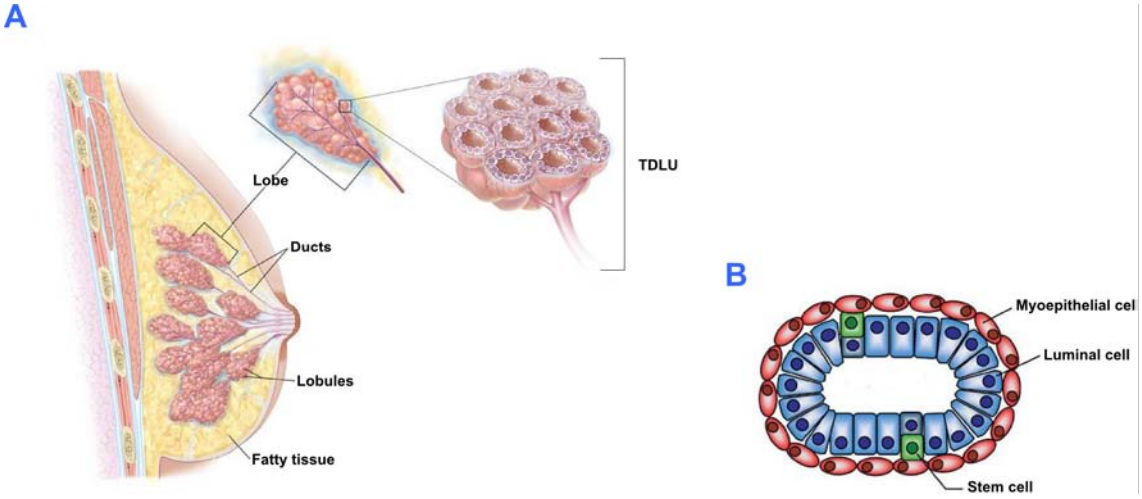

Figure 1. **Mammary gland structure**. (A) Sagital section of the mammary gland. Adapted from © 2012 Terese Winslow LLC. (B) Cellular structure of the mature mammary duct, composed of a myoepithelial layer and a luminal layer with stem cells. Adapted from Tiede *et al*. 2011.

1.2. Incidence and biology of breast cancer

Breast cancer is the most frequent type of malignancy and the leading cause of cancer deaths of women in developed countries; it constitutes 23% of total cancer cases and 14% of the cancer deaths. Incidence rates are high in Western, Northern Europe, Australia/New Zealand, and North America and low in sub-Saharan Africa and Asia (52).

Breast cancer progresses from benign epithelial atypia and atypical ductal hyperplasia (ADH), to malignant ductal carcinoma *in situ* (DCIS), or less frequently lobular carcinoma *in situ* (LCIS), and finally to invasive ductal carcinoma (IDC). DCIS consists of disorganized malignant cells that express E-cadherin and are enclosed by the basement membrane. However, in invasive ductal carcinoma cells break through the basement membrane and spread to the surrounding breast tissues. (22).

The breast cancer staging is based on the TNM (Tumour, Node, Metastasis) classification of primary tumour. The stage of a patient is designated after knowing the localization, size and spreading of primary tumour, as well as, the regional lymph nodes affectation and the appearance of metastases. The main stages are 0, I, II, III and IV, being stage 0 *in situ*, stage I early invasive state, and it progress to the stage IV which presents distant metastases. Normally the stage is inversely related to prognosis (45).

1.3. Types of breast cancer

Invasive ductal carcinomas can be classified into subtypes that have distinct histological features, molecular expression signatures and clinical outcomes. The five major subtypes based on the immunohistochemical expression of Estrogen receptor (ER), Progesterone receptor (PR) and Human epidermal growth factor receptor 2 (HER2 or ERBB2) are: basal-like, HER2-like, normal breast–like, luminal A, and luminal B. Basal-like tumours are characterized by expression of cytokeratin-5 and cytokeratin-17; HER2-like overexpress HER2 and related genes; normal-breast like tumours, express genes from adipose and other non-epithelial cells. Luminal A and B are ER positive tumours with high levels of cytokeratin-8 and cytokeratin-18; they differ in the levels of ER expression, as well as, in the proliferation rate (36,96,109).

A breast cancer group highly aggressive with reduced therapeutic options due to their heterogeneity and the absence of well-defined molecular targets is triple-negative breast cancer (TNBC). TNBC is characterized by the absence of ER expression, as well as, PR and does not have HER2 amplification. The majority of TNBC are basal-like (50-70%) (2); although, a new subtype was recently defined, termed claudin-low. This subtype was originally included in basal-like subtype, although it exhibits its own molecular characteristics including down-regulation of claudin-3, claudinin-4 and claudinin-7, reduced expression of Ki67, increased expression of epithelial-mesenchymal transition markers and of mammary cancer stem cells (CSCs) markers such as $CD44^{+}$,$CD24^{-/low}$ phenotype (48). TNBCs constitute 10 – 20% of all breast cancer and more frequently affect younger patients (67).

Among TNBCs basal-like (recently assigned as claudin-low subtype), a commonly studied cell line is the MDA-MB-231 (48). This human epithelial cell line was established from pleural effusion and is characterized by epidermal growth factor receptor (EGFR) overexpression and carries a mutant tumour suppressor protein p53 (23).

2. SRC FAMILY KINASES

In 1911, Peyton Rous discovered a virus that caused tumours in chickens, later termed Rous sarcoma virus (RSV). Years later, v-src was defined as the only RSV gene required for cell transformation. At the late 70's, the v-src gene product, $pp60^{v\text{-}src}$, or v-Src, was identified as the first protein tyrosine kinase. During this time, the counterpart cellular homologue c-Src was discovered, which allowed to establish the concept of proto-oncogene (10,78,79).

c-Src is the prototypic member of the Src family of tyrosine kinases (SFKs) that comprises nine members, c-Src, Yes, Fyn, Lyn, Blk, Lck, Hck, Fgr and Yrk. Three of them, c-Src, Yes and Fyn are ubiquitously expressed whilst Lyn, Blk, Lck, Hck, Fgr and Yrk are mainly expressed in hematopoietic cells (37,119).

2.1. Structure and regulation of SFKs

All family members have a conserved domain organization: a myristoylated and/or palmitoylated amino-terminal region, important for membrane localization; a unique domain, which varies the most among Src family members; SH3 and SH2 scaffold domains and a linker between SH2 and kinase domains. The catalytic domain is composed of two lobes separated by the catalytic cleft, where the ATP-binding site (K298) and substrate-binding site are located; the cleft contains the activation loop, which controls the accessibility of substrates and has a positive-regulatory autophosphorylation residue Y419 within the activation loop. The carboxyl-terminal tail has the negative-regulatory Y530 (Figure 2).

The inactive close conformation of SFKs occurs when Y530 at C-terminal domain is phosphorylated and binds to SH2 domain. Besides, this interaction is stabilised by binding of SH3 domain to the linker region. The result is a close molecular structure with a reduced access of substrates to the kinase domain. When SFKs is activated the intramolecular interactions are lost, giving rise to an open conformation. The active conformation of Src is stabilized by autophosphorylation at Y418 (Figure 2).

Chicken c-Src and human c-Src share a common structure, although differs in three amino acids that are present in the unique domain of human c-Src. On the other hand, v-Src contains 12 substituted carboxy-terminal amino acids, several point mutations throughout the molecule and does not have C-terminal regulatory region, thus is constitutively active.

c-Src can be regulated by several mechanisms, including intramolecular regulation, activation mediated by receptor or by localization. Concerning intramolecular regulation, c-Src tyrosine kinase (CSK) and its homolog Csk-homologous kinase (Chk) are able to inactivate c-Src by phosphorylation of Y530. Conversely, this phosphorylation can be removed by several tyrosine phosphatases such as Protein tyrosine phosphatase-α (PTPα), Protein-tyrosine phosphatase 1B (PTP1B), SH2-containing tyrosine phosphatase 1 (SHP1) or SHP2. Activation of growth-factor and cytokines receptors, including EGFR, PDGFR, IGF1R, VEGFR, FGFR, HER2 and ER, leads to their association with SH2 domain, which displaces inhibitory intramolecular interactions to promote SFKs activation. The localization of SFKs is important for their regulation, since inactive SFKs are localized at perinuclear sites, and active SFKs indirectly

interact by their SH3 domain with actin to be translocated to the plasma membrane. The localization of SFKs allows for interactions with transmembrane receptor tyrosine kinases and integrins. Other mechanisms of SFKs regulation include ubiquitylation to be degraded by proteasome (133). Src is normally found in an inactive state in quiescent cells and it is transiently activated during the G1 phase for induction of DNA synthesis and at the G2/M transition for cell division. SKFs are constitutively activated in aberrant conditions, including cancer (10,119).

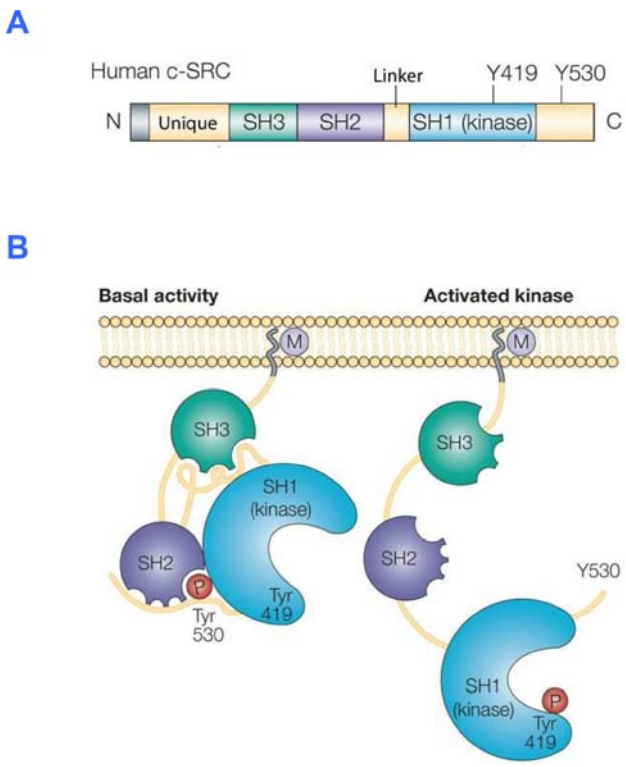

Figure 2. **Structure and activation of c-Src.** (**A**) Molecular structure of human c-Src. (**B**) Inactive conformation of human c-Src where phospho-Y530 from C-terminal region interacts with SH2 domain and linker region binds to SH3 domain. Dephosphorylation at Y530 results in an open active conformation. Adapted from Yeatman et al. 2004.

2.2. SFKs in different types of cancer

Among SFKs it is mainly Src that has been implicated in the development of human cancer. Like oncogenic v-Src, activated mutants of c-Src can transform cells in culture and induce tumours in chickens (37). Increases in Src kinase activity correlates with the progression of malignancy (106). Overexpression of c-Src or aberrant activation have been identified in various human cancers, although activating mutations and genomic amplifications are very rare (49). In gastrointestinal-tract cancer such as colorectal cancer shows a progressive increase in c-Src activity as the tumour stage

advances. Furthermore, an enhanced c-Src activity is observed in hepatocellular, pancreatic, gastric and oesophageal malignancies, as well as in breast, ovarian and lung cancers. In head and neck squamous cell carcinoma (HNSCC) and non-small cell lung carcinoma (NSCLC) cells, c-Src promotes cancer cell survival through STAT3 signalling (106). Hepatocellular cancers and colon carcinomas overexpress c-Src whilst underexpress the negative regulatory c-Src molecule, CSK, leading to higher levels of c-Src activation (133). Increased activity and expression of Yes were observed in human melanoma cells respect to normal melanocytes, as well as, in brain melanoma metastatic cells lines. In pancreatic cancer c-Src participates in the cell growth, invasion and metastasis. In ovarian cancer c-Src has an important role, since down-regulation of c-Src expression decreased anchorage-independent growth, tumour growth in mice, as well as, reduced VEGF expression and tumour vascularization. In bladder carcinoma, inhibition of SFK blocked epithelial-mesenchymal transition, suggesting that contributes to invasion. There are less evidences that link SFKs with brain and neuronal tumours, however, it has been shown that Src-Fak (Focal adhesion kinase) complex may enhance the proliferation of anaplastic astrocytoma cells by means of Extracellular signal-regulated kinase 2 (ERK2) activation as well as, the expression of cyclin D and E (111).

2.3. SFKs in breast cancer

A mouse model of mammary tumourigenesis consisting of mice carrying polyomavirus middle T antigen (PyVmT) under the control of mammary-specific promoter (MMTV) developed mammary tumours. However, mice with disrupted c-Src function often developed cystic hyperplasia and less frequently tumours; indicating that c-Src is important for mammary tumourigenesis in this model (44). The MMTV/PyVmT model of breast cancer with mammary epithelial-specific c-Src disruption, shown that c-Src deletion in mammary epithelium delays tumour onset and decreases tumour burden (77). Besides, it has been shown that high Src kinase activity is observed in breast cancer tissue compared with normal breast tissue (36,51). A sample-matched study revealed that 37 of the 52 pairs exhibit an increased Src family kinase expression or activity in the breast carcinoma tissue compared to matched normal tissue (99). Regarding breast tumour hormone receptor status, a study revealed a significant inverse correlation between ERα and Src expression levels. It is shown that Src protein levels are higher in $ER\alpha^-$ and PR^- compared to $ER\alpha^+$ and PR^+ tumours; in fact, the highest levels are found in triple-receptor negative tumours (27). Subsequently confirmed by Tryfonopoulos and colleagues, that observed an increase of Src in triple-negative compared to non triple-negative breast cancer samples, particularly of

membrane-associated Src (122). Furthermore, Src activity is increased in invasive respect to noninvasive breast cancer cell lines. Inhibition of SFKs activity in breast cancer cell lines reduces motility and invasion (114). It has been reported that SFKs activation phosphorylates Phosphatase and tensin homolog (PTEN), promoting its inhibition, which triggers PI3K/Akt signalling pathway. Furthermore, in HER2-overexpressing cancer cells, trastuzumab treatment exerts its antitumour activity by inhibiting Src binding to HER2. Thus, Src is not activated and provokes an increase in membrane location and activity of the tumour suppressor, PTEN (73,88).

Likewise, we previously shown that the conditional expression of a dominant negative form of Src (SrcDN, K295M/Y527F) in the non-metastatic, oestrogen-receptor positive, MCF7 cell line, provokes a significant decrease of cell migration, proliferation and spreading, as well as, causes tumour regression in nude mice (41).

These reports clearly show that Src family kinases play an essential role in cellular growth and proliferation, angiogenesis, migration and invasion.

3. METASTATIC PROCESS

Metastasis arises following the spread of cancer cells from a primary site and the formation of new tumours in distant organs. It represents the primary cause of cancer mortality (18).

Metastasis is a multistep process that requires numerous and well-defined timed changes in the tumour. Tumour cells detach from surrounding tissue and move through the extracellular matrix (invasion), entering into the blood or lymph circulatory systems (intravasation). Tumour cells must survive into circulatory system reaching secondary sites where they extravasate and colonize the new target tissue. The small population of tumour cells may remain latent until it is reactivated and growths, giving rise to a secondary tumour. New blood vessels formation (angiogenesis) is required for further tumour expansion (Figure 3).

Metastasis from solid tumours displays different organ tropism. In some cases it mainly involves one organ, such as prostate cancer metastasis to bone or sarcoma metastasis to lung; whilst in other cases it relapses in multiple organs, such as, triple-negative breast cancers, skin melanomas and lung cancers (125).

SFKs are involved in cancer metastasis by stimulating tumour cell migration and invasion that allow the entry into bloodstream. Furthermore, SFKs regulate cancer cell survival and proliferation, processes required for metastatic cell growth (43,119).

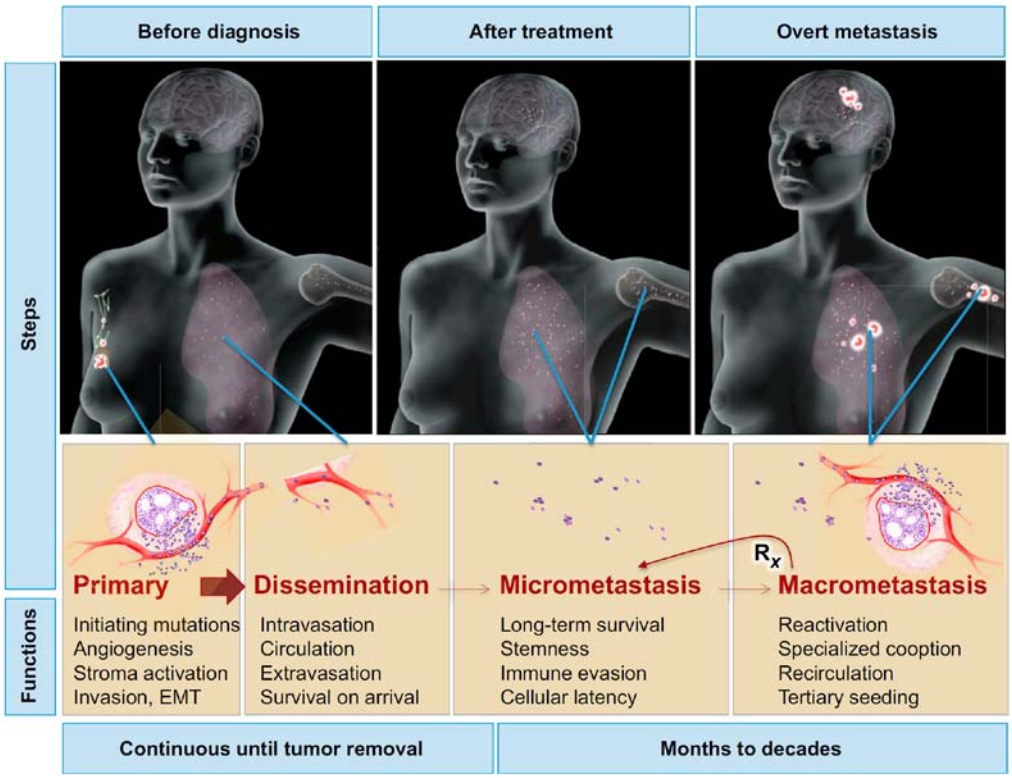

Figure 3. **Metastasis steps.** Metastatic process starts with dissemination of cancer cells from the primary tumour and ends in the formation of clinically detectable macrometastasis. The thickness of the arrows represents the efficiency in each step. Residual tumour cells remaining after treatment (Rx). Taken from Vanharanta *et al*. 2013.

3.1. Role of SFKs in survival and proliferation

The proto-oncogene c-Src is involved in the regulation of cell cycle progression. It participates in growth factor receptor signalling to promote DNA synthesis. Src exerts its effects through several mechanisms including Shc phosphorylation that triggers MAPK signalling, PI3K stimulation, as well as, activation and/or phosphorylation of receptor tyrosine kinases. Src activity is required during G1 phase to induce DNA synthesis, but also, is involved in G2/M transition. Cdk2 activates Src by phosphorylation during mitosis. Besides, microinjection of Src family neutralizing antibodies provokes cell arrested during mitosis (119).

Src phosphorylates $p27^{Kip1}$, which impairs inhibitory activity of $p27^{Kip1}$ over cyclin E-Cdk2, facilitating $p27^{Kip1}$ proteolysis. Besides, elevated c-Src activity has reduced $p27^{Kip1}$ levels (28).

We have previously shown that SFKs regulate G1-S transition in the breast cancer cell line MCF7. The proliferation rate is reduced after SrcDN expression in serum-starved, as well as serum- and EGF-supplemented conditions. It provokes an accumulation of cells in G1 phase and a reduction of activated Akt together with an

increase in $p27^{Kip1}$ expression after serum or EGF stimulation (41). Liu *et al.* in MCF7 obtained similar results by after c-Src knockdown or Src activity inhibition by PP2. They observed that Src regulates G1 progression by modulating $p27^{Kip1}$, cyclin D1 and E expressions through Akt/GSK3β and ERK1/2 pathways.

Integrin-dependent adhesion or growth factor-induced signalling stimulates Src, which in turn activates Fak, by phosphorylation at Y925. This event creates a binding site for the SH2 domain of Grb2, which transmits signal to MAPK (also termed ERK) pathway through Ras. However, signalling from integrins can occur by phosphorylation of Shc adaptor protein by Src, activating Ras/MEK/ERK pathway and cell cycle progression. Besides, phosphorylated Y397-Fak can bind p85 regulatory subunit of PI3K leading to stimulation of PI3K/Akt pathway, which enhances survival and proliferation (43).

Src acts as a mediator in growth-promoting pathways, induced by a variety of growth factors and cytokines that promote breast cancer, including oestrogen, progesterone, prolactin and epidermal growth factor.

Besides, Src is involved in activation of Signal transducer and activator of transcription (STAT) by receptors tyrosine kinase and, in breast cancer cell lines with high levels of EGFR, inhibition of Src reduced STAT3 activity (36).

We have previously shown that c-Src participates in cell proliferation induced by prolactin through two independent signalling pathways, Fak-ERK1/2 and PI3K, which in turn promotes c-Myc and cyclin D1 expression in the human breast cancer cells T47D and MCF7 (1).

3.2. SFKs in cytoskeletal rearrangement, cell adhesion and migration

Src kinases are involved in cell adhesion and migration, which require spatiotemporal rearrangement of cytoskeleton. Two main subcellular structures regulate adhesion, invasion and motility, focal adhesions and adherens junctions, both of them are regulated by c-Src. Focal adhesions are dynamic structures where cytoskeletal and signalling proteins are recruited by integrins clustering that attach the extracellular matrix to the actin stress fibers. They may comprise up to 100 structural and signalling molecules such as talin, vinculin, α-actinin, tensin, etc. Among the multiple molecules of focal adhesions c-Src, Fak, p130CAS, ERK and paxillin, play essential roles in their regulation. Adherens junctions allow cells to adhere to each other, by homotypic interactions between E-cadherin molecules (Figure 4). Focal adhesions tend to inhibit cellular migration unless there is a disruption of adherens junctions. c-Src is able to disrupt cellular junctions when is activated and promotes the focal adhesions turnover (133).

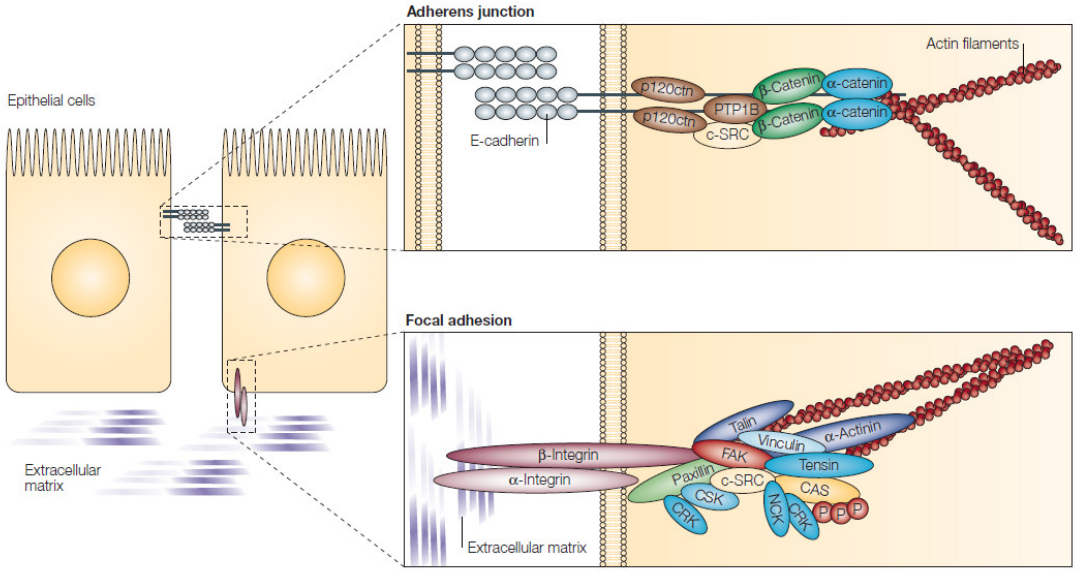

Figure 4. **Adherens junctions and focal adhesion.** Adhesion in epithelial cells is mediated by two main structures, adherens junctions and focal adhesions. Adherens junctions facilitate cell-cell adhesion through E-cadherin homotypic binding. E-cadherins, in turn, bind to actin filaments by a molecular complex consisting of p120-catenin, α-catenin and β-catenin. c-Src associates with this complex. Focal adhesion complex is composed of α-integrin and β-integrin heterodimers that link extracellular matrix to actin cytoskeleton. The intracellular complex that connect integrins to actin filaments is composed of several proteins, including paxillin, talin, vinculin, tensin, α-actinin, Fak and c-Src. Taken from Yeatman *et al.* 2004.

Cell migration is a cyclic process that includes formation of cellular protrusions, lamellipodia and filopodia, at the cell front; formation of focal adhesions at the front and disassembly at the rear edge, contraction of cytoskeleton leading to cell propulsion of the cell body forward and finally cell-substrate detachment and retraction at the rear of the cell.

The Rho family GTPases Rac1, Cdc42 and RhoA are important mediators of cell motility since regulate focal adhesions turnover and cytoskeleton dynamics. At the cell front, Src controls the formation of lamellipodia and filopodia by activating Rac and promoting Rho suppression through the phosphorylation of p190RhoGAP. At the cell rear, Rho activity is high where regulates the actin fiber assembly, as well as, the contractility. The integrin-mediated activation of Src allows localization of the Rho suppression pathway at leading edge. On the other hand, Rac and Cdc42 regulate the initial recruitment of cytoskeletal and signalling proteins into small focal complexes, whereas Rho controls the maturation of these complexes into bigger focal adhesions, as well as, focal adhesion lifetime.

It has been shown that the Fak-Src complex, p130CAS, paxillin, ERK, and Myosin light-chain kinase (MLCK) are essential for adhesion turnover at the cell front. The Fak-c-Src complex phosphorylates paxillin and p130CAS, which in turn recruit other

molecules to focal adhesions, regulating actin cytoskeletal organization. Paxillin is phosphorylated in tyrosine in the dynamic adhesions, which provokes its disassembly. On the other hand, Fak-Src signalling controls contractility through ERK, which phosphorylates MLCK to regulate adhesion disassembly. Fak autophosphorylation at Y397 regulates efficient disassembly of focal adhesions (127).

In addition, caveolin 1, a substrate of Src, could play an important role in cell motility. It has been described that caveolin 1 overexpression is associated with a basal-like phenotype and predicting a worse breast cancer patient prognosis. Grande-García *et al*. shown that the phosphorylation of Y14-caveolin 1 by Src is necessary for polarization and directs motility of mouse fibroblasts. Caveolin 1–deficient cells have decreased Rho and increased Rac and Cdc42 GTPase activities (42).

Furthermore, Joshi and colleagues shown that Rho signalling via Rho kinase (ROCK) promotes tumour cell migration and invasion by regulating focal adhesion turnover through phosphorylation of Y14-caveolin 1. Phosphorylated Y14-caveolin 1 by c-Src is linked to Rho/ROCK signalling. Besides, it is localized to membrane protrusions of tumour cells and associated to Rho activation, Fak stabilization in focal adhesions, increasing focal adhesion dynamics, as well as, cell migration. Activated Rho is localized to the leading edge of motile cells, including metastatic breast carcinoma. Furthermore, phosphoY14-caveolin 1 is expressed in several metastatic cells lines such as MDA-MB-231 or PC3 (57).

For its part, p130CAS is phosphorylated in tyrosine by Src-Fak complex creating a binding site for the adaptor protein Crk. Crk interacts with DOCK180, which in turn, activates Rac, promoting actin polymerization, and in consequence cell migration (43). Furthermore, p130CAS overexpression may provoke an increase in tyrosine phosphorylation of Fak and paxillin. p130CAS can bind Src, independently from Fak, enhancing Src in an active state (83).

3.3. SFKs role in invasion and transendothelial migration

Invasion of surrounding tissues is the first step in metastatic cascade. Malignant tumour cells are able to degrade epithelial basal membrane, as well as, the extracellular matrix, reaching circulatory system. The Src-Fak complex plays an important role in invasiveness. Fak localizes to lamellipodia and to actin-rich plasma-membrane protrusions enriched in metalloproteases, termed invadopodia. Src family kinase members control invadopodia formation, since they participate in cytoskeleton remodelling but also increase expression of metalloproteinases MMP-2 and MMP-9. Their expression is regulated by Src-Fak complex through c-JUN amino terminal

kinase (JNK) signalling pathway. The degradation of extracellular matrix components by MMPs is required for tumour invasion of surrounding tissues. Furthermore, the loss of E-cadherin, that forms adherens junctions, facilitates invasion. c-Src negatively regulates E-cadherin levels, which probably favours invasion (133).

Besides, caveolin 1 is involved in MDA-MB-231 metastatic ability, since its silencing by shRNA reduces cell invasiveness. In particular, ROCK- and Src-dependent phosphorylation of Y14-caveolin 1 is important for cell migration and invasion (57).

Abl interactor 1 (Abi1) is found in invadopodia and regulates their formation. Besides, Src signalling controls Inhibitor of differentiation protein 1 (Id1) expression, which in turn, modulates MMP-9 expression in MDA-MB-231 cell line (112).

Src family kinase participates in transendothelial migration. In AGS gastric adenocarcinoma cells, Cyr61 increases Chemokine receptor 1 and 2 (CXCR1 and CXCR2) expression and transendothelial cell migration through integrin αvβ3/Src/PI3K/Akt pathway (68). VEGF, through Src kinase activity, disrupts endothelial barrier function, promoting tumour cell extravasation, as well as, lung and liver metastasis of murine CT26 colon carcinoma in mice (128).

3.4. Role of SFKs in anchorage-independent growth

An essential property of metastatic cancer cells is to survive in circulatory system in order to colonize distant sites. Metastatic cells avoid anoikis, programmed cell death induced by detachment from the extracellular matrix. In mammary epithelial cells, overexpression of EGFR and c-Src promotes anchorage-independent growth (30). Integrins initiate signalling by clustering and binding to extracellular matrix components. In pancreatic carcinoma cells recruitment of c-Src by integrin $\alpha_v\beta_3$ may promote anchorage-independent signalling, distinct from the Fak-dependent response provoked by integrin in adherent conditions. Furthermore, colony formation depends on p130CAS phosphorylation by c-Src. Besides, $\alpha_v\beta_3$ promotes anchorage-independent growth by means of c-Src in breast and cervical cancer cell lines (29).

In addition, HEK293 cells transiently transfected with caveolin 1 (wt), c-Src and Grb-7, shown an increase in the number of colonies as compare to cells transfected with the mutant caveolin 1 (Y14A) together with c-Src and Grb-7. Thus, phosphorylation of Y14-caveolin 1 by c-Src binds Grb7 which enhances anchorage-independent growth (129).

3.5. SFKs in breast cancer metastasis to bone, lungs, brain and liver

The most common metastatic sites of breast cancer are brain, liver, lung, bone and distant nodal. Breast cancer cells express the chemokine receptors CXCR4 and CCR7

at high levels. CXCL12 and CCL21, the ligands for these receptors, are abundantly expressed in lymph nodes, lung, liver and bone narrow (18). Distinct patterns of spreading are shown based on the breast cancer subtype. Kennecke *et al*. made a study with 3726 patients showing that luminal A and B types have low risks of brain metastasis. HER2-like and luminal/HER2 (normal breast-like) subtypes have a relatively high rate of metastasis to brain, bone, liver and lung. Whereas basal-like tumours exhibit high rates of brain, bone, lung and nodal metastases and a lower rate of liver metastases. Moreover, the rate of early relapse is higher in basal-like and triple negative non-basal subtypes (58).

Bone metastases from breast cancer cells are mainly osteolytic, caused by osteoclast stimulation (86). c-Src has a role in bone formation, since Src knockout mice are deficient in bone remodelling and develop osteopetrosis (108). In fact, it has been shown that c-Src kinase activity promotes the development of osteolytic bone metastases of MDA-MB-231 cells. Mice intracardiacally injected with MDA-MB-231 transfected with constitutively active Src, developed larger osteolytic bone metastases compared to those observed with MDA-MB-231 expressing Src wt or Src kinase dead (87). In a study by Zhang and colleagues, MDA-MB-231 bone metastatic derivate cell line (BoM-1833) injected into left ventricle of mice caused dead with bone metastasis in 70 days, meanwhile c-Src knockdown extended survival by approximately 25 days. Thus, Src plays an important role in bone metastasis by promoting survival of breast cancer cells in bone marrow, since Src is necessary for CXCL12 activation of Akt and cell survival, as well as, for resistance to the proapoptotic effect of TRAIL (138).

Animal model of lung metastasis, consisting of tail vein injection, shown that after inoculation of Src kinase dead-transfected MDA-MB-231 cells, a lower number of foci was detected in lung with respect to inoculation of control cells. Therefore, Src tyrosine kinase activity has a role in lung metastases of MDA-MB-231 cells (87).

Many patients with breast cancer finally develop brain metastasis with a survival of less than one year. Clinically, HER^+ and TNBC patients have a higher risk for brain metastasis relapse. Zhang and colleagues observed an increased Src expression and activity in brain-seeking cell lines from BT474 and MDA-MB-231 compared to parental cell lines. Besides, immunohistochemistry of brain metastasis tumours revealed a strong staining of pY416-Src, that was significantly increased compared to primary breast tumours (unmatched). In an *in vitro* model of blood–brain barrier, they also observed that Src-wt or SrcY527F (constitutively active Src) promoted invasion, whereas shRNA-c-Src suppressed it. In addition, Src wt and Src-Y527F MDA-MB-231 cells shown an increased brain metastasis *in vivo* respect to control cells (137).

Multivariate analyses of 615 human breast tumours demonstrated an association between SRS (Src-responsive signature) status, a gene expression signature that denotes Src activity, and liver metastasis for ER^+ patients with a low significance (138).

4. INHIBITORS OF SFK ACTIVITY

Several inhibitors of Src family kinase activity have been described. Some of them such as PP2 and SU6656 have been used in preclinical trials; whereas Dasatinib is used in chronic myeloid leukaemia (CML) and in first phases of clinical trials for solid tumours. The three ATP-competitive inhibitors are selective compounds, and therefore, they not only inhibit Src family kinase activity, but also, other kinases with similar structure of the ATP-binding site.

4.1. Dasatinib

Dasatinib is a potent biochemical inhibitor of Bcr-Abl and Src kinases but also affects Lck, Yes, c-Kit, PDGFRβ and p38 among other kinases. *In vivo* activity was assayed in a xenograft model of chronic myelogenous leukaemia by using nude mice implanted with K562. Tumour regressions were observed at multiple dose levels (71). Preclinical studies in several solid tumour cell lines, such as prostate, breast and glioma have shown that Dasatinib induced an inhibition of cell proliferation, invasiveness and metastasis. Sensitivity to Dasatinib was determined by proliferation assay of 39 human breast cancer cell lines classified into luminal and basal subtypes. A strong correlation between sensitivity to Dasatinib and TNBC basal subtype was found. Since Src signalling has an important role in osteoclast activity, Dasatinib could prevent osteolytic metastases by inhibition of Src activity. This compound inhibited osteoclast proliferation in bone marrow cell culture and diminished serum calcium levels in a rat model of bone resorption (5). Furthermore, Zhang et al. shown that the bone metastatic activity of MDA-MB-231 bone metastatic derivate cell line was reduced by Dasatinib treatment (138). Several phase 1 and 2 studies have been performed using Dasatinib in combination with other compounds in solid tumours (5) (Figure 5A).

4.2. PP2

PP2 has inhibitory effects on SFKs members, including Src and Lck but also on other protein kinases, such as RIP2, CK1δ, CSK, Eph-A2 and FGFR1 (6). The inhibition of Src family kinases by PP2 reduced liver metastasis in a metastatic model consisting of orthotopic implantation of human colon cancer cell line HT29 (89).

Furthermore, inhibition of phosphoY418-c-Src by PP2 reduced cell proliferation and growth in the cervical cancer cell lines HeLa and SiHa (61) (Figure 5B).

4.3. SU6656

SU6656 is considered a potent inhibitor of Src family members. However, Bain *et al.* found that it also affected AMPK, BRSK2 and MST2 at a similar degree to Src and Lck inhibition. SU6656 inhibited Aurora B and C kinases even more effectively than Src or Lck *in vitro*. CaMKK*α*, CaMKK*β*, CHK2 and SRPK1 were found to be additional targets of SU6656 (6). Blake *et al*. observed that this compound inhibited PDGF- or serum-stimulated NIH 3T3 cell proliferation (11) (Figure 5C).

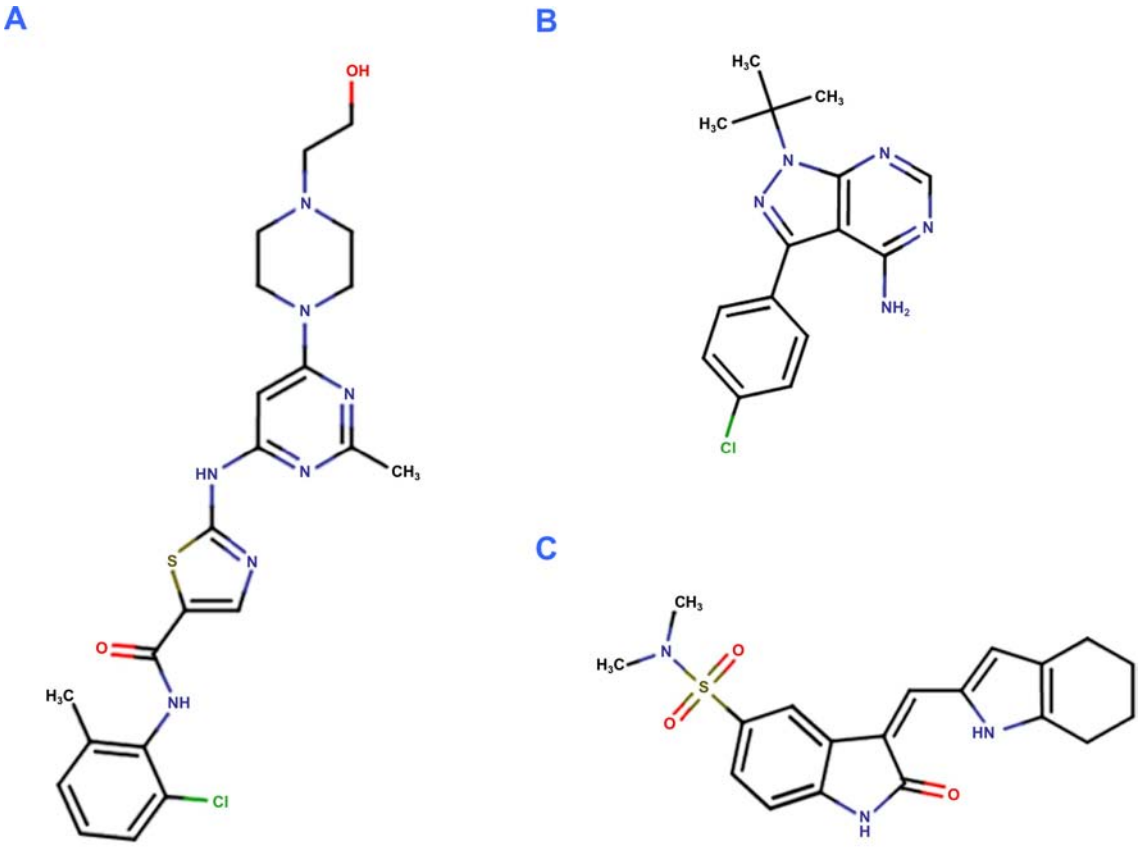

Figure 5. Structures of SFKs selective inhibitors. The molecular structure of Dasatinib (**A**), PP2 (**B**) and SU6656 (**C**) is depicted. Taken from Protein Data Bank.

OBJECTIVES

Several aspects of SFKs in breast cancer cells are extensively studied, however little is known about the specific role of their catalytic and scaffold functions in the process that lead to the metastasis of a highly invasive human breast cancer cell line, MDA-MB-231.

The main goal of this Doctoral Thesis is the *in vitro* characterization of proliferation, migration, invasion and transendothelial migration of MDA-MB-231 that depend on Src kinase activity or on c-Src by using three different but complementary approaches: inhibition of SFKs enzymatic activity, conditional suppression of c-Src and expression of SrcDN (K295M/Y527F).

The specific aims for the elaboration of this Thesis project are:

- To study process dependent on SFKs catalytic activity, by using three different selective SFKs inhibitors, Dasatinib, PP2 and SU6656.

- To investigate the role of c-Src, by knocking down its expression using a specific short hairpin RNA for c-Src under the tetracycline control in a Tet-On system.

- To determine the functionality of the endogenous members of SFKs expressed in MDA-MB-231 cells by conditional expression of SrcDN (K295M/Y527F).

MATERIALS AND METHODS

1. CELL LINES AND FUNCTIONAL STUDIES

1.1. Reagents

Stealth RNAi siRNA-Cyr61 (s7244) and scramble siRNA (12935-300) were from (Life-Technologies Corporation, Carlsbad, CA, USA). Anti-BrdU FITC-conjugated antibody and Matrigel™ were from BD-Biosciences (Bedford, MA, USA). MTT, trypan blue, propidium iodide (PI), esiRNA human Rab27a (esiRNA1), SU6656 and doxycycline (Doxy) were from Sigma-Aldrich (St. Louis, MO, USA). PP2 was from Tocris (Ellisville, MO, USA) and Dasatinib was from LC-Laboratories (Woburn, MA, USA). Blasticidin and zeocin were from InvivoGen (IBIAN Technologies, Zaragoza, Spain). Tet-Free-FCS (PAA Laboratories GmbH, Passching, Austria). Dharmafect 4 were from Thermo Scientific (Rockford, IL, USA).

1.2. MDA-MB-231 cell lines

Three human breast adenocarcinoma cells lines were used to perform experiments, MDA-MB-231, MDA-MB-231-Tet-On-shRNA-c-Src and MDA-MB-231-Tet-On-SrcDN (K295M/Y527F).

To generate MDA-MB-231 cell line with conditional expression (Tet-On) of short hairpin RNA-c-Src (shRNA-c-Src) or c-Src dominant negative (SrcDN), MDA-MB-231 cells were transfected with a vector encoding the Tetracycline repressor (TetR) (pcDNA6/TR; Life Technologies) by calcium phosphate method and selected 48 h later with 6 µg/ml of blasticidin. Clones were grown and tested for the expression of TetR by Western Blot. Clone TR8 was chosen for its maximal expression of TetR and transfected with pENTR™/H1/TO containing shRNA-c-Src sequence #944 (Life Technologies) 5'-CACCGCCTCAACGTGAAGCACTACACGAATGTAGTGCTTCACGT TGAGC-3'.

Cells were cultured in medium supplemented with blasticidin and 300 µg/ml of zeocin. Selected clones were grown in presence or absence of 2 µg/ml of Doxycycline (Doxy) for 72h and tested for expression of c-Src by Western Blot.

For MDA-MB-231 Tet-On SrcDN cell line generation, clone TR8 was used to transfect pcDNA4/TO with SrcDN sequence. After selection with 6 µg/ml of blasticidin and 300 µg/ml of zeocin, several clones were grown in medium supplemented or not with 1 µg/ml of Doxy for 72h and tested for expression of SrcDN by Western Blot. Clones with no basal expression of SrcDN in absence of Doxy that highly induce SrcDN upon addition of Doxy were selected, pooled to carry out experiments.

1.3. Cell culture

MDA-MB-231 cell line from the ATCC was maintained in Dulbecco´s Modified Eagle's Medium (DMEM) supplemented with 5% FCS, 2mM glutamine, 100 IU/ml penicillin, and 100 µg/ml streptomycin. MDA-MB-231 cells were authenticated by means of short tandem repeat (STR) analysis (PowerPlexW 1.2 System; Promega) at the Genomic Service of the Institute. MDA-MB-231-Tet-On-shRNA-c-Src and MDA-MB-231-Tet-On-SrcDN were cultured in the previous medium with 5% Tet-Free-FCS, 3 µg/ml blasticidin and 100 µg/ml zeocin. Cells were maintained at 37ºC in 5% CO_2 and splitted at approximately 80-90% confluence.

SYF cell line (Src, Yes, and Fyn deficient fibroblasts) from ATCC was maintained in DMEM supplemented with 5% FCS, 2mM glutamine, 100 IU/ml penicillin, and 100 µg/ml streptomycin.

1.4. Metabolic activity and proliferation assays

The effect of the SFKs activity inhibitors on MDA-MB-231 metabolic activity was assessed by using 3-(4,5-dimethylthiazol-2-yl)-2,5-diphenyl tetrazolium bromide (MTT) assay. A graph was generated depicting the metabolic activity as percentage of cells treated with each inhibitor at different concentrations respect to the control, DMSO-treated cells. Exponentially growing cultures were harvested after trypsinization and seeded at 1.5 x 10^4 cells/well in a 96-well plate in 100µl of complete medium for 24h. Then, medium was replaced with fresh medium supplemented with DMSO (1:1000, Control), Dasatinib (10, 100, 500, 1000 nM), PP2 or SU6656 (1, 5, 25, 50 µM). Following 72h treatment, 10 µl of MTT Formazan were added to each well to a final concentration of 0.5 mg/ml and incubated at 37 ºC for 4h. Formazan crystals were solubilized with 100 µl of 10% SDS/10 mM HCl at 37 ºC for 2 h and absorbance was measured at 570 nm in a VersaMax Elisa microplate reader.

For MDA-MB-231-Tet-On-shRNA-c-Src and MDA-MB-231-Tet-On-SrcDN cell lines, 24h after seeding, medium was changed and 2 or 1 µg/ml of Doxy, respectively, were added to cultures. Six wells per condition were prepared in three independent experiments.

Cell proliferation was determined by trypan blue exclusion assay. Cells were cultured at a density of 1.5 x 10^5 cells / 35-mm plate, 24 h later medium was changed and DMSO, 100 nM Dasatinib, 5 µM PP2 or 5 µM SU6656 were added. For MDA-MB-231-Tet-On-shRNA-c-Src and MDA-MB-231-Tet-On-SrcDN cells medium was supplemented with Doxy (concentrations as above). After 72 h, adherent and detached cells were collected, mixed with a 0.4% solution of trypan blue in PBS (1:1) and counted with a haemocytometer.

1.5. Cell cycle analysis

Cell cycle studies were performed by flow cytometry using double bromodeoxyuridine (BrdU) and propidium iodide (PI) labelling. Cells were plated at a density of 1.5 x 10^6 cells / 60-mm plate in complete medium. Next day cells were pre-treated for 2 h with DMSO or inhibitors and pulse-labelled with 30 µM of BrdU for 30 min, washed three times with culture medium and incubated in fresh medium with DMSO, Dasatinib, PP2 or SU6656 for 3, 9, 24 and 36 h. Cells at time 0 h were collected after washes. At given times, adherent and detached cells were harvested and fixed in 1 ml of 70% ethanol in distilled water for at least 1 h at 4 ºC. Then cells were incubated at 37 ºC in a solution of 2 ml HCl 2M with 10 µl pepsin buffer (20 mg/ml pepsin in 0.1M HCl) for 20 min. After two washes with PBS cells were labelled with anti-BrdU conjugated to fluorescein isothiocyanate (FITC) in a solution of 0.5% Tween-20 / 0.5 % FCS in PBS. Cells were washed with PBS, stained with PI / RNase (20 µg/ml) and analysed by flow cytometry (FACScan, Becton Dickinson & Company, Franklin Lakes, NJ, USA). Background signals were set by BrdU-unlabelled cells incubated with anti-BrdU-FITC.

For cell cycle analysis with PI labelling after 24 h and 72 h treatment with DMSO, Dasatinib (100 nM), PP2 (5 µM), SU6656 (5 µM) or ZM447439 (5 µM), detached and adherent cells were collected, washed with PBS and fixed in 70% ethanol for at least 1 h at 4 ºC. Then, PBS was added, cells were pelleted by centrifugation and resuspended in 1 ml of PBS, incubated with 20 µg/ml of PI / RNase and analysed by flow cytometry. At least 10,000 events per sample were acquired and analysed using Cell Quest Pro software (BD).

1.6. Cell migration assays

Cell migration was analysed by wound healing assay seeding 8 x 10^5 MDA-MB-231 cells per 60-mm plate in complete medium. Next day medium was changed and supplemented with DMSO or inhibitors (concentrations as before). After 24 h the confluent monolayer was scratched with a sterile 200 µl tip and plate was washed twice with fresh medium without serum to remove floating cells. Complete medium with DMSO, for control, or inhibitors was added to cultures. Same fields were photographed at 0 h and 20 h with a Nikon Eclipse TS100 inverted microscope (Nikon Instruments Europe B.V., Kingston, Surrey, England) equipped with Olympus DP20 digital camera (Olympus Europe GmbH, Hamburg, Germany) at a magnification of 100x.

For MDA-MB-231-Tet-On-SrcDN cell line, 24h after seeding cells were grown in presence or absence of 1 µg/ml of Doxy. Migration assay was performed as above.

For MDA-MB-231-Tet-On-shRNA-c-Src, 3.5 x 10^5 cells/well in 6-well plate were seeded in complete medium. Next day, fresh medium with or without 2 µg/ml of Doxy was added. After 48 h, the monolayer was scratched, washed twice with serum-free medium and complete medium with or without Doxy was replaced. Microphotographs were taken at 0 h and 20 h with a Microscope Cell Observer Z1 system (Carl Zeiss MicroImaging GmbH, Jena, Germany) equipped with a controlled environment chamber (37°C and 5% CO_2) and Camera Cascade 1k, under 4x objective.

Migration was quantified using Wound-healing tool of ImageJ. Each value represents the percentage of wound-healing area at 20 h respect to 0 h in three independent experiments.

Random migration assay was carried out by seeding MDA-MB-231-Tet-On-shRNA-c-Src cells at a low density (5 x 10^4 cells) in a 6-well plate. After 48 h of Doxy-treatment, cells were washed with serum-free medium and placed in 2% FBS medium. Three fields per well (three wells per condition) were photographed with the Microscope Cell Observer with a 10x objective, every 15 min for 22 h. Directionality, mean velocity, accumulated and Euclidean distances travelled were quantified from at least 63 cells per condition (7 per field) by using ImageJ. The experiment was repeated three times.

1.7. Transendothelial migration assay

MDA-MB-231-Tet-On-shRNA-c-Src cells were seeded in complete medium at 4.5 x 10^5 cells / 60-mm plate. At the same time, 5 x 10^4 human umbilical vein endothelial cells (HUVEC) in 120 µl of EGM medium (Lonza) were added over 0.2 % gelatin-coated cell culture inserts for 24-well plate (8 µm-pore PET membranes) (Falcon, BD Biosciences). Next day shRNA-c-Src cells were treated with or without 2 µg/ml of Doxy. After 48h treatment, 5 x 10^4 shRNA-c-Src cells in 120 µl serum-free DMEM were placed on the top of HUVEC monolayer. The lower chamber was filled with 600µl of 20% FBS-supplemented medium. As control, in order to test the spontaneous migration of HUVEC cells, two HUVEC-coated filters were placed in the same conditions, without seeding shRNA-cSrc cells. After 22 h, transmigrated cells were detached from the bottom of the filter and counted in a haemocytometer. The number of Doxy-treated transmigrated cells was expressed as the percentage respect to control transmigrated cells (100%). c-Src suppression was determined by Western blot before plating shRNA-c-Src cells over HUVEC monolayer and at 22 h.

1.8. Invasiveness assay

Invasion assay of MDA-MB-231 cells was performed in cell culture inserts of 8 µm pore in a 24-well plate. The chamber insert was coated with 100 µl of Matrigel diluted in

serum-free medium at a final concentration of 250 µg/ml and allowed to gelify overnight at room temperature. Next day, 5 x 10^4 cells were seeded in 200 µl of complete medium on the top of each Matrigel-coated filter. Cells were allowed to attach and then medium was replaced with fresh serum-free medium containing DMSO or inhibitors. Lower chamber was filled with 300 µl of medium supplemented with 10% FBS and DMSO or inhibitors. After 24 h, the cells on the top of inserts were removed and invasive cells attached to the bottom were fixed in methanol and stained with DAPI/PBS (10 µg/ml), mounted on slides with ProLong antifade-reagent. Photomicrographs of at least 4 fields/insert were taken with a Plan 20x/0.50 objective using Eclipse 90i fluorescence microscope equipped with Digital Sight DS-Qi1 camera and NIS-Elements BR imaging software (Nikon). DAPI-stained nuclei were counted. Four assays were made in triplicate.

MDA-MB-231-Tet-On-shRNA-c-Src and MDA-MB-231-Tet-On-SrcDN cells were cultured at a concentration of 5 x 10^5 / 60-mm plate. Next day medium was changed by fresh medium supplemented with Doxy (2 or 1 µg/ml of Doxy, respectively). After 48 h, cells were detached with trypsin and assay was performed as previously described for MDA-MB-231 cell line, in presence or absence of Doxy.

1.9. Soft-agar colony formation assays

The anchorage-independent growth of MDA-MB-231-Tet-On-shRNA-c-Src cell line was evaluated by soft-agar colony formation assay. Three milliliters of 0.5% agar in DMEM 10% FCS with or without 2 µg/ml of Doxy was solidified in the bottom of 60-mm plates. Exponentially growing cells were resuspended in a prewarmed solution of 0.3 % agarose in complete medium, with or without Doxy, and seeding at a density of 1 x 10^5 cells / agar precoated dish. Cells were re-fed every 3 days with complete medium (300 µl / plate) with or without Doxy. After 20 days of growth, plates were stained with 0.5 ml of 0.005 % crystal violet in distilled water for at least 1 h. Colonies measuring more than 0.1 mm were counted under a Nikon Eclipse TS100 inverted microscope. Two independent experiments were performed in triplicate.

1.10.Three-dimensional culture assay

For three-dimensional (3D) analysis of morphology, 3D embedded assay was performed as previously described (66). Cell culture dishes (24-well plates) were precoated with 50 µl of undiluted growth factor-reduced Matrigel (10 mg/ml) per well and allow to gel for 30 min at 37 °C. To analyse the effects of SFKs selective inhibitors on 3D cell growth, 1 x 10^4 cells per well were resuspended in 300 µl of complete medium/Matrigel (1:3) containing DMSO (control), Dasatinib (100 nM), PP2 (5 µM) or

SU6656 (5 µM) seeded over the gelified coat Matrigel and incubated for at least 30 min at 37 °C. Then, 500 µl of complete medium containing DMSO or SFKs selective inhibitors was added to the cultures and changed every 2–3 days for 21 days. To assess the effects of the inhibitors on MDA-MB-231 spheres already formed, compounds were added after 21st day of growth and maintained for additional 7 days. Treatments were performed in triplicate and assays were repeated twice. Representative fields were photographed at 10x magnification using the Nikon Eclipse TS100 inverted microscope equipped with Olympus DP20 digital.

1.11.Mammosphere formation assay

Cell suspensions of MDA-MB-231-Tet-On-shRNA-c-Src cell line were plated at low density of 1 x 10^3 cells/ml in ultra-low attachment 6-well plates (Falcon, Corning Life Sciences, Tewksbury MA, USA) in mammosphere culture medium: DMEM/F12 medium containing B27 (1:50; Life Technologies), 20 ng/ml EGF and bFGF (PeproTech EC Ltd., London, UK), 5 µg/ml insulin, 1µg/ml hydrocortisone (Sigma). To exclude sphere formation due to cell aggregation (47), mammosphere assay was also performed by plating cells in 96-well ultralow attachment plates at very low density (10 cells/100µl/well). To examine the effect of Src suppression on mammosphere formation, 2 µg/ml of Doxy was added in the growth medium at seeding and every 3 days. After 20 days, mammospheres were manually counted using the Nikon-Eclipse TS100 under 4x magnification. Sphere forming efficiency (SFE) was calculated as number of sphere-like structures (diameter≥ 50 µm) formed in 20 days divided by number of seeded cells and expressed as percentages of the means ±SD.

1.12.Time-lapse video microscopy

MDA-MB-231 cells were seeded in complete medium in 35 mm µ-dishes (1 x 10^5 cells / dish). After 24h, cells were treated with DMSO (Control) or SU6656 (5 µM). Images were taken every 15 min, 3h after inhibitor addition until 20 h. Live cell imaging was obtained with a 20x Plan Apochromat objective, using microscope Cell Observer Z1 system. Time-lapse movies were formatted using imaging software AxioVision 4.8 (Zeiss).

1.13.Transient transfection of siRNA-Cyr61 and esiRNA-Rab27a

Silencing of Cyr61 or Rab27a was achieved using transient transfection of siRNA-Cyr61 (s7244) or esiRNA-Rab27a. MDA-MB-231 cells (1 x 10^5 cells/well) were seeded in 2 ml of complete media without antibiotics in a 6-well plate. Next day, transient

transfection was performed. Briefly, 5 µl of Dharmafect 4 were diluted in 195 µl of DMEM with L-glutamine. In another tube, siRNA was diluted with DMEM with L-glutamine to a final concentration of 20 nM for siRNA-Cyr61, 50 nM for esiRNA-Rab27a or and 20/50 nM for scramble siRNA (Life Technologies), respectively. After 5 min incubation at room temperature, both mixes were incubated together for 20 min. Then, medium from cells was removed and replaced with 1.6 ml medium without antibiotics and 400 µl of appropriate transfection mix were added to each well. Cells were incubated at 37 ºC for 8 h and then medium was replaced. After 40 h of transfection, cells were detached with trypsin and used for invasion, transendothelial migration or Western blot (72h) assays, as previously described. When esiRNA-Rab27a was employed, medium was changed after 72h and cells were then maintained 24h in serum-free media. Secretome and total cell extracts were used for Western blot analyses.

1.14.Statistical analysis

All results are expressed as mean ± standard deviation (SD) of at least three independent experiments. Parametric bilateral Student *t*-test was used for statistical analyses. Two-sided p-values less than 0.05 were considered statistically significant.

2. PROTEIN-BASED ASSAYS

2.1. Reagents

Anti-c-Src 327 was a gift of Joan S. Brugge (Harvard University). Anti-Tet-repressor (Mobitec, Göttingen, Germany). Anti-Fak (A17), anti-p120-catenin (S-19), anti-c-Myc (N262), anti-Cyr61 (sc-13100), anti-Oct3-4 (C-20) and anti-cyclin D1 (H-295) were from Santa Cruz Biotechnology (Santa Cruz, TX, USA). Anti-Cis-Golgi-gp74 25H8 was a gift of Ignacio Sandoval (Centro de Biología Molecular Severo Ochoa, Madrid) (4). Anti-Rab27a polyclonal antibody was a gift of Peter van der Sluijs (University Medical Center Utrecht) (91). Anti-CD63 (63PU-S, Inmuno-Step, Salamanca, Spain; Calbiochem OP171, Merck-Millipore), antibodies to MMP-2 (AB6003), MMP-9 (AB19016), anti-pS10-histone H3, phosphotyrosine 4G10, anti-avian Src mouse mAb clone EC10 and Nanog (AB9220) were from Millipore (Merck Millipore Corporation, Billerica, MA, USA). Anti-MMP-7 (AP6212a) was from Abgent (San Diego, CA, USA). Anti-pY925-Fak, anti-pS473-Akt and anti-pY118-paxillin were from Cell Signaling Technologies (Danvers, MA, USA). Anti-aurora B and anti-histone H3 were from ABCAM (Cambridge, UK). Anti-paxillin, anti-p130CAS, anti-caveolin, anti-pY14-

caveolin, anti-β-catenin and anti-$p27^{Kip1}$ were from BD-Biosciences. Anti-Sox2 was from Neuromics (Edina, MN, USA). Anti-pY397-Fak, anti-pY418-Src, secondary horseradish peroxidase-conjugated antibodies, goat-anti-mouse IgG Alexa-Fluor 546, goat-anti-rabbit IgG Alexa-Fluor 488, DAPI (D1306), ProLong anti-fade-reagent were from Life-Technologies Corporation. Purified histone H3 was from Roche Applied Science (Indianapolis, IN, USA). Acrylamide/Bis-acrylamide (29:1), SDS and ammonium persulfate were from Bio-Rad Laboratories (Hercules, CA, USA). ECL was from GE Healthcare Biosciences (Pittsburgh, PA, USA). BCA protein assay was from Thermo Scientific.

2.2. Protein extraction and quantification

Subconfluent cell cultures from three 60-mm dishes were washed twice in ice-cold PBS and lysed in ice-cold lysis buffer (10 mM Tris-HCl, pH 7.5, 50 mM NaCl, 30 mM sodium pyrophosphate, 5 mM EDTA, 5 mM EGTA, 1% Triton X100, 50 mM NaF, 0.1 % SDS, 0.1 mM Na_3VO_4, 1mM phenylmethylsulfonyl fluoride, 1 mM benzamidine, 1 mM iodacetamide, 1 mM ortho-phenantroline). The cell lysates from three plates for each condition were pooled. The supernatants from a centrifugation of 15,000 xg for 30 min at 4 ºC were collected and protein concentration was determined by BCA protein assay in a microreader plate. Extracts were compensated for differences in protein concentration with lysis buffer, boiled in SDS sample buffer (62.5 mM Tris-HCl, pH 6.8, 5% β-mercaptoethanol, 2% SDS, 10% glycerol) and stored at -20 ºC until further use.

2.3. Western blotting

Equal amounts of protein (30 µg) were separated by SDS-PAGE and electrotransferred to a polyvinylidene difluoride (PVDF) membrane for 45 min at 2.5 mA/cm^2. Nonspecific binding on the PVDF filters was minimized by blocking with 5% non-fat dry milk in TBST (10 mM Tris-HCl, pH 7.4, 0.1% Tween-20), or 5% bovine serum albumin in TBST for anti-phosphoproteins immunodetection for 1 h at room temperature. Membranes were then incubated with specific primary antibodies in blocking buffer overnight at 4 ºC. After three washes with TBST, filters were incubated with suitable secondary antibody conjugated to horseradish peroxidase for 1 h at room temperature. Membranes were washed three times with TBST and proteins were detected with enhanced chemiluminescence reagent (ECL). X-ray films were scanned and signal was measured by densitometry using ImageJ program. Protein expression was determined relative to loading control signal; control condition (DMSO or Doxy untreated cells) was arbitrarily assigned a value of 1.

2.4. Aurora B kinase activity assay

Exponentially growing cultures were lysed in buffer B (50 mM Hepes, pH 8, 600 mM KCl, 0.5% Nonidet P40, 1 mM Na_3VO_4, 1mM DTT, 0.1 mM protease inhibitors) at 4 ºC. Aurora B kinase was immunoprecipitated from total cell extracts, as described previously (Tardaguila et al. (117)). Immune-complexes were incubated with 1 µg of histone H3 for 30 min at 37 ºC in kinase assay buffer (20 mM Hepes, pH 7.4, 150 mM KCl, 5 mM $MnCl_2$, 5 mM NaF, 1 mM DTT, 30 µM cold ATP) in presence or absence of 1 µM SU6656. pS10-H3, H3 and Aurora B kinase expression were determined by Western blot.

2.5. Immunofluorescence and confocal microscopy

For immunofluorescence studies, MDA-MB-231 cells seeded on sterile coverslips were treated for 24 h with DMSO or inhibitors, fixed with 3.7% paraformaldehyde in PBS for 10 min at room temperature, permeabilized with 0.1% Triton X-100 in PBS for 5 min at room temperature and blocked for 30 min with 1% BSA in PBS. Coverslips were incubating at 37 ºC for 1h with TRITC-labelled phalloidin (1:200 in PBS-1% BSA) or with primary antibodies, anti-α-tubulin (1:50) and anti-phosphohistone H3 (1:200). Following washes with PBS, cells were probed with Alexa Fluor 488 goat anti-mouse or Alexa Fluor 546 goat anti-rabbit, secondary antibodies (1:200) for 1 h at 37 ºC. DAPI/PBS (10 µg/ml) was used for 10 min at 37 ºC to counterstain the cells, after washing with PBS. Then coverslips were mounted on slides with ProLong anti-fade reagent. Samples were photographed with a Plan Apochromat 60x/1.40 objective using a Nikon Eclipse 90i fluorescence microscope equipped with Digital Sight DS-Qi1 camera and NIS-Elements BR imaging software (Nikon).

For confocal microscopy assays, MDA-MB-231 cells 24 h-treated with or without inhibitors, as well as, MDA-MB-231-Tet-On-shRNA-c-Src cells, treated or not with Doxy for 72 h, were fixed and permeabilized as above, blocked with 5% normal goat serum/PBS and washed with PBS-1% BSA. MDA-MB-231 cells were incubated with anti-pY118-paxillin (1:50), anti-pY925-Fak (1:50), anti-β-catenin (1:100) or anti-p120-catenin (1:100). MDA-MB-231-Tet-On-shRNA-c-Src cells were incubated with the primary antibodies rabbit polyclonal anti-Cyr61, anti-IGFBP4 in combination with mouse monoclonal anti-25H8 or anti-CD63 (1:100). Coverslips were washed with PBS and then incubated with secondary antibodies diluted 1:400 in 5% normal goat serum/PBS. Samples were mounted after DAPI/PBS counterstaining. Images were acquired using an inverted Zeiss LSM 710 laser-scanning microscope with a Plan Apochromat 60x/1.40 objective. Sequential scanning mode was used to avoid crosstalk

between channels. Z-optical stacks with 0.6 µm intervals through the cell Z-axis were recorded. Images were processed with ZEN 2009 software (Zeiss) and Adobe Photoshop CS5 (Adobe Systems In., USA).

2.6. Secretome analysis

2.6.1. Secretome fractionation

Cultures of MDA-MB-231-shRNA-c-Src were grown for 48h in the absence or presence of Doxy (2 µg/ml) in complete media. Cells were then washed three times with serum- and phenol red-free DMEM and then incubated for additional 24h in this medium in absence or presence of Doxy. Conditioned media from control or Doxy-treated shRNA-c-Src cells were used to prepare total secretome or soluble and exosomal fractions of secretome by differential centrifugation, as described (118). Briefly, the culture media was spin down at 300 xg for 10 min and supernatant was then centrifuged at 2,000 xg 10 min to remove alive and dead cells obtaining total secretome. Total secretoma from MDA-MB-231-Tet-On-SrcDN cells was prepared as above, growing cells with or without 1 µg/ml of Doxy. In order to prepare soluble secretome and exosomal fraction, additional centrifugation steps were performed at 10,000 xg for 30 min and 100,000 xg for 70 min. The proteins from supernatant of 100,000 xg, were concentrated by methanol/chloroform precipitation (soluble secretome). Microvesicle pellet was resuspended in PBS-5mM EDTA for Western blot analyses (Figure 1).

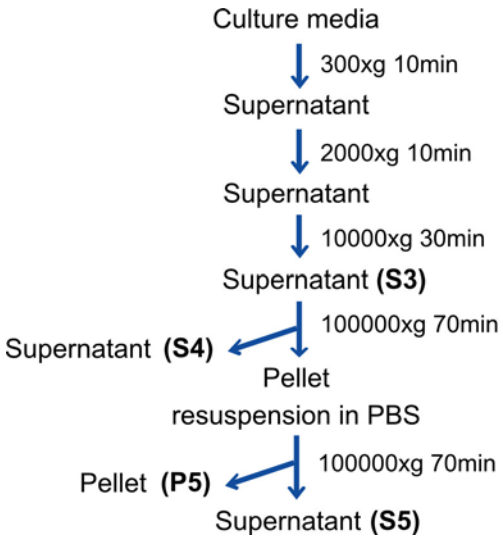

Figure 6. Outline of differential ultracentrifugation of secretome to isolate exosomes. Adapted from Thery *et al*.

2.6.2. Secretome protein digestion and iTRAQ-4-plex® labelling

Total secretome from MDA-MB-231-Tet-On-shRNA-c-Src was obtained from culture media as described above, and the pellet was discarded. For digestion, 20 µg of protein from each secretome condition (-/+ Doxy) were precipitated with methanol/chloroform. Twenty micrograms of protein from each condition were reduced with TCEP [Tris(2-carboxyethyl)phosphine], alkylated with MMTS (methyl methanethiosulfonate), digested with trypsin and labelled with iTRAQ reagent. Samples labelled with iTRAQ tags 116 and 117 were used for control conditions and 114 and 115 for Doxy-treated replicates. After peptide labelling with iTRAQ reagents, the four reaction mixtures of each experiment were then combined into a single tube and labelling reaction stopped by evaporation in a Speed Vac. Each digested, labelled and pooled samples were desalted using Sep-Pak C18 cartridges (Waters), vacuum concentrated and reconstituted with 0.1% heptafluorobutyric acid (HFBA).

2.6.3. Secretome protein separation and analysis by RP-LC-MALDI TOF/TOF MS

The resulting peptide mixtures were separated by Tempo nano multidimensional liquid chromatography coupled to mass spectrometry for protein identification (AB SCIEX, Foster City, CA, USA). After separation in nanoMDLC HPLC, peptides were then eluted onto an Onyx monolith C18 column (150mm x 0.1mm i.d.) (Phenomenex, Aschaffenburg, Germany). A 1.5 µl/min flow rate of 3 mg/ml α-cyano-4-hidro-cinnamic acid MALDI matrix diluted in 70% acetonitrile and 0.1% TFA aqueous solution, were mixed post-column with the eluted peptides. Spots were deposited on the MALDI-plate (Opti-TOF™ LC MALDI Insert, AB SCIEX, Foster City, CA, USA) by a fraction collector Suncollect (SunChrom GmbH, Friedrichsdorf, Germany). A MALDI TOF/TOF 4800 (AB SCIEX) mass spectrometer was used for acquisition and processing of the data. MS data from the spots were acquired in positive reflector ion mode in the mass range of 800-3500m/z by accumulation of 1200 laser shots. MS/MS spectra were generated by 2kV collisions with air. Maximal 2000 laser shots were accumulated for MS/MS spectra.

Raw files containing a peak list of the precursors and fragment ions were filtered and exported with the ABI-Extractor tool (Peaks-Bioinformatics Solutions, Waterloo, Canada). Protein identification and quantitation on each of the two data sets were done by using MASCOT v2.3.01 (Matrix Science, London, UK) and Phenyx v2.6 (GeneBio, Geneva, Switzerland) search engines. The searches were performed against the UniProtKB/Swiss-Prot human database (40,478 sequences; 22,568,758 residues) to estimate the false discovery rate (FDR) below 1%, which boosted the reliability of the data. The confidence interval for protein identification was set to≥ 95% ($p<0.05$) and

only peptides with an individual ion score above the 1% FDR score threshold were considered correctly identified. Differential expression of proteins between controls and Doxy-treated samples was determined by calculating the weighted average ratios of the peptides for each identified protein. Only proteins having at least two quantitated peptides were considered in the quantitation.

3. GENE EXPRESSION PROFILING

3.1. RNA extraction and quantification

MDA-MB-231 or MDA-MB-231-Tet-On-shRNA-c-Src cells were treated for 72 h with inhibitors (100 nM Dasatinib, 5 µM PP2 or SU6656) or with 2 µg/ml Doxy, respectively. Total RNA from cultures at 70% confluence was extracted using RNeasy kit (Qiagen, Hilden, Germany), following manufacturer's instructions, from three independent experiments made in triplicate. RNA quantity and quality was assessed by NanoDrop and using the RNA 6000 Nano Assay kit on an Agilent 2100 Bioanalyser (Agilent Technologies, Santa Clara, CA, USA). RNA samples with an integrity value higher than or equal to 8 from each treatment per experiment were pooled. cDNA was synthesized using random octamer primers with kit High Capacity cDNA Reverse Transcription (Applied Biosystems, Life Technologies) following manufacturer's instructions.

3.2. Real time quantitative PCR analysis (qRT-PCR) of c-Src mRNA and gene expression analysis

c-Src mRNA expression was determined by using TaqMan probe for human c-Src (Hs01082246_m1), TBP (TATA-box binding protein) was used as endogenous control (Life Technologies). For CCN1 (Cyr61) qRT-PCR was carried out using SYBR Green Master Mix (Life Technologies) according to manufacturer's instructions. For Cyr61 the primers 5'-TCCAGCCCAACTGTAAACATCA-3' and 5'-GGACACAGAGGAATGCAGCC-3' were used and for endogenous control, GAPDH, 5'-GTGAAGGTCGGAGTCAACG-3' and 5'-TGAGGTCAATGAAGGGGTC-3', as described previously (136). Gene expression was then calculated as the difference in threshold cycle (ΔCt) between the target gene and TBP and GAPDH respectively; ΔΔCt was the difference between theΔCt values of the test sample and that of the control. Relative expression of target genes was calculated as $2^{-\Delta\Delta Ct}$.

Ten micrograms of total RNA from DMSO or inhibitors-treated cells were used to prepare probes, then targets were hybridized to Agilent Sure Print G3 Human GE

8x60k Microarray (Santa Clara, USA) following manufacturer's instructions. Differential expression analysis was performed using R platform for statistical analysis (R Foundation for Statistical Computing, Vienna) and several packages from the Bioconductor Project (http://www.bioconductor.org/). The raw data were imported into R and preprocessed using half method for background correction and the quantile method for normalization. Probes with expression level below the detection control probe in all samples were removed. To identify differentially expressed genes, we used the limma package. Correction for multiple hypotheses testing was accomplished by using Benjamini and Hochberg False Discovery Rate (FDR) adjustment (8). Genes were selected as differentially expressed with an adjusted P value ≤ 0.05. Hierarchical clustering analysis of gene expression profiles was carried out using the complete linkage method.

3.3. Gene Set Enrichment Analysis (GSEA)

Gene Set Enrichment Analysis (110) was applied to define gene sets based on prior biological knowledge about biochemical pathways using Biocarta, KEGG and Reactome databases and based on Src gene set previously reported (9). Genes were ranked based on limma moderate t statistic. After Kolmogorov-Smirnov testing, those gene sets showing FDR ≤ 0.05, were considered significantly enriched among compared treatments.

RESULTS

1. GENERATION OF MDA-MB-231-Tet-On-shRNA-c-Src AND MDA-MB-231-Tet-On-SrcDN (K295M/Y527F)

Clones from MDA-MB-231-Tet-On-shRNA-c-Src cells were analysed by Western Blot for reduction of c-Src expression upon induction of shRNA-c-Src by addition of Doxy (2 µg/ml, 72h) to cultures. Those clones with a significant reduction of c-Src expression were chosen and pooled. Pool #11 was tested for c-Src mRNA and protein levels in absence or presence of distinct concentrations of Doxy (data not shown) and at different time-points (0 , 14 , 24, 48 and 72 h). In view of the results, pool #11 was used for the experiments, that were usually performed at 2 µg/ml Doxy for 72 h (Figure 7A and 7B).

The generation of MDA-MB-231-Tet-On-SrcDN gave rise to several clones, that were tested for SrcDN expression by Western Blot. The clones with SrcDN expression upon induction with 1 µg/ml of Doxy for 72h and absence of SrcDN expression without Doxy were selected and pooled. Pool #20, was selected by its expression in presence of Doxy and absence without Doxy (Figure 7C).

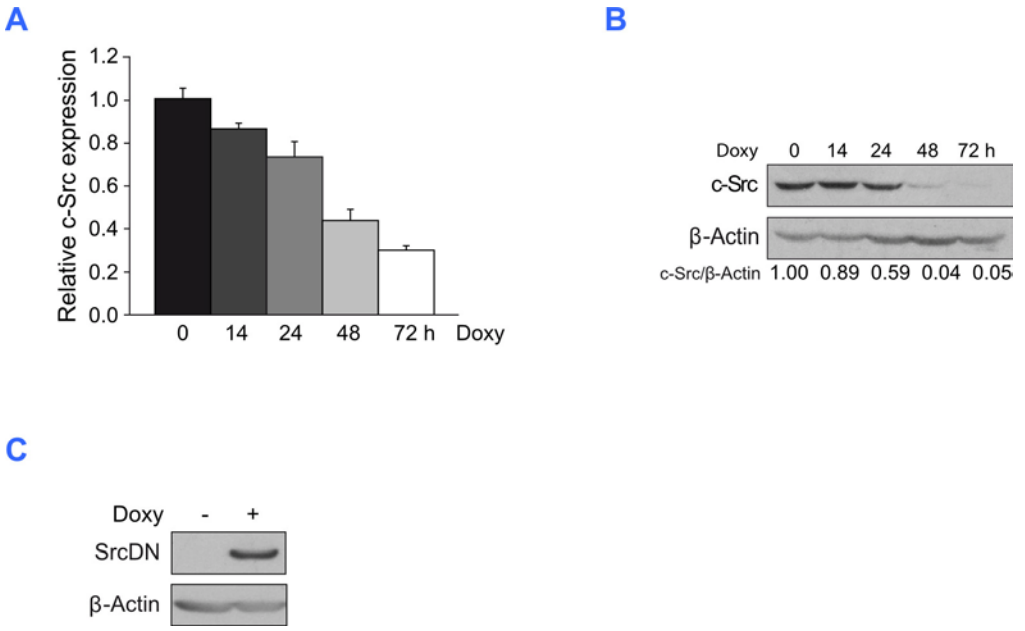

Figure 7. Analysis of c-Src and SrcDN expression in MDA-MB-231. (A) Relative c-Src mRNA levels after 2 µg/ml of Doxy treatment for the indicated times. (B) Whole-cell lysates treated with Doxy for the indicated times were analysed by SDS-PAGE and immunoblotting using anti-c-Src (mAb 327) and anti-β-actin, as loading control. (C) The expression of SrcDN and β-actin were detected by Western Blot in cell lysates of MDA-MB-231-Tet-On-SrcDN cells treated or untreated with 1 µg/ml of Doxy (72 h) using the specific anti-avian Src mAb (EC10). Representative blots of three experiments are shown.

2. EFFECTS OF KINASE ACTIVITY INHIBITION, c-Src SUPPRESSION AND SrcDN EXPRESSION ON PROLIFERATION, CELL CYCLE AND MORPHOLOGY

SFKs are involved in survival and proliferation in different cancer cells, including breast cancer (111). In this context, we previously showed that c-Src participated in the control of G1-S transition in the non-metastatic breast cancer cell line, MCF7 (41). Therefore, we performed *in vitro* proliferation assays by trypan blue exclusion method, as well as by MTT to measure the metabolic activity, in MDA-MB-231 with inhibition of Src family kinase activity, depletion of c-Src or SrcDN expression. Since inhibitors of SFKs enzymatic activity are not fully specific and can affect other tyrosine kinases, we used three SFKs selective inhibitors, Dasatinib, PP2 and SU6656. It allows to distinguish the effects caused by Src kinases activity from those produce on additional kinases activity.

2.1. Anti-proliferative effects of SFKs kinase activity inhibition with Dasatinib, PP2 and SU6656

To determine concentrations of the selective inhibitors to be used in this study, we examined the metabolic effects of Dasatinib, PP2 and SU6656 on MDA-MB-231 cells for 72h by MTT assay. As shown in Figure 8A at 100 nM Dasatinib (Das) and 5 µM PP2 and SU6656 (SU) the mitochondrial conversion of the tetrazolium salt, MTT, to its formazan product was reduced to about 55% with respect to control-treated cells (DMSO). At these concentrations of the selective inhibitors, Src activity was decreased as revealed by Western blot analysis of pY416-Src. Dasatinib reduced 90% the extent of Src phosphorylation at Y416, PP2 70% and SU6656 40%, approximately (Figure 8B).

MTT assay for shRNA-c-Src or SrcDN expression induced by Doxy (2 µg/ml or 1 µg/ml, respectively) for 72 h revealed no significant differences in metabolic activity (Figures 8C and 8D). Cell viability was studied by trypan blue exclusion test after 72h treatment at Doxy concentrations previously tested. Dasatinib and PP2 reduced proliferation by about 30% and SU6656 nearly 70% (Figure 8G). Furthermore, the number of cells positive for trypan blue was lower than 5% (data not shown), suggesting no cytotoxic effects at these concentrations. In contrast, shRNA-c-Src or SrcDN expression had no significant effect on cell proliferation (Figures 8E and 8F).

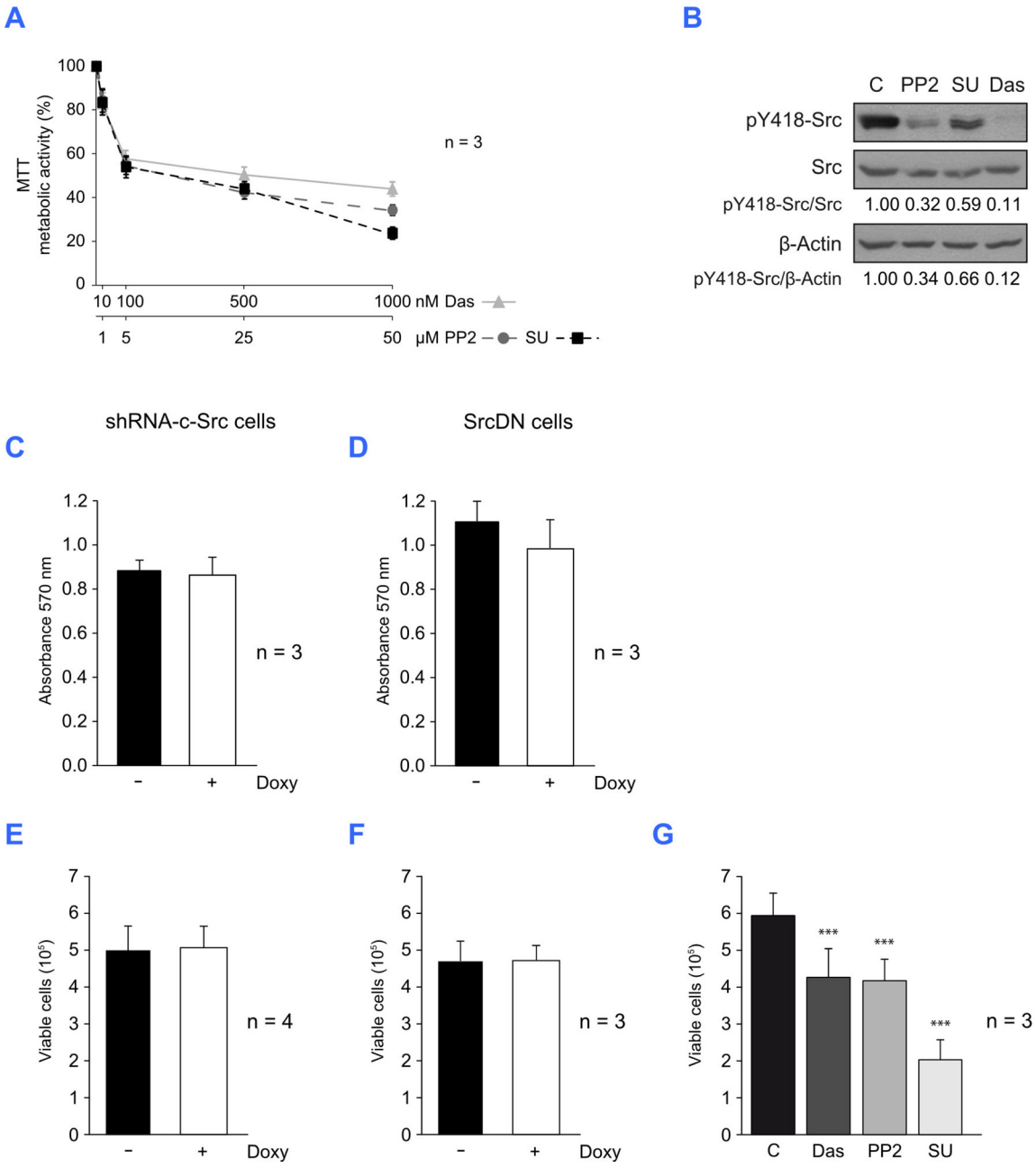

Figure 8. SFKs inhibitors cause a reduction in proliferation. (A) MTT metabolic activity of MDA-MB-231 cells treated with DMSO (control), Dasatinib, PP2 and SU6656 treated for 72 h. Results are shown as curves displaying the percentage relative to the vehicle-treated sample. (B) Whole-cell lysates treated with DMSO (1:1000), Das (100 nM), PP2 (5 µM) and SU (5 µM) for 16 h were analysed by SDS-PAGE and immunoblotting using the indicated antibodies. Representative blots of three experiments are shown. (C and D) MTT metabolic activity of cells treated 72 h with 2 µg/ml Doxy to induce shRNA-c-Src (C) or 1 µg/ml for SrcDN (D). (E, F and G) Cell viability was assessed by Trypan blue exclusion assay after 72 h treatment with DMSO, Das, PP2 and SU (as above) for MDA-MB-231 (G) or Doxy at previous concentrations (E and F). Data presented summarize the mean (±SD) of at least three independent experiments made in sextuplicate for MTT assay or triplicate for Trypan blue exclusion assay.*** $p \leq 0.001$ (Student *t*-test).

2.2. Changes in cell cycle distribution caused by SFKs inhibitors

Since cell viability was reduced by inhibition of SFKs catalytic activity, we performed a BrdU pulse-chase assay with PI labelling to determine alterations in cell cycle. The FACS analyses revealed that treatment with Dasatinib or PP2 induced accumulation of cells in G1 and reduced the fraction of cells in S and G2/M phases, as compared to control-treated cells. In contrast, the analysis of SU6656-treated cells showed an altered cell cycle, with a progressive decrease in G1 cells and increase in G2/M cells until 24 h. At this time appeared a new cell population with >4N DNA content that progressively increased with time (Figure 9A).

To confirm these results, PI labelling of cells treated with inhibitors or DMSO (control) at a longer time (72 h) was performed. Dasatinib and PP2 treated cells shown a higher proportion of G1 cells compared to 38 h treatment. However, the >4N compartment remained unaltered compared to control cells. In SU6656 treated cells, G1 and S fractions were reduced and the fraction of cells in G_2/M phases was increased, whereas the polyploid population was the most represented, about 60-70% (Figure 9B). Consistently, this compound did not inhibit DNA duplication, but it probably blocked cell cycle completion, according to the strong reduction (about 70 %) in the number of cells determined by trypan blue assay respect to control cells (Figure 8G).

The percentage of cells present in the subG1 fraction was no significant in the treatment with the inhibitors compared to control. Furthermore, no PARP degradation was observed (data not shown), suggesting that these compounds, under these experimental conditions, did not induce apoptosis.

Moreover, the increase of $p27^{Kip1}$ and the decrease of c-Myc expression provided further evidence for the G1 arrest of Dasatinib and PP2 treated cells. No modifications in $p27^{Kip1}$ or c-Myc levels were observed in cells treated with SU6656 compared to control cells (Figure 9C).

Since the SFKs inhibitors Dasatinib, PP2 and SU6656 are able to inhibit other targets, we wondered whether the effects on cell cycle could be due to the inhibition of additional kinases. To investigate this hypothesis, we performed a PI labelling to analyse cell cycle of SYF cells, fibroblasts derived from triple *c-src*, *yes* and *fyn* knockout mice (60). Analyses of cell cycle at 24 h showed no significant differences in G1 fraction between Dasatinib, PP2 or DMSO (control) treated cells. However, SU6656 provoked cell cycle alterations similar to those observed in MDA-MB-231 cells (reduction in G1 and S phases and increase in G2/M and >4N compartments) (Figure 9D).

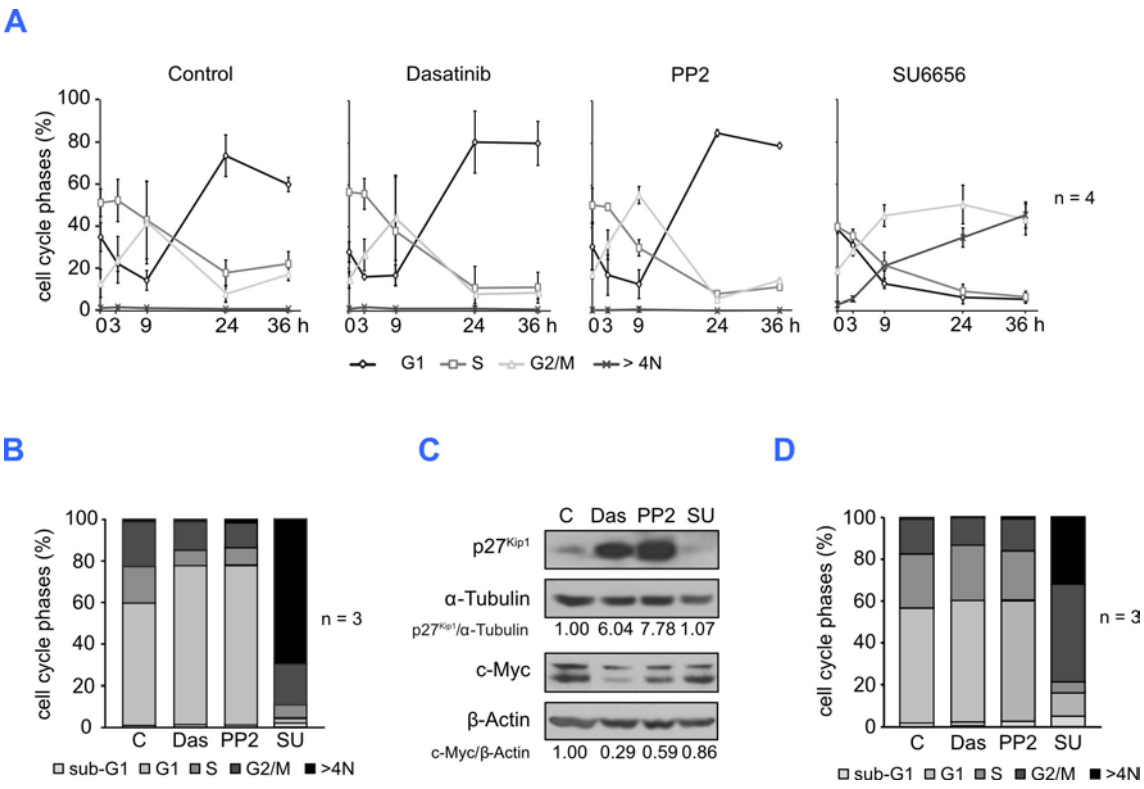

Figure 9. Effects of SFKs inhibitors on cell cycle of MDA-MB-231 and SYF cells. (A) Cell cycle analyses by pulse/chase BrdU and PI labelling of MDA-MB-231 cells treated with DMSO (control), Dasatinib (100 nM), PP2 (5 μM) and SU6656 (5 μM). Results represent the average ±SD of four independent experiments. (B) Cell cycle of MDA-MB-231 by PI labelling after 72 h inhibitors treatment. (C) Whole-cell lysates from MDA-MB-231 cells treated 24 h with DMSO (C), Das, PP2 or SU were probed for $p27^{Kip1}$ and c-Myc. Membranes were reblotted for α-tubulin and β-actin, respectively, as loading controls. Blots are representative of three independent experiments. (D) Cell cycle analyses after PI labelling of SYF cells treated 24 h with DMSO (C), Das, PP2 or SU (concentrations as above).

2.3. Effects of SU6656 on cell cycle: Aurora B kinase

Since SU6656 is a kinase inhibitor, we hypothesized that a kinase involved in regulation of mitosis could be affected. Polyploidy and enlarged cell size phenomena observed in MDA-MB-231 were similar to those detected by Giet *et al.* in distinct human tumour cell lines by inhibiting of an enzyme that belongs to the chromosome passenger protein family, Aurora B kinase (40). Besides, SU6656 has been described as an Aurora B kinase inhibitor *in vitro* (6,63). Therefore, we used a selective inhibitor of Aurora B kinase, ZM447439 (31), to compare its effects on cell cycle profile with those provoked by SU6656, used at the same concentration (5 μM). PI labelling after 24 h treatment with SU6656 or ZM447439 showed a similar pattern; a reduction in the percentage of cells in G1 and S phases and an increase in G2/M and >4N compartments compare to control cells (Figure 10A).

A canonical substrate of Aurora B kinase is serine-10 of histone H3 (31,40,100,117), then we analysed the expression of pS10-H3 by Western blot in subconfluent cultures treated with DMSO (control), ZM447439 (positive control) and SU6656 for 24 h. A reduction in pS10-H3 levels was observed in both SU6656 and ZM447439 treated cells (Figure 10B). To confirm that SU6656 directly inhibited Aurora B kinase in MDA-MB-231 we performed an *in vitro* kinase assay. Aurora B kinase was immunoprecipitated from cultures 24 h-treated with DMSO or SU6656 and incubated with 1 µg of purified histone H3 in kinase assay buffer. A strongly reduction in pS10-H3 was observed in SU6656 immune-complexes (Figure 10C). To further confirm these results DMSO, SU6656 and ZM447439 treated cells (24 h) were analysed under fluorescence microscope after staining with DAPI, α-tubulin and pS10-H3. Analysis of mitotic cells treated with SU6656 or ZM447439 shown cells with multiple spindle poles and a decreased expression of pS10-H3, compared to control (Figure 10D).

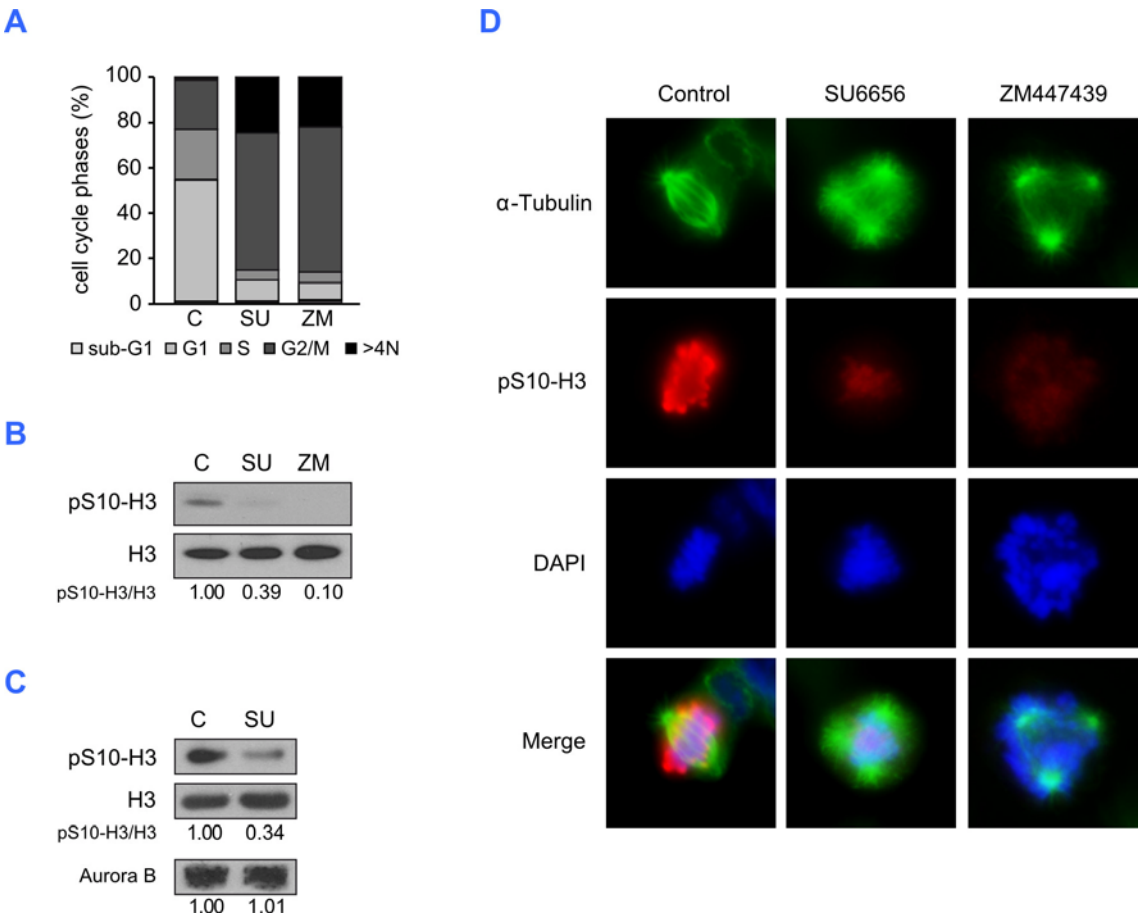

Figure 10. Comparative effects of SU6656 and ZM447439 in MDA-MB-231 cells. (A) Cell cycle analyses by PI labelling after 24 h treated with DMSO (control), SU6656 (5 μM) and ZM447439 (5 μM). (B) Immunoblot analyses of histone H3 and its phosphorylation in S10 from cells treated with DMSO (C), SU or ZM for 24 h at concentrations as above. (C) Aurora B kinase was immunoprecipitated from cultures treated with DMSO (C) or SU (5 μM) for 24 h. Immune-complexes were incubated with histone H3 in the presence or absence of SU6656 (1 μM) and ATP; the phosphorylation of S10-H3 was determined by Western blot. (D) Representative immunofluorescence micrographs of mitotic MDA-MB-231 cells. Control and SU- or ZM-treated cells for 24 h were labelled for DNA (DAPI, blue), microtubules (anti α-tubulin, green) and pS10-histone H3 (anti-pS10-H3, red).

2.4. Effects on 3D growth pattern caused by SFKs activity inhibition

Three-dimensional (3D) cultures better mimic the tumour extracellular microenviroment to study tumour cell progression. Given the effects observed on cell proliferation in two-dimensional conditions, we studied the effects of SFKs inhibition on 3D cultures. MDA-MB-231 cells were growth embedded in Matrigel in presence or absence of the selective inhibitors. After 21 day-growth in the presence of Dasatinib or PP2, colonies size decreased respect to DMSO-treated cells (control). However, SU6656 prevented colony formation inducing the appearance of enlarged cells (Figure 11A). We also tested if these compounds could affect already-formed spheres. After 21-day growth, addition of PP2 or SU6656 for further 7 days provoked no effects, however Dasatinib reduced colony size (Figure 11B).

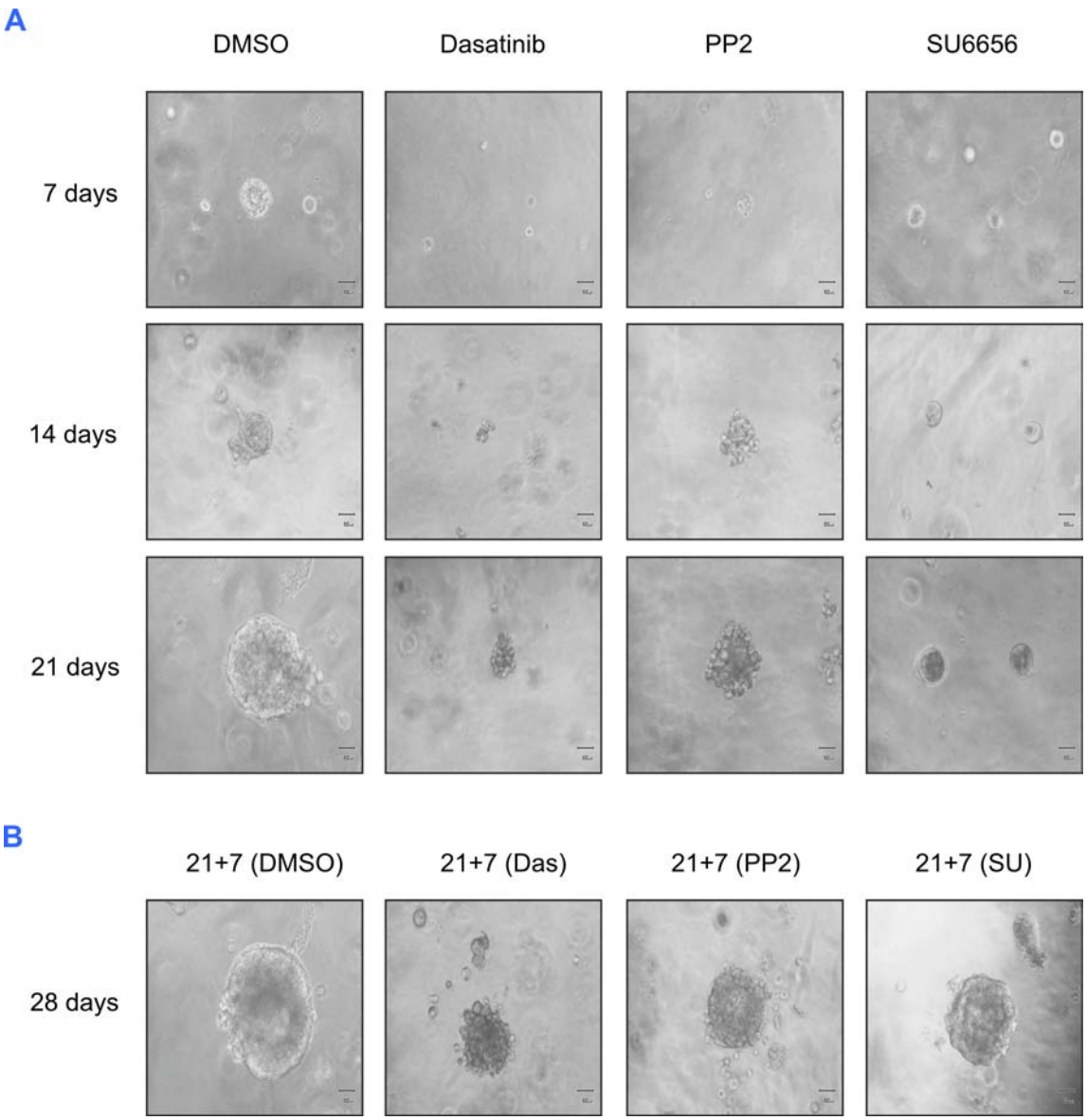

Figure 11. 3D structures of MDA-MB-231 after SFKs inhibition. (A) Representative photos from contrast-phase microscopy shown colonies at 7, 14 and 21 days growth embedded in Matrigel in presence of DMSO, Das (100 nM), PP2 or SU6656 (5 μM). (B) Effects of 7 day-inhibitor treatments after 21 days of colonies growth. Scale bar, 10 μm.

2.5. Alteration of cell morphology caused by inhibition of SFKs

Analysis of cell morphology by phase contrast microscopy showed that the inhibition of Src kinase activity for 24 h by Dasatinib produced rounded cells, meanwhile PP2 generated spindle cells and SU66565 increased cell size (Figure 12A). However, c-Src suppression or SrcDN expression did not altered cell phenotype (Figure 12B and 12C).

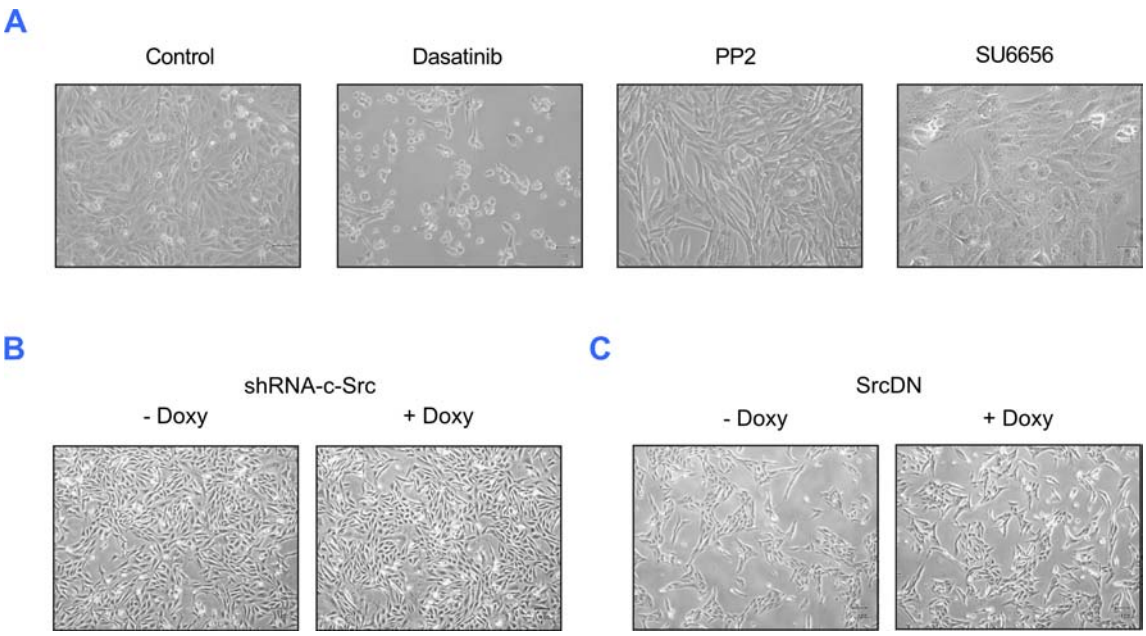

Figure 12. Analysis of morphological features of MDA-MB-231 cell cultures by phase contrast microscopy. (A) Induction of three different phenotypes in cells treated for 24 h with Dasatinib (100 nM), PP2 or SU6656 (5 μM) versus DMSO (control). Scale bar, 50 μm. (B) MDA-MB-231-shRNA-c-Src cells treated with 2 μg/ml Doxy for 72 h showed no cell shape modifications as compared to untreated cells. (C) MDA-MB-231-SrcDN cells treated with 1 μg/ml Doxy for 72 h depict no phenotypic changes. Scale bar, 100 μm.

To further characterize these changes, MDA-MB-231 grown as previously, were labelled with α-tubulin and DAPI and observed under fluorescence microscope. Dasatinib-treated cells showed partially collapsed microtubule structure defining a pseudo-spherical shape. In PP2 and SU6656-treated cells microtubule cytoskeleton was similar to control cells, although in presence of PP2 cells appeared elongated and with SU6656 cell size increased and multinucleation was induced (Figure 13A). These effects of SU6656 on cell morphology support the hypothesis that this compound blocked cell division.

To confirm this presumption, a time-lapse video microscopy of cell cultures was carried out in presence of DMSO or SU6656 for 24 h. While control cells progressed through the cell cycle, SU6656 treated cells detached from the plate and before cytokinesis occurred they re-attached giving rise to enlarged multinucleated cells (Suppl. Videos S1 and S2).

To test whether the effects on cell morphology were due to inhibition of SFKs catalytic activity, SYF cells were double-labelled with α-tubulin and DAPI. Analysis by fluorescence microscopy revealed that Dasatinib or PP2 did not provoke significant

shape changes. In contrast, SU6656 induced the appearance of enlarged and multinucleated SYF cells (Figure 13B).

Furthermore, MDA-MB-231 cells treated with SU6656 showed an increase in cell size and multinucleation similar to those provoked, by ZM447439, inhibitor of Aurora B kinase (Figure 14). These results, together with the cell cycle profile and the histone H3 phosphorylation, suggest that SU6656 inhibited cell division of MDA-MB-231 cells by inhibiting Aurora B kinase activity.

To further characterize modifications in cell shape caused by Dasatinib, PP2 and SU6656 in MDA-MB-231 cells, we analysed β-catenin and p120-catenin distribution as well as actin cytoskeleton organization by confocal microscopy. We observed β-catenin and p120-catenin relocalization to the cytoplasmic membrane in cells treated with the three compounds when compared with control cells, while total expression levels of both proteins remained unaltered (Figure 15A and 15B).

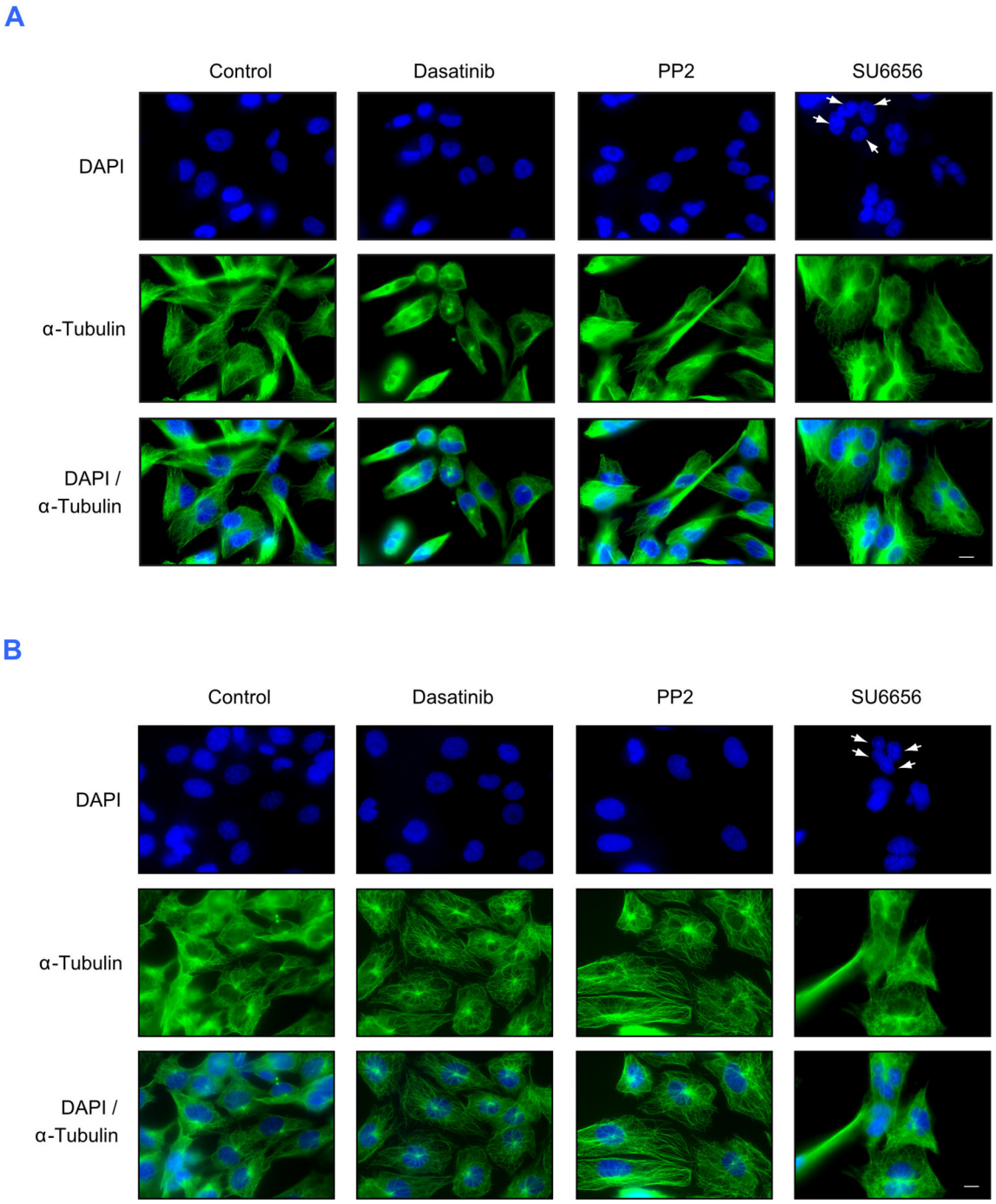

Figure 13. Morphological alterations caused by SFKs inhibitors. Representative immunofluorescence images of cultures treated with DMSO (Control), Dasatinib (100 nM), PP2 and SU6656 (5 μM) for 24 h of MDA-MB-231 cells (A) or SYF cells (B). Cells were labelled for DNA (DAPI, blue) and for microtubules (anti-α-tubulin, green). Scale bar, 10 μm. Arrows show multinucleated cells.

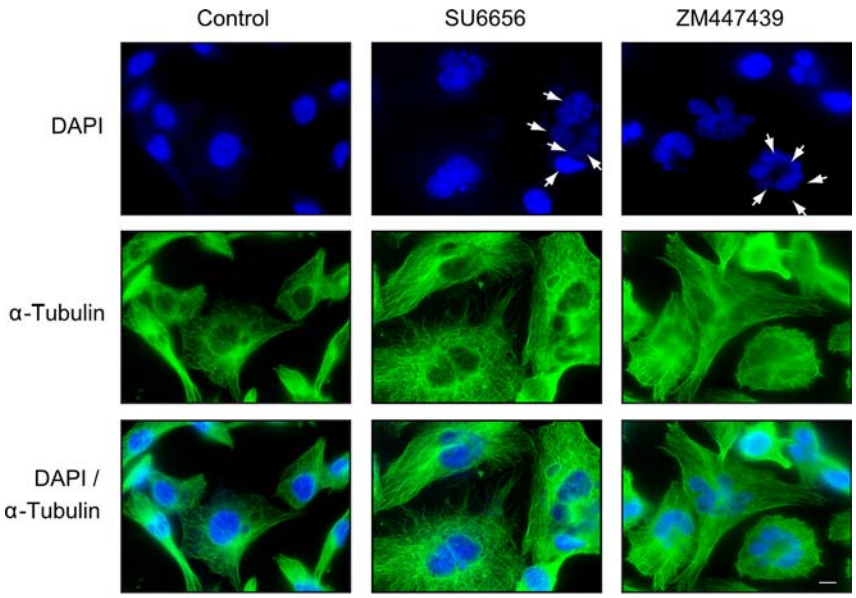

Figure 14. Comparative effects of SU6656 and ZM447439 on MDA-MB-231 cell morphology. Immunofluorescence micrographs of cells treated with DMSO (Control), SU6656 or ZM447439 (5 µM) for 24 h. Cells were labelled for DNA (DAPI, blue) and for microtubules (anti-α-tubulin, green). Scale bar, 10 µm. Arrows show multinucleated cells.

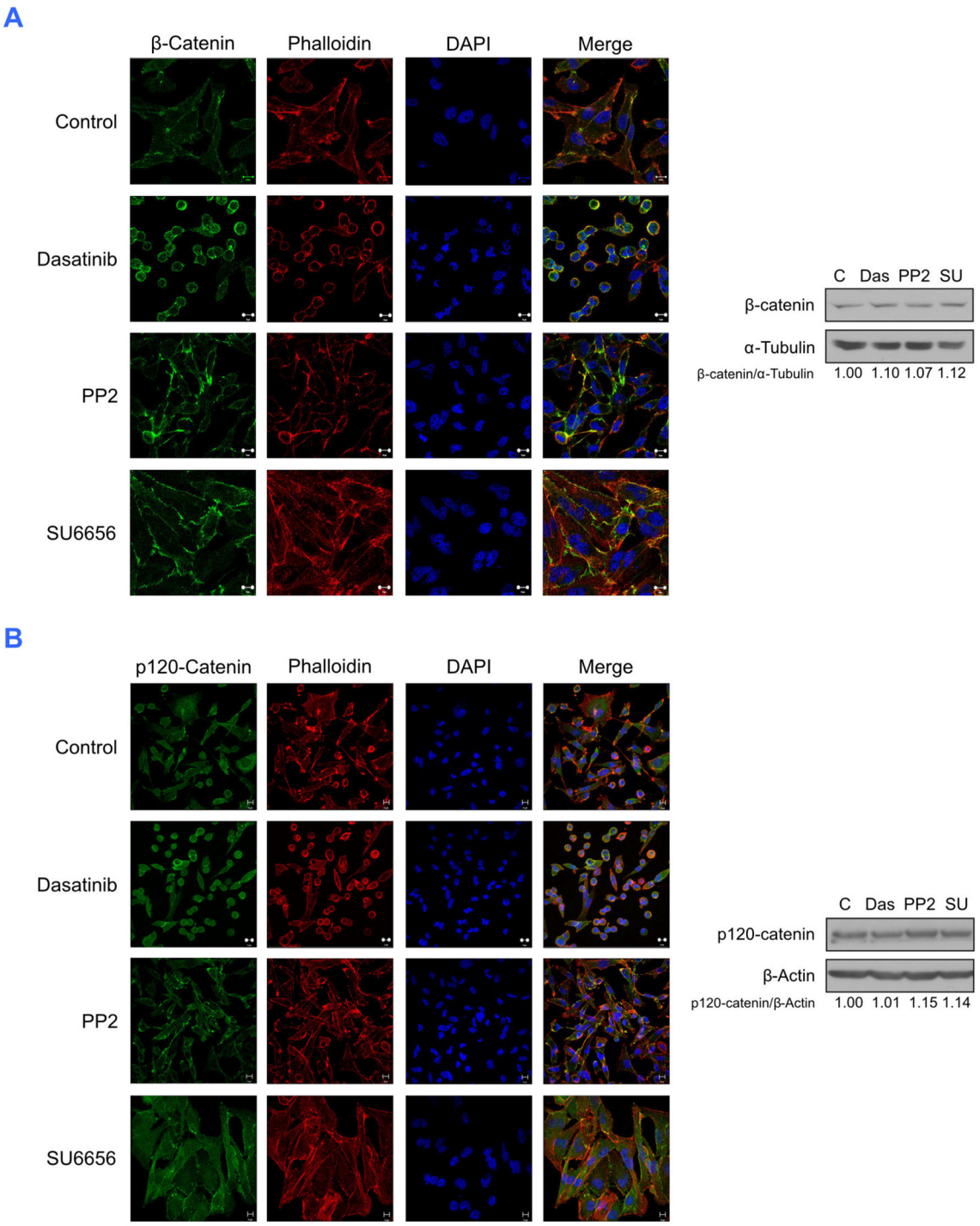

Figure 15. Immunofluorescence analysis of β-catenin and p120-catenin localization in MDA-MB-231 treated with SFKs inhibitors. Confocal microscopy analyses of cells grown in presence of DMSO (Control), Dasatinib (100nM), PP2 (5μM) or SU6656 (5μM) for 24h. Western blot analysis from total cell extracts in the same conditions for β-catenin, p120-catenin, α-tubulin and β-actin as loading controls. Representative blots are shown. (A) Cells were labelled for β-catenin (green) or p120-catenin (B), microfilaments (TRITC-labelled phalloidin, red) and DNA (DAPI, blue). Representative images captured with a 60x/1.40 NA oil objective using a Zeiss LSM 710 laser-scanning microscope are shown and correspond to the maximum intensity projections of the stacks. Scale bar, 10 μm.

2.6. Distinct gene expression profiling induced by Dasatinib, PP2 and SU6656

Since SU6656 provoked different effects compared to Dasatinib and PP2 in cell cycle regulation and morphology, we engaged analyses of gene expression profiles induced by these compounds. All studies were carried out in triplicate and RNA was used to hybridize Agilent microarrays. One of SU6656 triplicate was discarded because it did not pass quality control standards. All treatments resulted in gene expression changes. Using a statistical cut-off of adjusted P value ≤0.05, we obtained 1866 differentially expressed probes (1641 annotated sequences) after Dasatinib treatment, 21 after SU6656 (15 annotated sequences) and 16 probes after PP2 treatment. The complete list of genes is provided in Suppl. Table 1. Unsupervised hierarchical clustering of all individual data representing all selected differentially expressed sequences is shown in Figure 16A. There are two clearly defined clusters on x-axis, one for Dasatinib treatment and the other for PP2, SU6656 and control. Into this group were defined two clusters PP2 and SU66565-control. Therefore, Dasatinib defined a strong differential gene pattern compared to control. On the contrary, SU6656 gave rise a gene expression profile similar to control, except for two groups of genes. PP2 shown a gene pattern intermediate between Dasatinib and SU6656, in most cases effects were similar to Dasatinib but at lower intensity. On y-axis is shown relative intensity of the probes and two main clusters of differentially expressed genes (up-regulated and down-regulated) were defined. The comparisons of each individual treatment versus control using plot profile representations are shown in Figure 16B. These plots show expression values along different samples for probes selected as differentially expressed in the three treatment groups. The data indicated that Dasatinib produced dramatic changes of gene expression that diverged from control and SU6656 samples and to lower degree from PP2. Although only a reduced number of genes passed the statistical analysis after PP2 treatment, the plots showed that there was a great similarity between PP2 and Dasatinib. The PP2 versus Control analysis showed two main clusters, PP2-Dasatinib, and SU6656-Control. Instead, in the evaluation of SU6656 versus Control, a set of genes defined in an individual group that differed from the rest of treatments. In addition, almost all genes selected in PP2 and Dasatinib groups did not alter their expression after SU6656 treatment.

Furthermore, to study pathways of gene expression related to biological functions analysed above upon different treatments, GSEA (110) was applied using annotations from BioCarta, KEGG and Reactome pathway databases together with Src gene set previously reported (9). The analyses (Suppl. Table 2) showed that most of the pathways detected were down regulated in each treatment. Exceptionally, glycolysis

was up-regulated in Dasatinib-treated cells, while asthma and autoimmune thyroid disease were increased in PP2-treated cells. Dasatinib, PP2 and SU6656 shared some pathways, such as, pathways involved in different processes of cell cycle regulation, immune system and metabolism of lipids and lipoproteins. However, other pathways were more specific. Dasatinib and PP2 shared pathways involved in signalling by EGFR in cancer, by GPCR and by NGF. In addition of cell cycle regulation, metabolism of carbohydrates was common in PP2 and SU6656, while pathways involved in renal cell carcinoma, pancreatic, bladder and colorectal cancer and WNT signalling appeared to be specific for SU6656. Interestingly, GSEA analyses of Src gene pathway (Suppl. Table 3) showed a significant reduction upon SU6656 treatment (FDR=0.024), while PP2 and Dasatinib treatments had FDR >0.05 (0.083 and 0.193, respectively).

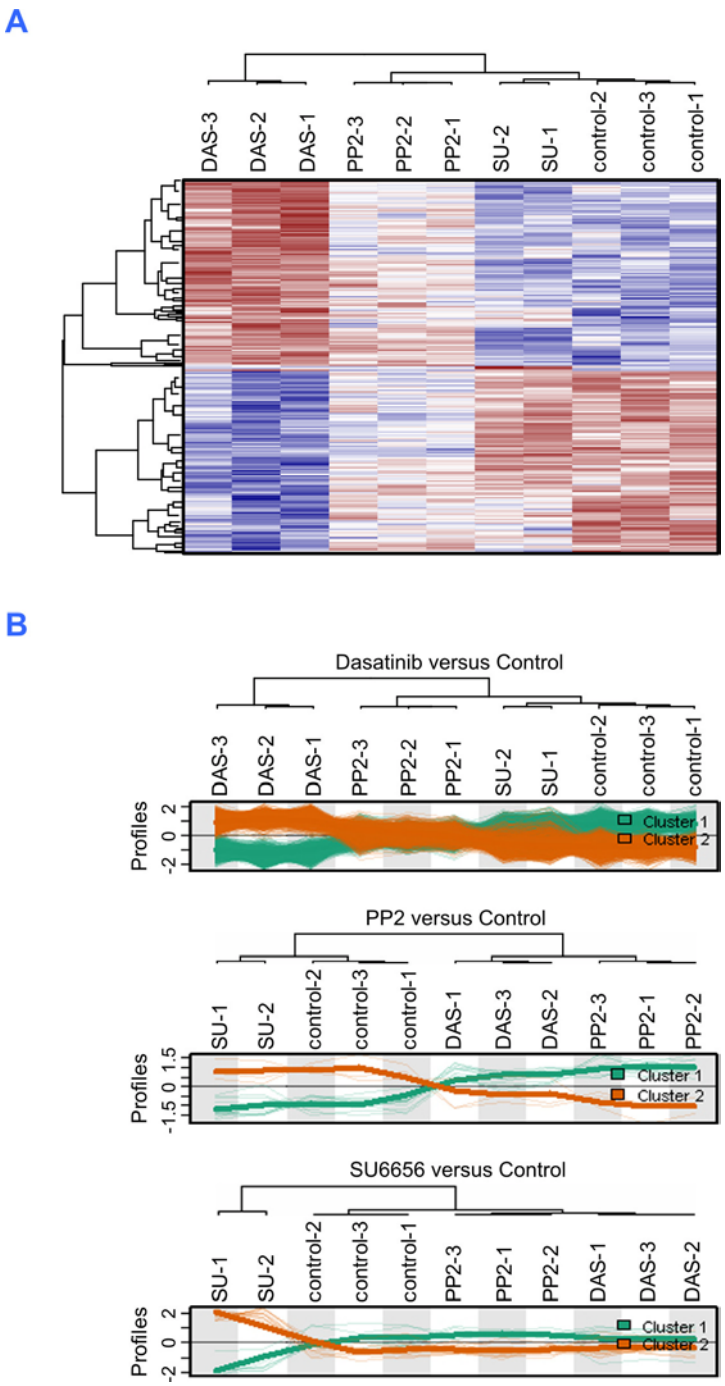

Figure 16. Gene expression profiles regulated by Dasatinib, PP2 and SU6656. (A) Hierarchical clustering (heat map) of all individual data representing the differentially expressed sequences after three treatments at P-*adjust* ≤0.05. Columns correspond to samples; row corresponds to individual probe sets. Intensities were normalized across the rows. Normalized log intensity values of probes were centred to the median value of each probe set and coloured on a range of + 2 (red) and - 2 (blue). (B) Comparisons between effects of Dasatinib, PP2 and SU6656 treatments are shown in plot profiles. Signal intensities are normalized as in heat map and expression values are coloured based on the overall pattern. For each pattern, a loess (logical weighted polynomial regression) fit line describes the overall profile of corresponding group. This tendency profile is plotted up-regulated sequences (Cluster 1,green) and down-regulated sequences (Cluster 2, orange).

3. INHIBITION OF MIGRATION AND INVASION CAUSED BY SFKs INHIBITORS, c-Src DEPLETION AND SrcDN EXPRESSION

3.1. Effects in SFKs substrates involved in migration, invasiveness and cell motility

Src Family Kinases, play key roles in regulating cell adhesion and migration by promoting changes in membrane dynamics through modulation of Rho GTPase activity (121), focal adhesion turnover (35) and actin cytoskeletal rearrangement (21,116). Src associates with focal contacts where phosphorylates Fak, p130CAS and paxillin, promoting focal adhesion turnover. Besides, caveolin 1 is an effector of Rho/ROCK signalling in the regulation of focal adhesion turnover and, its phosphorylation in tyrosine 14 is dependent on Src (57). Therefore, phosphorylation of these proteins was tested by Western blot from cells grown in presence of Dasatinib, PP2 or SU6656 for 24 h or in presence of Doxy for 72 h to induce shRNA-c-Src or SrcDN expression. A decrease in phosphorylation levels of Y925-Fak, Y118-paxillin, pYp130CAS and Y14-caveolin was observed after inhibition of the catalytic activity of SFKs and c-Src suppression. Additionally, c-Src depletion provoked a reduction in the autophosphorylation site Y397 of Fak. No modification or increased in some proteins including pY118-paxillin or pY14-caveolin was observed after SrcDN expression (data not shown). However, the inhibition of SFKs activity, as well as the expression of SrcDN (Figure 17A and 17C) or, in a lesser extent, c-Src suppression provoked a diminished phosphorylation of S473-Akt (Figure 17B). The serine/threonine kinase Akt is also involved in migration and invasion of cancer cells (132).

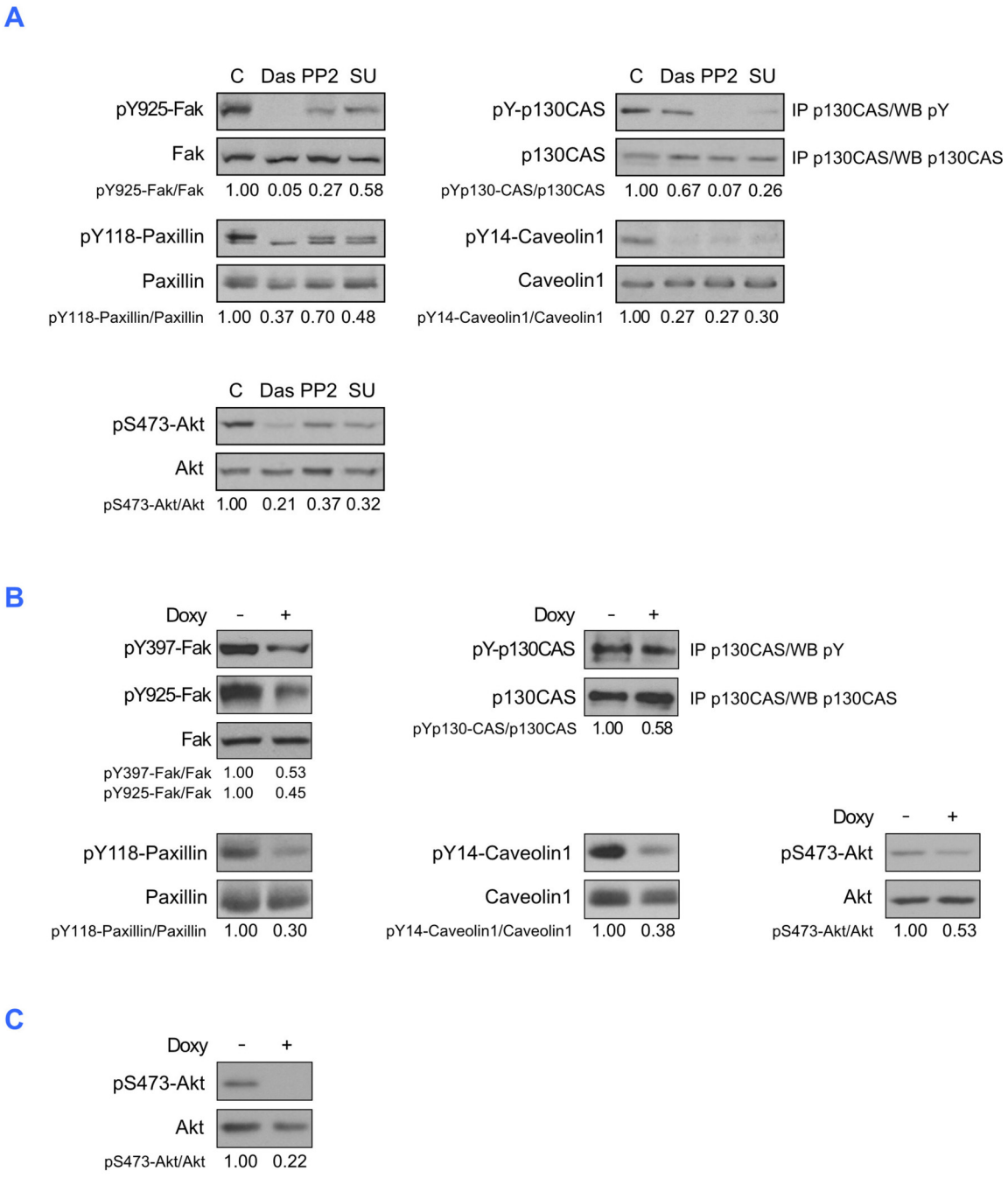

Figure 17. Inhibition of SFKs activity or c-Src depletion leads to changes in phosphorylation of focal adhesion proteins. (A) MDA-MB-231 cells were grown in presence of DMSO, Dasatinib (100 nM), PP2 or SU6656 (5 μM) for 24 h. Whole-cell extracts were analysed by Western blot analysis of pY925-Fak, pY118-paxillin, pY14-caveolin 1, total Y-phosphorylation of p130CAS and pS473-Akt. (B) MDA-MB-231-Tet-On-shRNA-c-Src cells incubated with or without 2 μg/ml Doxy for 72 h were lysed and protein extract was analysed by Western blot for proteins previously described. (C) Cell lysates from treated or untreated (1 μg/ml Doxy, 72 h) MDA-MB-231-Tet-On-SrcDN cells analysed by Western blot with anti-pS473-Akt and anti-Akt. Representative blots from three independent assays are shown.

3.2. Inhibitors of Src family kinase activity, c-Src suppression or SrcDN expression reduced cell migration

In view of the effects on phosphorylation of proteins from focal adhesion complex, we tested cell migration by performing a wound-healing assay. SFKs catalytic activity inhibition by addition of Dasatinib, PP2 or SU6656 to cultures for 20 h resulted in a highly significant reduction of migration ability as compared to control DMSO-treated cells. Dasatinib reduced migration by 75%, while PP2 and SU6656 by nearly 60% (Figure 18A). Suppression of c-Src, also inhibited cell migration although to a lower extent than SFKs selective inhibitors, 10% (Figure 18B). To confirm the low reduction in migration by shRNA-c-Src cells, we deeply analysed migration by random migration assays in subconfluent conditions. A significant reduction of mean velocity and distance travelled by c-Src depleted cells was observed as compared to Doxy-untreated cells (Figure 18C). For its part, the induction of SrcDN caused similar effects on cell migration, with a significant reduction of 23% compared to control cells (Figure 18D).

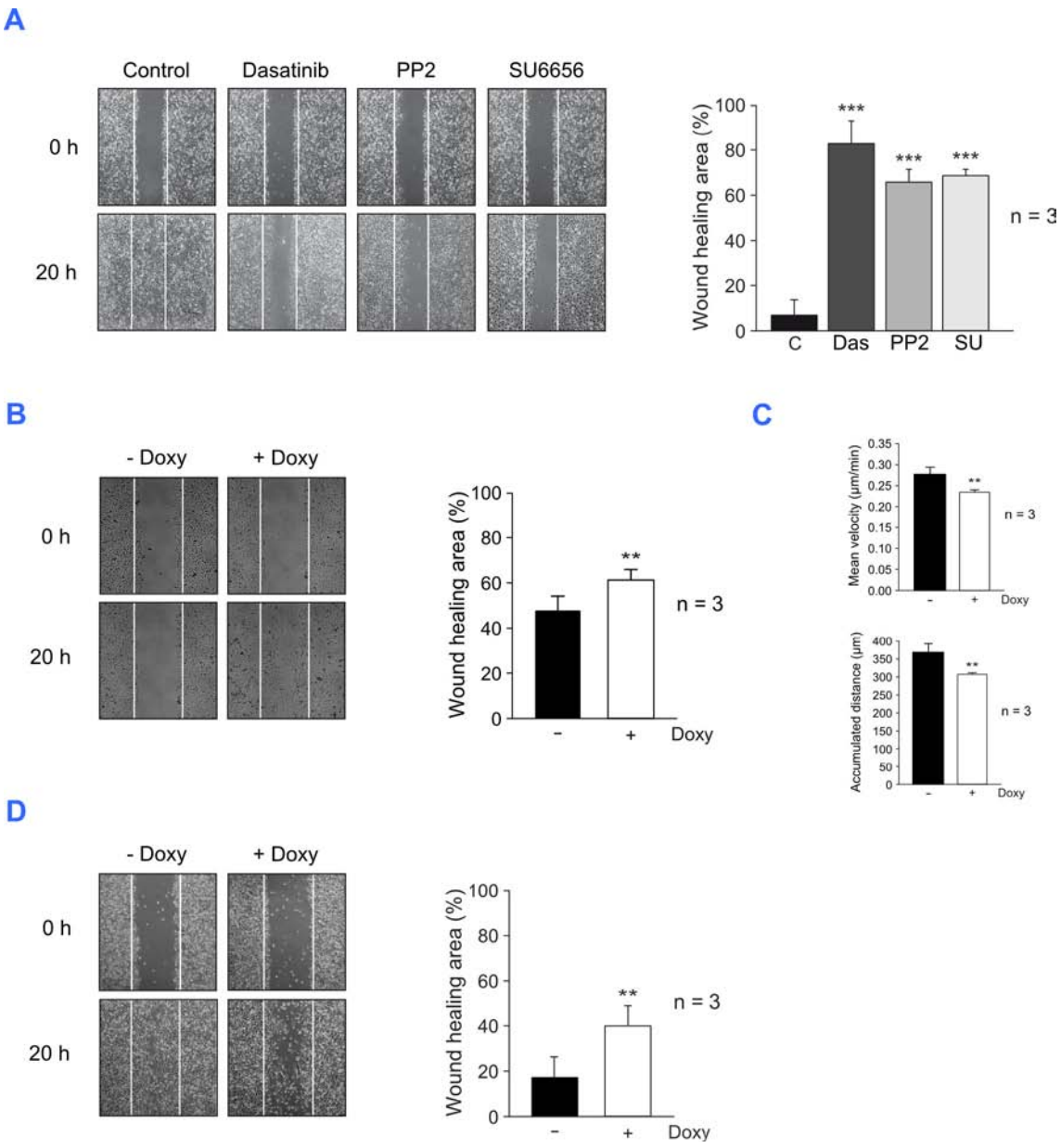

Figure 18. Inhibition of SFK activity, c-Src depletion or SrcDN expression reduced MDA-MB-231 cell migration. Wound-healing migration assay was performed to determine cell motility. Cell monolayers were wounded with a sterile 200 µl pipette tip and washed with serum-free medium. Cells were photographed at 0 h and after 20 h incubated in complete medium. Cell motility was quantified with Image J and wound healing area was calculated relative to control at 0 h (100%). (A) Representative images of wound-healing assay from MDA-MB-231 cells treated with DMSO (control), Dasatinib (100 nM), PP2 or SU6656 (5 µM) for 20 h. (B) MDA-MB-231-Tet-On-shRNA-c-Src cells in presence or absence of 2 µg/ml Doxy for 72 h, to suppress c-Src. (C) Mean velocity and accumulated distance was calculated with Image J from at least 63 c-Src depleted cells in random migration assays. (D) Wound-healing assay after SrcDN expression with 1 µg/ml Doxy. Graphs represent mean ± SD of three independent experiments. **p<0.01 and ***p<0.001 (Student *t*-test).

3.3. Invasiveness alteration by SFKs inhibition, c-Src depletion or SrcDN expression

Src family kinases are essential to form invadopodia, structures involved in ECM degradation enriched in proteases such as matrix metalloprotreases 2 and 9 (MMP-2 and MMP-9) (13,84). An *in vitro* invasion assay with Matrigel-coated transwells was carried out to determine the effects of SFKs activity inhibition, as well as, expression of shRNA-c-Src and SrcDN. A significantly reduction in cell invasion was observed after treatment with either of the three inhibitors (Figure 19A). Furthermore, c-Src suppression and SrcDN induction caused a similar effect on cell invasion with a significant reduction of 65% and 50%, respectively (Figures 19B and 19C). Cellular expression of proteases by Western blot analysis revealed that neither c-Src depletion nor SrcDN expression modified protein levels (data not shown). Therefore, we determined secreted MMP levels after shRNA-c-Src and SrcDN expression by 72 h of Doxy treatment. Immunoblot analysis revealed a reduction in MMP-2, MMP-7 and MMP-9 in both cases (Figure 19D), which is consistent with reduced cellular invasion.

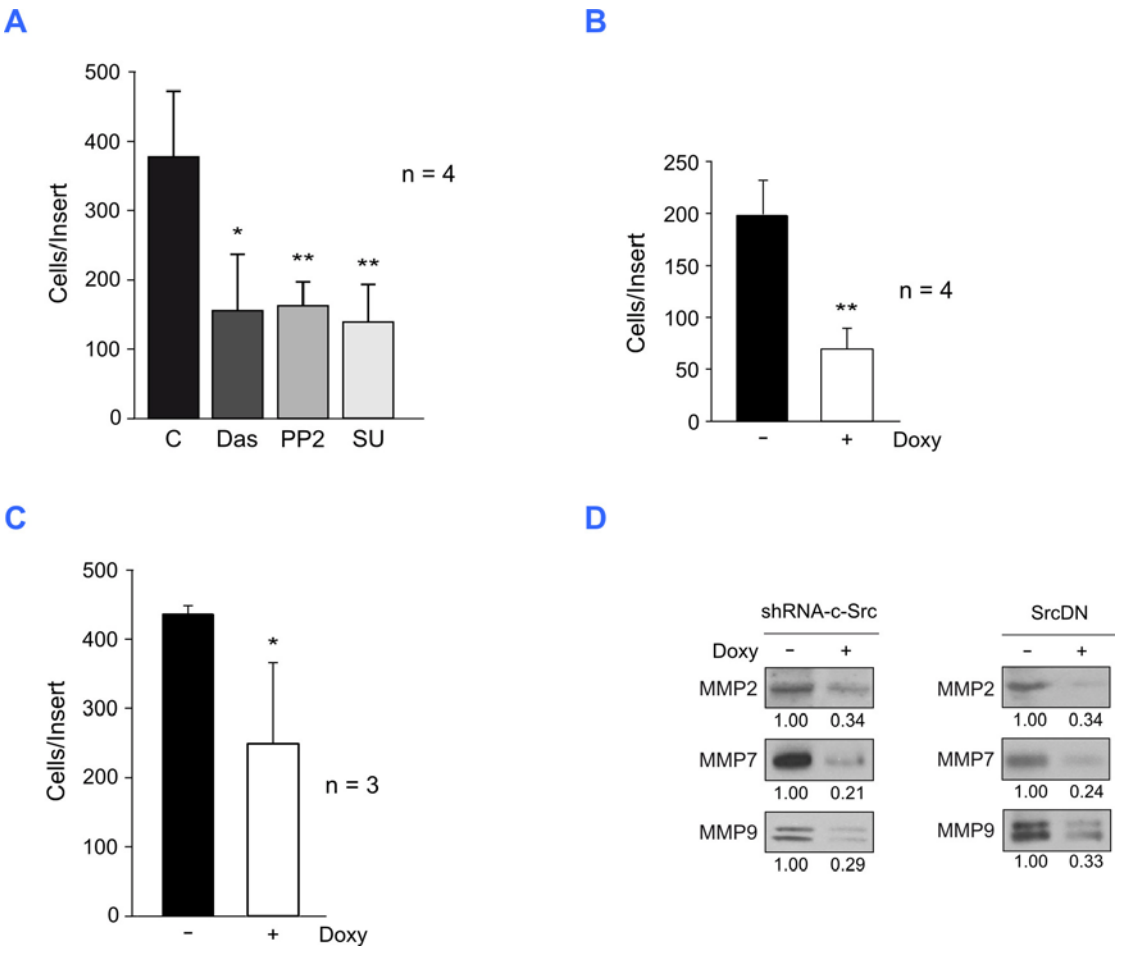

Figure 19. Reduced invasion capacity of MDA-MB-231 by inhibition of SFK activity, c-Src suppression or SrcDN expression. Boyden chamber assay was performed on Matrigel-coated transwell (8 µM membrane) by seeding 5x10^4 cells in serum-free medium. (A) After 24 h- incubation in presence of DMSO (C), Das, PP2 or SU, the lower surface of the filters were stained with DAPI and at least 4 fields/insert were counted.(B) Invasion of c-Src depleted cells after 48 h of Doxy (2 µg/ml) treatment. (C) Invasiveness of cells with induced expression of SrcDN by 1 µg/ml of Doxy for 48 h. Assays were quantified as above and the number of invasive cells were determined after 24 h. Graphs display mean ± SD of at least three independent experiments made in triplicate (*p<0.05, **p<0.01 and ***p<0.001; Student *t*-test). (D) Western blots of MMP-2, 7 and 9 from secretome extracts of cells with c-Src depletion or SrcDN expression for 72 h are shown. Representative blots from three independent experiments are shown.

3.4. shRNA-c-Src expression induced modifications in secretome

In order to determine additional proteins specifically controlled by c-Src involved in cell migration and invasion, we characterized the secretome from shRNA-c-Src cells. To this end, cell cultures were treated with Doxy (2 µg/ml, 72 h) for the last 24 h cells were grown in serum free medium and the conditioned medium was collected. These medium was spin down, labelled with iTRAQ and analysed by MALDI TOF/TOF. Protein identification and quantitation were done by using MASCOT v2.3.01 and

Phenyx v2.6 search engines. Twenty proteins differentially expressed were identified, 13 down-regulated and 7 up-regulated (Table 1). Among down-regulated proteins in Src-suppressed cells appeared Cyr61, β-2 Microglobulin (B2M), Insulin-like growth factor binding protein 4 (IGFBP4), Conective tissue growth factor (CTGF), etc. The most underexpressed protein, approximately 3.5-fold change, was Cyr61, an extracellular matrix-associated signalling protein, involved in migration, angiogenesis, as well as, tumourigenesis and breast cancer progression (68,123). We then determined cellular mRNA and protein expression levels of Cyr61 by qRT-PCR and Western blot, respectively. No differences in CCN1 levels (mRNA of Cyr61) between c-Src depleted and control cells were found. Besides, Cyr61 protein levels from total extracts resulted unaltered. However, secreted Cyr61 was reduced in c-Src depleted cells compared to control cells, according to proteomic analysis (Figure 20A). Similarly, in SrcDN induced cells, Cyr61 mRNA and protein levels were unaltered. Furthermore, Cyr61 expression was reduced in total secretome (Figure 20B). In contrast, Dasatinib and PP2 decreased Cyr61 expression in total MDA-MB-231 cell extracts compared with DMSO treated cells (control). No effects on Cyr61 expression were observed after SU6656 treatment (Figure 20C). In addition, to test if the presence of Doxy in culture medium could affect directly to Cyr61, total secretome from control and Doxy-treated MDA-MB-231 cells was collected. Proteins were precipitated with methanol/chloroform and analysed by western blot; no differences were observed in Cyr61 expression (Figure 20D).

PROTEIN AC	Description	Mascot Average Ratio Ctrl/Doxy		Phenyx Average Ratio Ctrl/Doxy	
		iTRAQ1	iTRAQ2	iTRAQ1	iTRAQ2
O00622	Protein CYR61 OS=Homo sapiens GN=CYR61 PE=1 SV=1	3.569	4.423	3.512	3.470
P61769	Beta-2-microglobulin OS=Homo sapiens GN=B2M PE=1 SV=1	1.608	1.568	1.575	1.368
P22692	Insulin-like growth factor-binding protein 4 OS=Homo sapiens GN=IGFBP4 PE=1 SV=2	1.546	1.415	1.408	1.292
P29279	Connective tissue growth factor OS=Homo sapiens GN=CTGF PE=1 SV=2	1.519	1.414	1.541	1.370
P01034	Cystatin-C OS=Homo sapiens GN=CST3 PE=1 SV=1	1.441	1.352	1.402	—
P16035	Metalloproteinase inhibitor 2 OS=Homo sapiens GN=TIMP2 PE=1 SV=2	1.440	1.459	1.426	1.438
P07996	Thrombospondin-1 OS=Homo sapiens GN=THBS1 PE=1 SV=2	1.433	1.454	1.337	1.303
P80188	Neutrophil gelatinase-associated lipocalin OS=Homo sapiens GN=LCN2 PE=1 SV=2	1.431	1.492	1.487	1.523
Q16270	Insulin-like growth factor-binding protein 7 OS=Homo sapiens GN=IGFBP7 PE=1 SV=1	1.425	1.434	1.381	1.376
Q14697	Neutral alpha-glucosidase AB OS=Homo sapiens GN=GANAB PE=1 SV=3	1.414	—	1.279	—
P04004	VTNC_HUMAN Vitronectin OS=Homo sapiens GN=VTN PE=1 SV=1	—	—	1.235	1.613
O00300	TR11B_HUMAN Tumor necrosis factor receptor superfamily member 11B OS=Homo sapiens GN=TNFRSF11B PE=1 SV=3	—	1.342	—	1.409
P07858	Cathepsin B OS=Homo sapiens GN=CTSB PE=1 SV=3	1.214	1.420	1.214	1.313
P04179	Superoxide dismutase [Mn], mitochondrial OS=Homo sapiens GN=SOD2 PE=1 SV=2	0.789	0.707	0.789	0.708
Q5QNW6	Histone H2B type 2-F OS=Homo sapiens GN=HIST2H2BF PE=1 SV=3	0.739	0.668	0.588	0.706
P29401	Transketolase OS=Homo sapiens GN=TKT PE=1 SV=3	0.707	0.678	0.767	0.848
P02768	Serum albumin OS=Homo sapiens GN=ALB PE=1 SV=2	0.580	0.630	0.624	0.655
P62805	Histone H4 OS=Homo sapiens GN=HIST1H4A PE=1 SV=2	0.569	0.609	0.567	0.647
Q71DI3	Histone H3.2 OS=Homo sapiens GN=HIST2H3A PE=1 SV=3	0.543	0.528	0.558	0.594
P0C0S8	Histone H2A type 1 OS=Homo sapiens GN=HIST1H2AG PE=1 SV=2	0.443	0.513	0.461	0.513

Table 1. Summary of secreted proteins identified by MALDI TOF/TOF. Thirteen secreted proteins were down-regulated and seven were up-regulated in shRNA-c-Src cells after Doxy treatment ($p<0.05$).

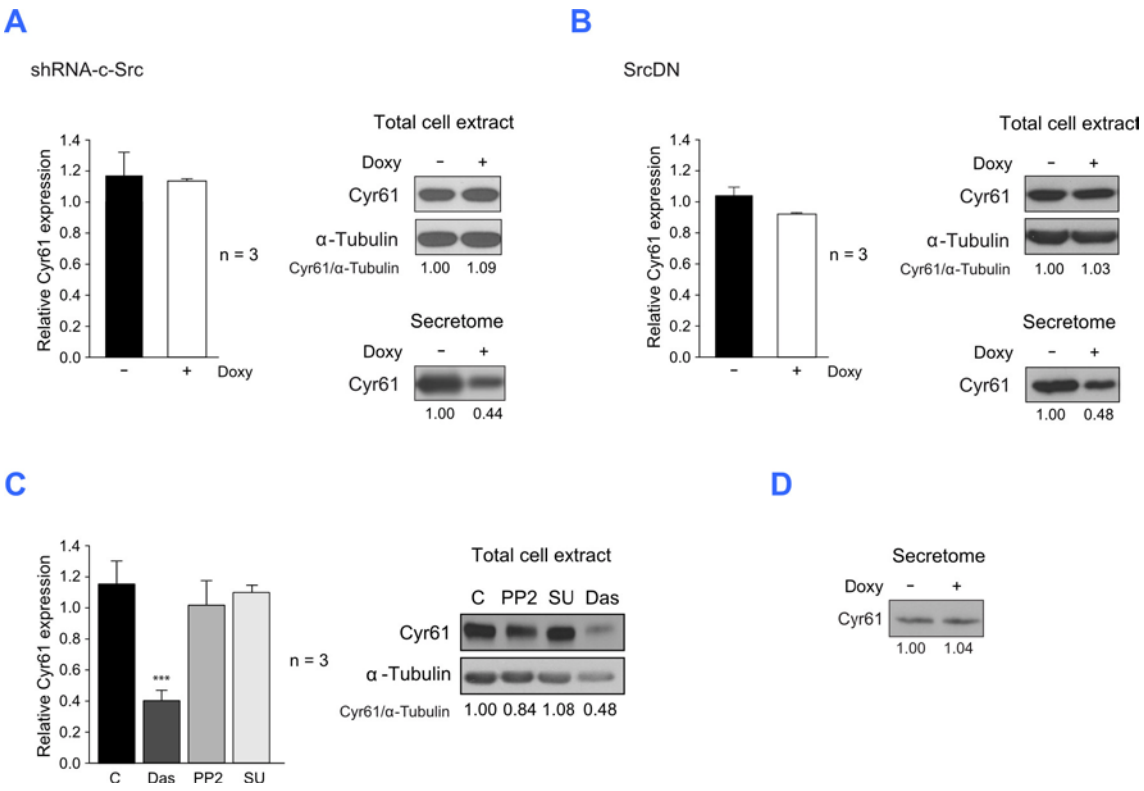

Figure 20. Cyr61 expression in secretome and whole-cell extracts . (A) MDA-MB-231-Tet-On-shRNA-c-Src cells were grown in presence or absence of 2 µg/ml Doxy for 72 h. mRNA was extracted to quantify by qRT-PCR the relative expression of CCN1 (Cyr61) using GAPDH as endogenous control. Lysates from whole-cell extracts or protein precipitated from secretome were used to determine Cyr61 protein levels by Western blot. (B) MDA-MB-231-Tet-On-SrcDN cells were treated or not with 1 µg/ml Doxy for 72 h, mRNA and Cyr61 protein levels were determined as above. Graphs depict mean ± SD of three distinct experiments. (C) MDA-MB-231 cells treated with DMSO (C), PP2, SU6656 (5 µM) or Das (100 nM) for 24 h, mRNA was determine as above and Cyr61 protein levels of total cell lysates were determined by Western blot. (D) Doxy at 2 µg/ml for 72 h had no effects on Cyr61 levels in secretome of MDA-MB-231 cells. Representative blots from at least 3 independent experiments are shown.

3.5. Colocalization of Cyr61 with secretory pathway structures in MDA-MB-231-Tet-On-shRNA-c-Src cells

Given the fact that no modifications in mRNA and intracellular protein levels of Cyr61 were observed, we hypothesized that secretory pathway could be altered. Lechner *et al.* described for first time that the human Cyr61 localized to the secretory pathway in human osteoblasts (65), so we analysed by immunofluorescence microscopy cellular distribution of gp74. This membrane glycoprotein is found mainly in cis-Golgi network but also in tubulovesicular structures and ER foci (4). The partial colocalization between Cyr61 and gp74 observed in shRNA-c-Src cells (Pearson's coefficient > 0.5) (12) was not modified by c-Src depletion (Figure 21A). Furthermore,

we studied colocalization with CD63, a tetraspanin present in late endosomes, lysosomes and exosomes (98). We found that suppression of c-Src did not affect the partial colocalization between Cyr61 and CD63 (Pearson's coefficient > 0.5) (Figure 21B). Altogether, these results suggest no alteration in Cyr61 cellular distribution upon c-Src suppression.

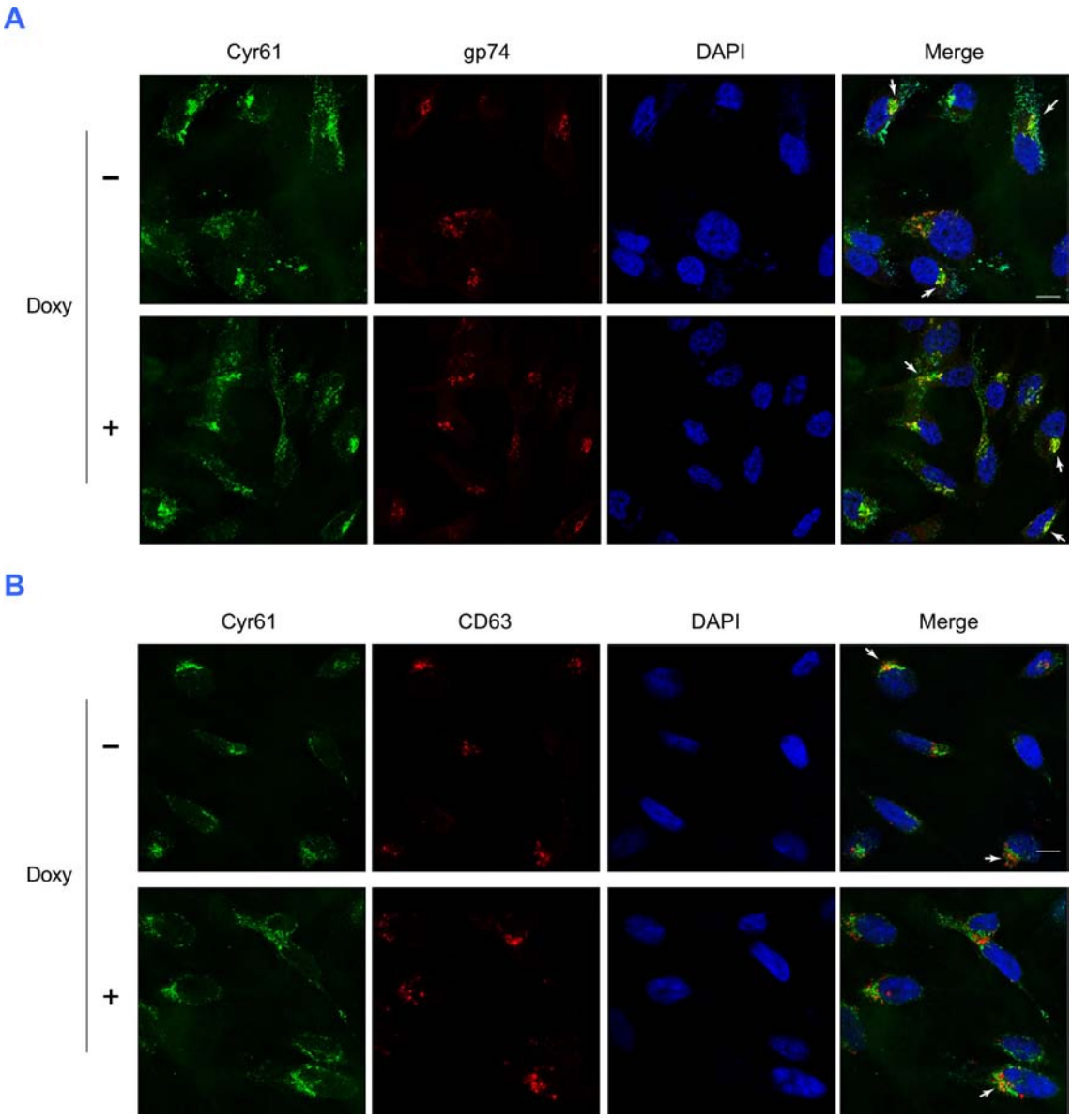

Figure 21. Confocal immunofluorescence localization of Cyr61 and gp74 or CD63. (A) Partial colocalization of Cyr61 (green) and the cis-Golgi marker, gp74 (red) in MDA-MB-231 unaltered by suppression of c-Src by 2 μg/ml of Doxy treatment for 72 h. (B) Immunofluorescence of Cyr61 (green) and the endosomal and exosomal marker, CD63 (red) in MDA-MB-231 cells with or without c-Src depletion for 72 h. Scale bar, 10 μm. Random fields are shown.

3.6. Cyr61 is associated with the exosomal fraction

Based on the relation of Cyr61 with the endosomal compartment, as a partial colocalization between Cyr61 and CD63 was observed, and since is an extracellular protein, we hypothesized that Cyr61 could be secreted in exosomes. To test this hypothesis, a differential centrifugation of secretome from shRNA-c-Src cells treated or untreated with 2 µg/ml Doxy for 72 h was carried out to obtain exosome-enriched fraction. After the last centrifugation at 100,000 xg 70 min, microvesicle pellet corresponding to exosomes (118) was resuspended in PBS-5mM EDTA. Supernatant proteins were concentrated by methanol/chloroform precipitation. Western blot analysis shown that Cyr61 was mainly found in fraction described by Thery *et al.* as exosome fraction (pellet P5) and a minor part was free in medium (supernatant S3). Furthermore, the tetraspanin CD63, described as exosome marker, was mostly detected in pellet P5. The quantification of three independent experiments by densitometry revealed a consistent reduction of Cyr61 in exosomes (Figure 22A). To confirm this finding, we transiently transfected esiRNA-Rab27a or scramble siRNA (control) in MDA-MB-231. The small GTPase Rab27a plays an essential role in exosome secretion (93). We observed a significant knockdown of Rab27a in the cells, together with a significant decreased of Cyr61 and CD63 in secretome (Figures 22B and 22C). Altogether, these findings suggest that Cyr61 is located in exosomes.

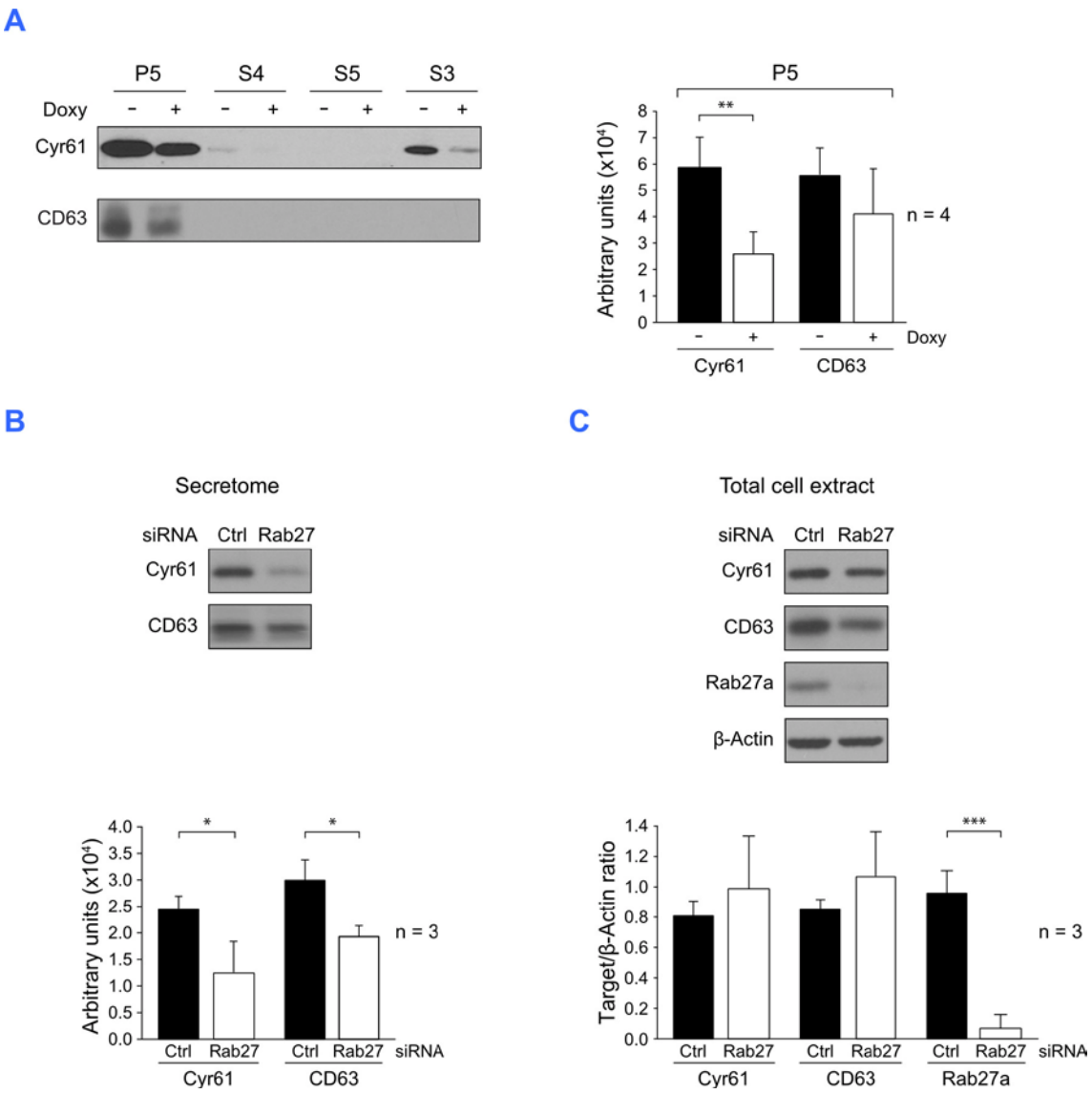

Figure 22. Localization of Cyr61 in exosomes. (A) Differential centrifugation was used to isolate exosomal fraction (P5) from secretome of control (Doxy -) or c-Src depleted (Doxy +), Supernatants 3, 4 and 5 (S3, S4 and S5) and pellet 5 (P5) were blotted with anti-Cyr61 and anti-CD63. (B and C) MDA-MB-231 cells transiently transfected with scramble siRNA or esiRNA-Rab27a for 96 h. (B) Analysis of secretome by Western Blot for Cyr61 and CD63. (C) Anti-Cyr61, anti-CD63, anti-Rab27a and β-actin, as loading control, were used to determine their expression by Western blot in total cell extracts. Graphs represent mean ± SD from densitometric analysis of the indicated proteins for three independent experiments. Results are expressed in arbitrary units (for P5 and for secretome) or as target/β-Actin ratio (for total cell extract). Student *t*-test (*p<0.05, **p<0.01 and ***p<0.001). Representative blots from 3 independent experiments are shown.

3.7. Decrease in transendothelial migration caused by c-Src depletion

Lin *et al.* described that Cyr61 contributed to transendothelial migration and intravasation in AGS human gastric carcinoma cells (68). Then, we studied whether Cyr61 reduction in secretome provoked by c-Src suppression was involved in extravasation event during metastatic cascade by performing a transendothelial migration assay *in vitro*. Control or 48 h Doxy-treated MDA-MB-231-Tet-On-shRNA-c-Src cells were seeded on top of HUVEC monolayer grown over gelatin-coated transwells. In parallel, HUVEC spontaneous migration was tested by seeding the endothelial cells alone over gelatin-coated transwells. c-Src suppression caused a significantly reduction in transendothelial migration after 22 h (Figure 23); which is consistent with the reduction of gelatinases, matrix metalloproteases 2 and 9, observed in total secretome (Figure 19D).

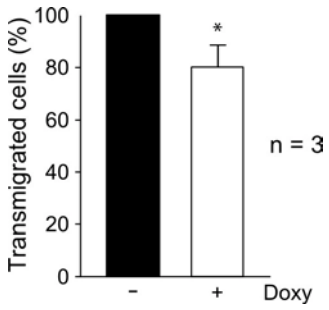

Figure 23. Reduced transendothelial migration of c-Src depleted cells. Transendothelial migration assay was performed in MDA-MB-231-Tet-On-shRNA-c-Src cells after 48 h-treatment with 2 µg/ml Doxy. $5x10^4$ cells were seeded onto HUVEC monolayer and transmigrated cells were detached and counted in a haemocytometer at 22 h. Transmigrated cells were expressed as percentage respect to control cells (100%). The average ± SD of three independent experiments made in triplicate are shown. *p<0.05 (Student t-test).

3.8. Silencing of Cyr61 reduced invasion and transendothelial migration

To determine if Cyr61 mediated the effects on invasiveness and transendothelial migration, MDA-MB-231 cells were transiently transfected with Cyr61-siRNA or scramble-siRNA (Ctrl, Figure 24A), then invasion assay in Matrigel-coated transwells and transendothelial migration assay were performed. A decrease in invasion and transendothelial migration abilities were observed in Cyr61 suppressed cells compared to control ones (Figures 24B and 24C).

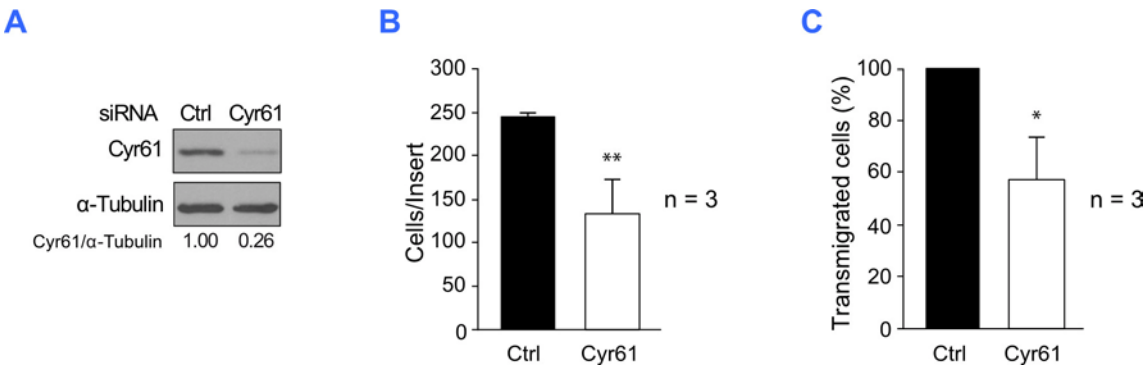

Figure 24. Silencing of Cyr61 reduces invasion and transendothelial migration. (A) Cell lysates from MDA-MB-231 cells transiently transfected with either scramble-siRNA (Ctrl) or siRNA-Cyr61 for 72 h were analysed by Western blot with anti-Cyr61 and anti-α-tubulin, as loading control. (B) Invasion assays were carried out with siRNA-Cyr61 and siRNA-control cells after 48 h transfection. The number of cells per insert was determined after DAPI stained. (C) Transendothelial migration assay was performed after 48 h siRNA-Cyr61 and siRNA-control transfection. Transfected cells were seeded onto HUVEC monolayer. At 22h transmigrated cells were detached and counted in a haemocytometer. Data are presented as percentage of siRNA-Cyr61 transmigrated cells compared to siRNA-control (100%). Graphs depict the average ± SD of three independent experiments performed in triplicate are shown. Student *t*-test (*p<0.05 and **p<0.01).

4. c-Src INVOLVEMENT IN ANCHORAGE-INDEPENDENT GROWTH AND MAMMOSPHERE FORMATION EFFICIENCY

The ability of cancer cells to proliferate in the absence of adhesion to extracellular matrix (ECM) proteins is a hallmark of transformed cells and reflects their metastatic potential, as allows tumour cells to expand, invade adjacent tissues and disseminate through the circulation to distant organs. We tested if c-Src played a role in anchorage-independent growth by performing a colony formation assay. To this end, MDA-MB-231-Tet-On-shRNA-c-Src cells were seeded in 0.3% agar in complete medium over a 0.5% agar layer, both of which in the presence or absence of Doxy. c-Src suppression significantly decreased the number of colonies detected after 20 days of growth (Figure 25A).

The ability of sphere formation is a property of cells with stemness features. To determine whether c-Src depletion modified this ability in MDA-MB-231 cells, mammosphere formation assays were performed. Sphere forming efficiency was significantly reduced by shRNA-c-Src induction after 20 days, compared to control cells (Figure 25B). In order to discard that spheres were cell aggregates instead of mammospheres formed from single cells, assays were also carried out in 96-well plate at very low cell density, obtaining comparable results (data not shown). Besides, according to Al-Hajj *et al.* $CD44^+$ $CD24^-$ / $Lineage^-$ defined a subpopulation of cells with

the highest tumourigenic potential, that could identify breast cancer stem cells (3). Then we determined the expression of these surface markers by flow cytometry. A significantly decrease in the percentage of $CD24^+$ cells was observed in samples obtained from mammospheres to those obtained from adherent cultures (Figure 25C), indicating that growth condition in a mammosphere defined medium could enrich the fraction of cells with stem-like properties. Doxy addition to mammosphere cultures slightly increased $CD24^+$ fraction, suggesting a partial involvement of c-Src in the maintenance of stem-like population. As regard CD44 expression, almost all cells, both from adherent and mammosphere cultures, were highly positive for this marker. In addition, c-Src suppression did not induce alterations in its expression pattern (Figure 25C, dot plot).

To deeply characterize stem cell population, we analysed by Western blot the expression of pluripotency markers Oct3/4, Nanog and Sox2 in lysates from mammospheres. The diminished expression observed in c-Src suppressed cells compare to control ones (Figure 25D) could be in agreement with the reduced mammosphere forming ability observed in Doxy-treated samples (Figure 25B).

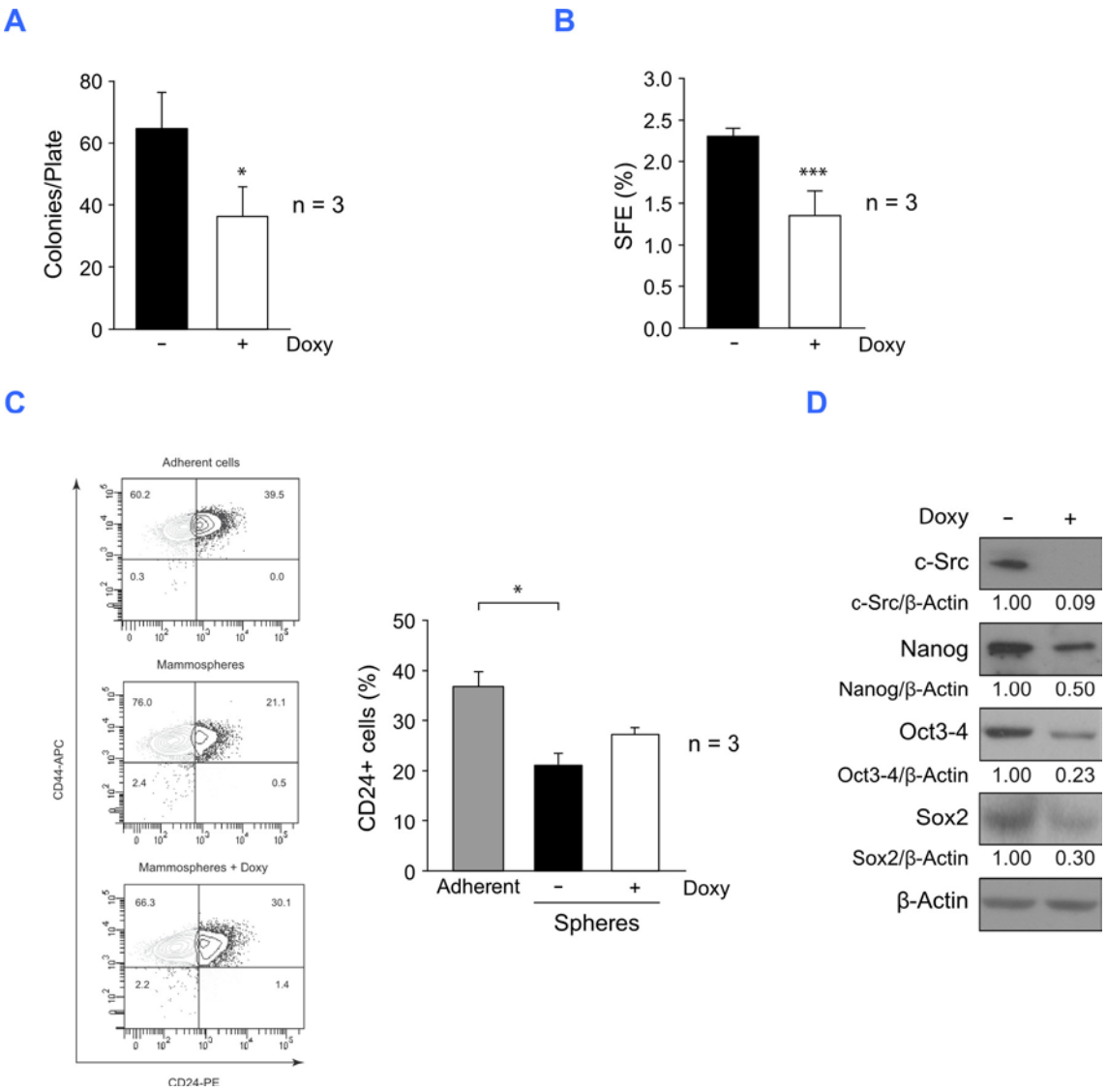

Figure 25. c-Src suppression affects colony formation in soft agar and mammospheres. (A) Average ± SD of number of colonies in soft agar with or without c-Src expression are shown. Colonies were counted after crystal violet stain in contrast-phase microscope. (B) Sphere formation efficiency (SFE) was calculated as the percentage of number of spheres ≥ 50 µm relative to number of seeded cells after 20 days growth in presence or absence of 2 µg/ml Doxy. Student t-test (***p<0.001). (C) Representative plots of CD24/CD44 labelled cells from adherent cultures and from dissociated mammospheres with or without c-Src suppression. Graph depicts mean ± SD of $CD24^+$ cells from adherent cultures or from dissociated mammospheres of three independent experiments (*p<0.05; Student *t*-test). (D) Analysis of c-Src, Nanog, Oct3-4 and Sox2 by Western blot from lysates of mammospheres treated or untreated with Doxy (as above). Representative blots from at least 3 independent experiments are shown.

DISCUSSION

Src family kinases are involved in tumour development and metastasis of cancer cells, exerting their effects on cell adhesion, migration, invasion, proliferation, differentiation and survival (37,49,106,133). Since metastasis is the main cause of cancer mortality (18) and SFKs are involved in breast cancer (36), we used a highly metastatic breast cancer cell line, MDA-MB-231, to analyse SFKs functionality. To address this aim we employed three approaches: inhibition of SFKs catalytic activity by Dasatinib, PP2 and SU6656, suppression of c-Src and expression of SrcDN. We generated conditional expression of shRNA-c-Src and SrcDN because we previously observed that constitutive suppression of c-Src was deleterious to MCF7 cells. Besides, conditional expression of SrcDN in MCF7 reduced cell proliferation (41).

1. INVOLVEMENT OF SFKs ACTIVITY IN MDA-MB-231 CELL PROLIFERATION

Given that SFKs are involved in cell proliferation, we determined cell growth by trypan blue exclusion and MTT assays. The inhibition of Src catalytic activity by three different selective inhibitors, Dasatinib, PP2 and SU6656, caused a reduction of pY418-Src and diminished proliferation of the triple-negative/basal-like breast cancer cell line, MDA-MB-231. However, no significant effects were observed on cell proliferation after c-Src suppression or SrcDN expression. This is in agreement with Brunton and collaborators work, where is shown that the expression of SrcDN or kinase defective Src (Src251) in KM12C colon epithelial cancer cell line did not alter *in vitro* or *in vivo* cell growth (14). However, in contrast to our findings, Rucci *et al*. showed a decreased in proliferation after constitutive expression of SrcDN in MDA-MB-231 cells (102).

Dasatinib and PP2 increased G1 and reduced S and G2/M cell cycle phases, together with an increase in $p27^{Kip1}$ and a reduction in c-Myc expressions. No modifications in cell cycle profiles were observed after Dasatinib or PP2 treatment on SYF fibroblasts suggesting that the effects on cell cycle are mediated by SFKs. The inhibition of G1 to S phase cell cycle transition was also detected after Dasatinib or PP2 treatment of different cell types, including MDA-MB-231, MCF7, T47D, head and neck squamous cell carcinoma, as well as, non-small cell lung cancer cell lines (56,97). Furthermore, treatment with each of the three inhibitors did not cause apoptosis, as no significant proportion of cells in subG1 phase was observed, as well as, no PARP degradation (data not shown), demonstrating that these compounds do not provoke apoptosis at the chosen concentrations. However, Dasatinib stimulated apoptosis in MDA-MB-468, by activating caspases-8 and -9, as well as, in bone sarcoma cell lines

(90,107). These observations are in contrast with our results, probably because of the dose used. Altogether these findings indicate that SFKs activity is involved in cell proliferation, by regulating G1-S transition through $p27^{Kip1}$ and c-Myc in MDA-MB-231 cell line. They are in accordance with previous results obtained in MCF7 cell line where it has been shown that SFKs are involved in G1-S progression, associated with an increase in $p27^{Kip1}$ (41).

In contrast, SU6656 provoked a progressive decrease in G1 and S phases, as well as, an increase in G2/M and >4N phases. The proportion of cells with DNA content higher than 4N increased with the time of treatment, reducing the amount of cells in the remaining phases, thus there is an accumulation of polyploid cells caused by SU6656. Besides, MTT metabolic assay can be used as a viability assay, since the transformation of tetrazolium salt into formazan only takes place in living cells with functional mitochondria. The results showed a discrepancy between trypan blue proliferation assay and MTT metabolic assay. The trypan blue assay revealed a proliferation rate of 30%, whereas metabolic activity determined by MTT assay was around 55%. It may due to cells progress through the cell cycle, duplicate organelles, including mitochondria, but they fail in cell division. Furthermore, since the effect of this inhibitor was similar in both MDA-MB-231 and SYF cells, we conclude that is not due to the inhibition of SFKs activity but to an additional kinase involved in mitosis. The main mitotic protein kinases described are Cyclin-dependent kinase 1 (Cdk1), Pole-like kinase 1 (Plk1), NIMA-related kinase 2 (Nek2) and Aurora kinases (92). The Aurora family of serine/threonine protein kinases is involved in centrosome separation and maturation, spindle assembly and stability, chromosome condensation, segregation and cytokinesis. In mammalian cells there are three members, Aurora-A, -B and –C, that are overexpressed in many types of cancers (40). Among the three Aurora kinases, Aurora-B and –C are inhibited *in vitro* by SU6656 (6). Although both Aurora kinases have similar functions, Aurora C kinase protein appears in germ cell in the testis (124), then Aurora B could be responsible for the effects caused by SU6656 in our cellular model. The use of other Aurora B kinase inhibitor, ZM447439 (31), gave rise to a cell cycle profile similar to that observed after SU6656 treatment, characterized by diminished G1 and S phases, as well as, increased G2/M and >4N phases. Furthermore, we observed that SU6656 and ZM447439 inhibited phosphorylation of the canonical substrate of Aurora B kinase, S10 of histone H3 (40,117). These findings were confirmed by immunofluorescence microscopy of mitotic MDA-MB-231 cells in presence of SU6656 or ZM447439, where a decreased staining of pS10-H3 was observed. *In vitro* kinase assay revealed a reduction of S10-H3 phosphorylation in presence of SU6656. Polyploidization and multinucleation induced by SU6656 were

also observed in SUM159 and MCF7 breast cancer cell lines (data not shown), and in leukaemic UT-7/TPO, K562 and HEL cell lines (63). The induction of these alterations both in p53 wt (MCF7) and in p53 mutant cell lines (MDA-MB-231, SUM159) indicate that the mechanism involved is p53 independent. Altogether, these findings suggest that SU6656 alters cytokinesis, as well as, previous mitotic events by inhibiting Aurora B kinase, an effect that is observed in other cell types.

GSEA analysis of gene set expression confirmed the results obtained, because the three inhibitors down-regulated pathways related to cell cycle, including DNA replication (KEGG), mitotic cell cycle, G1-S transition and DNA repair (Reactome). Interestingly, GSEA analysis also showed that SU6656 significantly reduced Src gene set expression.

Since c-Src suppression did not inhibit cell proliferation, we can suggest that c-Src is not essential in the process. Similarly, constitutive suppression of c-Src in bone-derived metastatic MDA-MB-231, BoM-1833 cells, did not alter cell proliferation (138). Interestingly, in the non-metastatic MCF7 cells, constitutive suppression of c-Src greatly reduces their proliferation (41). The immunoprecipitation of several SFKs members and the subsequent use of the pY418-Src antibody revealed that Src and Fyn were the main activated SFKs members in MDA-MB-231 (data not shown). Fyn has been associated with cell growth, particularly the expression of kinase dead Fyn reduced tumour weights in a mouse squamous cancer model (104). Lu *et al*. shown that the inhibition of Fyn and Src by Dasatinib or the knockdown by siRNA blocked EGFR-dependenty motility and tumour growth in glioblastoma (72). So, it is not strange that the catalytic activity of other SFKs members, such as Fyn, could be responsible for cell proliferation in MDA-MB-231.

Cell proliferation was not only affected in two-dimensional culture conditions, since we observed that the inhibition of Src family kinase activity decreased cell growth in three-dimensional Matrigel conditions. Particularly, Dasatinib and PP2 reduced the size of colonies, whereas SU6656 prevented their formation. Similarly to the results obtained in two-dimensional cultures, SU6656 inhibited cell division by altering cytokinesis. Addition of PP2 or SU6656 after 21 days of colony formation did not provoke any effect, whereas Dasatinib reduced colony size. These data suggest that the Src family kinase activity participates in colony development in three-dimensional cultures of MDA-MB-231 cells, and the effect of Dasatinib on colonies already formed is a side-effect caused by the inhibition of additional targets.

2. MORPHOLOGICAL ALTERATIONS AFTER SFKs ACTIVITY INHIBITION

Alterations of cell migration and invasion require dynamic reorganization of the actin cytoskeleton, which in turn can lead to a change in cell morphology. Inhibition of SFKs catalytic activity by Dasatinib, PP2 and SU6656 resulted in an altered phenotype. In contrast, c-Src suppression or SrcDN expression did not provoke significant morphological changes. Surprisingly, each compound gave rise to a different phenotype. SU6656-treated cells became enlarged and more flattened. As mentioned previously, SU6656 disrupted cytokinesis in MDA-MB-231 cells, as well as, in SYF fibroblasts, giving rise at similar shape in both cases. Besides, time-lapse imaging from SU6656-treated MDA-MB-231 cells showed that they detached from the plate to divide then reattached again without division, giving rise to enlarged cells. As SYF cells lack Src, Yes and Fyn, we can conclude that morphological alterations provoked by SU6656 occur in a Src kinase activity-independent manner.

Dasatinib caused rounded cells with a collapsed cytoskeleton, similar to the phenotype observed by Pichot and colleagues after treatment of breast cancer cells (97). Immunofluorescence micrographs of Dasatinib-treated cells showed relocalization of β-catenin and p120-catenin, as well as collapse of the actin cytoskeleton. Interestingly, expression of the thermo-sensitive LA29 v-Src in chicken fibroblasts by switching temperature, results in loss of organized actin stress fibers and focal-adhesion structures, giving rise to rounded morphology and reduced adhesiveness (38). PP2 gave rise to an elongated cell shape spindle-like phenotype caused by a lower effect over actin cytoskeleton. Besides, Dasatinib or PP2 did not significantly alter SYF morphology. Thus, altogether suggest that overactivation or inhibition of SFKs catalytic activity alters cellular morphology by disorganization of cytoskeleton as well as focal adhesions.

3. SFKs IN FIRST STEPS OF METASTASIS: MIGRATION AND INVASION

SFKs are involved in focal adhesion turnover and cytoskeleton reorganization that finally control cell motility and, in turn, cell migration and invasion. Cellular stimulation facilitates c-Src interaction with actin fibers and its movement from perinuclear region to plasma membrane, where participates in the focal adhesion complexes (35,105). Integrins link extracellular matrix to cytoskeleton through a complex of several proteins including Fak, whose autophosphorylation creates a binding site for SH2 domain of Src. Fak-Src complex phosphorylates other proteins such as p130CAS, paxillin or caveolin 1 promoting focal adhesion turnover and the movement of the cell (16,127). Inhibition

of SFKs catalytic activity by Dasatinib, PP2 and SU6656 resulted in reduction of phosphorylation of these Src-Fak substrates, and consequently a decrease in cell migration and invasion. Accordingly, Dasatinib, PP2 or SU6656 did not alter migration of SYF fibroblasts (data not shown). c-Src depletion or SrcDN also reduced cell migration. Similarly, in MCF7 cells constitutive suppression of c-Src or conditional expression of SrcDN inhibits cell migration (41). Similar findings were obtained after SrcDN constitutive expression in MDA-MB-231 cells (102). Altogether, these data suggest an essential role of the catalytic activity of SFKs, as well as, an important role of the prototypic member of SFKs, c-Src, in cell migration. Surprisingly, we did not observe a reduction in Y118-paxillin or Y14-caveolin 1 phosphorylation after SrcDN expression in MDA-MB-231, which is in contrast with observed in MCF7 cells (41) and in KM12C colon epithelial cancer cells after SrcDN expression. Furthermore, KM12C has an altered migratory phenotype after SrcDN expression, but phosphotyrosine content of Fak is increased, as well as, in SYF cells. Besides, it is shown that the SH2 domain of Src is essential for both recruitment of Src-Fak to focal adhesions and increased phosphorylation of Fak (14). Overall, these data might indicate that SrcDN in MDA-MB-231 recruits Fak to cell membrane where is constitutively associated with adhesion complexes avoiding dephosphorylation of focal adhesions proteins. Nevertheless, we observe decreased activation of Akt, measured by S473 phosphorylation, a protein involved in migration and invasion in several cancer cell types (19,59,81,95,132). SFKs inhibition, SrcDN expression and to less extent c-Src suppression reduced S473-Akt phosphorylation in MDA-MB-231. Knockdown of Abl interactor 1 (Abi1) in MDA-MB-231 cells decreases cell proliferation, migration and invasion (112,126). Wang *et al.* also found an alteration in lamellipodia formation, as well as, an alteration of PI3K/Akt pathway (126). Sun and colleagues also observed an inhibited Src-Id1-MMP-9 pathway and altered invadopodia formation, as well as, ECM degradation. Besides, PP2 treatment inhibited Src activation accompanied with a reduced Id1 expression and MMP-9 production (112).

Invasion assay revealed a similar reduction after SFKs enzymatic inhibition by Dasatinib, PP2 and SU6656. Also, c-Src suppression and SrcDN expression inhibited cell invasion. Besides, SrcDN expression or c-Src depletion reduced MMP-2, MMP-7 and MMP-9 in the secretome. Similarly, the SFKs catalytic inhibitor PH006 also inhibits MMP-2/9 and MDA-MB-231 cell invasion (75) and, in A549 and H1299 lung cancer cell lines, SU6656 inhibits expression of MMP-2/9 required for cell invasion (74). Also, in the head and neck human cancer cell lines 1483 and PCI-37a, SFKs catalytic activity is required for cell invasion (135). In MDA-MB-231 cells constitutive expression of SrcDN diminished cell invasion (102). Altogether these findings suggest that SFKs catalytic

activity is essential for invasiveness of MDA-MB-231. Furthermore, c-Src plays a key role in this process, since its suppression reduces it in a similar extent.

Several studies support our results, since Dasatinib reduces migration and invasion in TNBC cell lines MDA-MB-231 and MDA-MB-468 (122), and in SaOS-2 and U-2 OS human sarcoma cell lines, together with an inhibition of p130CAS (107). This compound also suppresses migration and invasion of human melanoma cell lines, A2058 and 1205-Lu (15). In the lung cancer cell line A549, PP2 treatment diminishes migration and invasion by approximately 50% (82).

In conclusion, MDA-MB-231 migration and invasion abilities are mediated by SFKs catalytic and scaffold functions through several pathways, including PI3K/Akt.

4. c-Src MODULATES SECRETOME OF MDA-MB-231 CELLS

The characterization of secretome in c-Src suppressed MDA-MB-231 cells resulted in 20 proteins differentially expressed; among them, 13 were down-regulated whereas 7 appeared up-regulated. Down-regulated genes include Cysteine-rich protein 61 (Cyr61), β-2-Microglobulin (B2M), Insulin-like growth factor-binding protein 4 (IGFBP4), and Connective tissue growth factor (CTGF). Among secreted up-regulated genes we found Manganese superoxide dismutase (SOD2), Transketolase (TKT), as well as, several histones, Histone H2B type 2F (HIST2H2BF), Histone H4 (HIST1H4A), Histone H3.2 (HIST2H3A), etc.

In secretome of c-Src depleted cells, down-regulation of Cyr61 by around 3.5 fold respect to control cells was confirmed by Western blot analysis. The treatment with the three selective SFKs inhibitors showed a diminished mRNA only in Dasatinib-treated cells, which is in agreement with gene expression analysis (Suppl. Table 1), as well as reduced protein levels of Cyr61, indicating a regulation of Cyr61 expression by this compound. Lai and colleagues found that cotransfection of the transcription factor TEAD with the coactivator TAZ in breast cancer cells significantly enhanced activation of Cyr61 promoter. Besides, TEAD4 has been described as the most important member of its family in TAZ-induced tumourigenesis (62). Thus, Dasatinib might regulate Cyr61 expression at transcriptional level through regulation of TEAD4, since gene expression analysis revealed down-regulation of TEAD4 in Dasatinib-treated cells, whereas it remained unaltered after PP2 or SU6656 treatment (Suppl. Table 1). PP2 caused a slight reduction of Cyr61 at protein level but not at mRNA level, which suggest post-transcriptional regulation. Since regulation of Cyr61 cellular expression by the SFKs catalytic inhibitors, Dasatinib, PP2 or SU6656 is different, and neither shRNA-c-Src nor SrcDN altered Cyr61 cellular expression, we can conclude that

control of Cyr61 cellular expression is independent of catalytic activity, c-Src or scaffold function of SFKs.

Confocal immunofluorescence microscopy analysis of Cyr61 and glycoprotein gp74, a cis Golgi marker (4), as well as Cyr61 and CD63, a marker of late endosomes, lysosomes and exosomes (34,80), show that Cyr61 is localized in secretory pathway. We observed that c-Src depletion did not change Cyr61 distribution, suggesting that c-Src may not regulate this part of the secretory pathway of Cyr61. However, c-Src depletion or SrcDN expression reduced Cyr61 in secretome, indicating that c-Src modulates the levels of secreted Cyr61.

Cyr61 involvement in metastasis is well documented. Lin and colleagues showed that the monoclonal antibody anti-Cyr61, 093G9, which inhibits Cyr61 functionality, reduced proliferation of MDA-MB-231, as well as, diminished lymph node metastasis *in vivo* (69). Besides, Cyr61 participates in metastasis of hepatocellular carcinoma and prostate cancer cells (113,134). This CCN family member mediates cell proliferation, migration, adhesion, angiogenesis and differentiation (25). Cyr61 is highly expressed in invasive and tumourigenic breast cancer cell lines, MDA-MB-231, MDA-MB-436, MDA-MB-157, T47D and BT474; whereas its expression is reduced in less tumourigenic ones, MCF7, BT-20 and ZR-57-1 (130). The ectopic expression of Cyr61 in MCF7 gave rise to oestrogen-independent growth, both in anchorage-independent and –dependent conditions. In mouse models, overexpression of Cyr61 in MCF7 cells, increases tumour growth, as well as, density of blood vessel in the tumours (123,130). Cyr61 is associated with the extracellular matrix and we found a small portion of Cyr61 as soluble-secreted protein. However, the majority of Cyr61 is released into exosomal microvesicles in breast carcinoma MDA-MB-231 cell line. Indeed, siRNA suppression of Rab27a in MDA-MB-231 cells significantly inhibited CD63 and Cyr61 in the secretome. In this context, Jenjaroenpun and co-workers determined exosomal mRNA and miRNA profiles by RNA sequencing, they found mRNA of Cyr61 in exosomes of MDA-MB-231 and MDA-MB-436 (53).

Exosomes are vesicles of endocytic origin that transfer information, such as, mRNA, miRNA and proteins to recipient cells. These microvesicles can act locally, on cancer cells and stroma to promote tumour growth, or distantly to prepare niche for cancer cell implantation and growth. Active MT1-matrix metalloprotease is secreted in exosomes to degrade type 1-collagen fibers. Invasive breast cancer cells released exosomes containing HSP90α, a chaperone that activates extracellular proteases, including MMP-2 and plasmin. Amphiregulin, EGF and TGF-α, HER ligands, are components of cancer exosomes. Furthermore, they induce angiogenesis and proteomic analysis revealed pro-angiogenic factors in their composition (46). Regarding to the modification of

metastatic niche, Peinado and colleagues showed that melanoma-derived exosomes promote metastatic niche formation through modification of bone marrow-derived cells. Besides, exosomal microvesicles from patients with metastatic melanoma have higher protein concentration. Exosomes derived from a metastatic melanoma cell line were injected in mice and later localized in lung, bone marrow, liver and spleen, common sites of melanoma metastasis. Furthermore, exosomes altered vascular permeability in the lung, that is an event in the formation of premetastatic niche (94). We observed a diminished invasive capacity in Matrigel after c-Src suppression, as well as, after transient silencing of Cyr61. Furthermore, c-Src depletion or knockdown of Cyr61 reduced transendothelial migration, which suggest that Cyr61 mediates, at least in part, the role of c-Src in invasion and extravasation. Moreover, c-Src also controls breast cancer cell dissemination by degrading the extracellular matrix, contributing to breast tumour cells extravasation.

Although the expression of secreted Cyr61 is the one most affected by c-Src suppression, we cannot exclude the contribution of other proteins, including IGFBP-4 or CTGF, in the regulation of MDA-MB-231 metastatic process.

IGFBPs modulate, activating or inhibiting, the biological activity of IGF, specifically IGFBP4 inhibits activity of Insulin-like growth factor 1 (IGF1). The cleavage of IGFBP4 by Pregnancy-associated plasma protein-A (PAPP-A) protease releases biologically active IGF (17,64). In 4T1.2 mouse mammary adenocarcinoma cells injected in an orthotopic model of breast cancer a protease-resistant IGFBP4 inhibits 4T1.2 tumour growth. Furthermore, authors suggest that it could increase tumour growth acting as a reservoir of IGF1. Nonetheless, wild-type IGFBP4 does not promote tumour growth in breast (103) whereas in other types of cancer, such as, in non-orthotopic murine models of colon and prostate cancers, IGFBP4 inhibits tumour growth (32,33). Our *in vitro* studies did not indicate an effect on cell growth, since the decrease of IGFBP4 secreted after c-Src depletion does not affect proliferation rate. Further studies are required to deeply characterize its contribution to tumourigenesis and/or metastasis in MDA-MB-231 cell line.

Xie and colleagues suggested a role for CTGF, WISP-1, as well as Cyr61, all members of the CCN family, in the progression of breast cancer. Particularly, they found that CTGF was related to stage, tumour size, lymph node metastasis and age. They observed that the 100% of primary breast cancers analysed with stage III or IV overexpressed CTGF. Furthermore, a significant correlation among CTGF, WISP-1 and Cyr61 expression was found in the primary breast cancer studied (131). MDA-MB-231 express high levels of CTGF whilst, MCF7, T47D or BT-474 express barely detectable levels. They indicate that CTGF provokes cytoskeleton rearrangement,

which affects migratory ability, through binding to integrin αvβ3. Besides they show that the prometastatic S100A4 gene is regulated by the CTGF-integrin αvβ3-Erk1/2 pathway and contributes to metastatic ability of MDA-MB-231 cells in a lung metastatic mouse model (24). Given the role of CTGF in the migration ability of breast cancer cells, we cannot exclude that its reduced levels in secretome of c-Src suppressed cells contribute to diminish the motility of MDA-MB-231 cells.

5. SFKs REGULATE ANCHORAGE-INDEPENDENT GROWTH AND SELF-RENEWAL ABILITY

Anchorage-independent colony formation is a measure of the capacity of cancer cells to escape from anoikis, and therefore to survive in absence of substrate. This characteristic is important for metastatic cells that must acquire the ability to survive in circulatory or lymphatic systems to colonize the target organs. We observed a reduction in the capacity of the MDA-MB-231 cells to form colonies in soft agar after c-Src suppression, indicating that c-Src affects survival in anchorage-independent growth conditions. SFKs catalytic activity and tropomyosin receptor kinase C (TrkC) have been implicated in the survival of the highly metastatic 4T1 mouse mammary cancer cells by using SU6656 in the colony formation assay (55). It also has been reported the involvement of c-Src enzymatic activity in anchorage-independent growth of MDA-MB-468, MCF7 and ZR-75-1 human breast cancer cell lines, as inhibitor PP1 significantly reduced the ability of these cell lines to form colonies in soft agar. Furthermore, the stable transfection of catalytically inactive c-Src into MDA-MB-468 and MCF7 reduced colony formation ability (50). Furthermore, Zheng *et al.* observed that siRNA-c-Src in MDA-MB-231, MDA-MB-435S, MDA-MB-436 and SKBR3 breast cancer cell lines diminishes colony formation in soft agar, as well as, apoptosis. Suppression of Fyn or Yes in MDA-MB-231 and MDA-MB-435S has no effect on anchorage-independent growth (139). Therefore, altogether indicates that c-Src and/or the tyrosine kinase activity of SFKs are needed for breast cancer cell growth in anchorage-independent conditions.

Among the population of breast cancer cells that are able to survive in vascular system to reach distant organ, it is believed that only a small subpopulation have the ability to form new tumours. These “tumour-initiating cells” are often termed cancer stem cells (CSCs). In acute myelogenous leukaemia, a subpopulation of leukemic cells with markers similar to normal hematopoietic stem cells was progressively enriched in clonogenic assays in non-obese diabetic/severe combined immunodeficient (NOD/SCID) mice. In this sense, Al-Hajj and colleagues described a subpopulation of

breast cancer cells, defined as $CD44^{+}$ $CD24^{-/low}$ $Lineage^{-}$, with the ability to form tumours more efficiently than other subpopulations with different phenotypes. This subpopulation seems to have properties of cancer stem cells (3). One of these properties is the self-renewal which allows the maintenance of stem cell population. Cancer cells have been demonstrated to possess this ability by serial tumour transplantation and sphere-formation assays (54,115). We observed that c-Src suppression significantly reduced the sphere forming efficiency of MDA-MB-231 cells, affecting the self-renewal of breast cancer stem cells. Furthermore, cells from mammospheres exhibited a significantly decrease of $CD24^{+}$ fraction cells compared to adherent cells, confirming that the spheroids are enriched in breast cancer stem or progenitor cells. Conversely, mammospheres from c-Src depleted cells showed a slight increase of $CD24^{+}$ cell percentage, although it was no significant. These data suggest that c-Src is essential to maintain the tumourigenic subpopulation in breast cancer cells.

It has been demonstrated that the transcription factors, Oct3/4, Nanog and Sox2 regulate and maintain the self-renewal and pluripotency of embryonic stem cells (7). They are involved in the development and malignant progression of various types of tumours. Ling *et al*. shown the expression of these pluripotency-associated transcription factors in three human breast cancer cell lines, MDA-MB-231 cells expressed high levels of Oct3/4 and low levels of Nanog and Sox2 compared to MCF7 and T47D cell lines (70). The knockdown of Sox2 in MCF7 decreased cell proliferation and tumour growth (26). In a study of 226 breast tumours biopsies, Rodriguez-Pinilla and collaborators found that Sox2 expression was higher in basal-like as compared to luminal or $HER2^{+}$ tumours (101). Down-regulation of Nanog inhibits breast, prostate and colon tumour development and the prostate cancer stem/progenitor cell population is enriched in Nanog (54). In bladder cancer higher Oct3/4 expression correlates with tumour progression and metastasis (20). Gidekel and colleagues showed that Oct3/4 sets the oncogenic potential of germ-cell tumours and acted in a dose-dependent manner (39). It is notable to point out the reduction in the expression of pluripotency markers Oct3/4, Nanog and Sox2 observed in mammospheres of MDA-MB-231 after c-Src suppression; indicating that c-Src is involved in the self-renewal ability of breast cancer stem cells *in vitro* by regulating the pluripotency-associated transcription factors Oct3/4, Nanog and Sox2.

CONCLUSIONS / CONCLUSIONES

1- The use of Dasatinib and PP2 revealed that SFKs catalytic activity is essential for MDA-MB-231 proliferation, since controls G1-S transition by regulating $p27^{Kip1}$ and c-Myc expressions. However, SU6656 provoked multinucleated polyploid cells affecting Aurora B kinase activity, which regulates cytokinesis. This effect is independent of Src family kinase activity and is common to several breast cancer cell lines.

2- Migration and invasion of MDA-MB-231 cells requires the kinase activity of SFKs, where c-Src plays an important role. These effects are mediated by phosphorylation of Y925-Fak, p130CAS, Y118-paxillin and Y14-caveolin 1, required for focal adhesion turnover, and cell motility. Furthermore, c-Src also controls secretion of matrix metralloproteases, MMP-2, MMP-7 and MMP-9 that degrade the components of extracellular matrix and therefore are important for cell invasive capacity.

3- c-Src also modulates the secretion of proteins involved in breast cancer progression or metastasis, including Cyr61, IGFBP4 and CTGF. Furthermore, we found a new exosomal protein, Cyr61, involved in invasion and transedothelial migration processes of MDA-MB-231 cells.

4- c-Src plays a key role in the anchorage-independent growth of MDA-MB-231 cells, which determines their ability to survive in absence of substrate, a fundamental step for the metastatic cascade.

5- c-Src is required to maintain the breast cancer stem/progenitor cell subpopulation by regulating the expression of pluripotency-associated transcription factors Oct3/4, Nanog and Sox2.

1- El uso de Dasatinib y PP2 reveló que la actividad de las SFKs es esencial para la proliferación celular, ya que controla la transición G1-S, regulando la expresión de $p27^{Kip1}$ y c-Myc. Sin embargo, SU6656 dio lugar a células poliploides multinucleadas al afectar a la actividad de Aurora B quinasa, que regula la citocinesis. Este efecto es independiente de la actividad quinasa de la familia Src y es común a varias líneas celulares de cáncer de mama.

2- La migración e invasividad de las células MDA-MB-231, necesita la actividad quinasa de las SFKs, donde c-Src juega un papel importante. Estos efectos están mediados por la fosforilación de Y925-Fak, p130CAS, Y118-paxilina y Y14-caveolina 1, las cuales son necesarias para el recambio de las adhesiones focales, y la motilidad celular. Además, c-Src también controla la secreción de las metaloproteasas de matriz, MMP-2, MMP-7 y MMP-9 que degradan componentes de la matriz extracelular y por tanto, son importantes para la capacidad celular invasiva.

3- c-Src también modula la secreción de proteínas implicadas en la progresión o la metástasis del cáncer de mama, incluyendo, Cyr61, IGFBP4 y CTGF. Además, encontramos una nueva proteína exosomal, Cyr61, implicada en los procesos de invasividad y migración transendotelial de las células MDA-MB-231.

4- c-Src tiene un papel importante en el crecimiento independiente de anclaje de las células MDA-MB-231, lo que determina su habilidad para sobrevivir en ausencia de sustrato, un paso fundamental para la cascada metastásica.

5- c-Src es necesario para mantener la subpoblación de células troncales/progenitoras de cáncer de mama mediante la regulación de la expresión de los factores de transcripción asociados a pluripotencia, Oct3/4, Nanog y Sox2.

REFERENCES

1. Acosta, J.J., R.M. Munoz, L. Gonzalez, A. Subtil-Rodriguez, M.A. Dominguez-Caceres, J.M. Garcia-Martinez, A. Calcabrini, I. Lazaro-Trueba, and J. Martín-Pérez. 2003. **Src mediates PRL-dependent proliferation of T47D and MCF7 cells via the activation of Fak/Erk1/2 and PI3K pathways**. *Mol Endocrinol*. 17:2268-2282.
2. Adamo, B., and C.K. Anders. 2011. **Stratifying triple-negative breast cancer: which definition(s) to use?** *Breast Cancer Res*. 13:105.
3. Al-Hajj, M., M.S. Wicha, A. Benito-Hernandez, S.J. Morrison, and M.F. Clarke. 2003. **Prospective identification of tumorigenic breast cancer cells**. *Proc Natl Acad Sci U S A*. 100:3983-3988.
4. Alcalde, J., G. Egea, and I.V. Sandoval. 1994. **gp74 a membrane glycoprotein of the cis-Golgi network that cycles through the endoplasmic reticulum and intermediate compartment**. *J Cell Biol*. 124:649-665.
5. Araujo, J., and C. Logothetis. 2010. **Dasatinib: a potent SRC inhibitor in clinical development for the treatment of solid tumors**. *Cancer Treat Rev*. 36:492-500.
6. Bain, J., L. Plater, M. Elliott, N. Shpiro, C.J. Hastie, H. McLauchlan, I. Klevernic, J.S. Arthur, D.R. Alessi, and P. Cohen. 2007. **The selectivity of protein kinase inhibitors: a further update**. *Biochem J*. 408:297-315.
7. Ben-Porath, I., M.W. Thomson, V.J. Carey, R. Ge, G.W. Bell, A. Regev, and R.A. Weinberg. 2008. **An embryonic stem cell-like gene expression signature in poorly differentiated aggressive human tumors**. *Nat Genet*. 40:499-507.
8. Benjamini, Y., and Y. Hochberg. 1995. **Controlling the False Discovery Rate: A Practical and Powerful Approach to Multiple Testing**. *J R Stat Soc Ser B* 57:289-300.
9. Bild, A.H., A. Potti, and J.R. Nevins. 2006. **Linking oncogenic pathways with therapeutic opportunities**. *Nat Rev Cancer*. 6:735-741.
10. Bjorge, J.D., A. Jakymiw, and D.J. Fujita. 2000. **Selected glimpses into the activation and function of src kinase**. *Oncogene*. 19:5620-5635.
11. Blake, R.A., M.A. Broome, X. Liu, J. Wu, M. Gishizky, L. Sun, and S.A. Courtneidge. 2000. **SU6656, a selective src family kinase inhibitor, used To probe growth factor signaling**. *Mol Cell Biol*. 20:9018-9027.
12. Bolte, S., and F.P. Cordelieres. 2006. **A guided tour into subcellular colocalization analysis in light microscopy**. *Journal of microscopy*. 224:213-232.
13. Bourguignon, L.Y., Z. Gunja-Smith, N. Iida, H.B. Zhu, L.J. Young, W.J. Muller, and R.D. Cardiff. 1998. **CD44v(3,8-10) is involved in cytoskeleton-mediated tumor cell migration and matrix metalloproteinase (MMP-9) association in metastatic breast cancer cells**. *J Cell Physiol*. 176:206-215.

14. Brunton, V.G., E. Avizienyte, V.J. Fincham, B. Serrels, C.A. Metcalf, 3rd, T.K. Sawyer, and M.C. Frame. 2005. **Identification of Src-specific phosphorylation site on focal adhesion kinase: dissection of the role of Src SH2 and catalytic functions and their consequences for tumor cell behavior**. *Cancer Res*. 65:1335-1342.

15. Buettner, R., T. Mesa, A. Vultur, F. Lee, and R. Jove. 2008. **Inhibition of Src family kinases with dasatinib blocks migration and invasion of human melanoma cells**. *Mol Cancer Res*. 6:1766-1774.

16. Carragher, N.O., and M.C. Frame. 2004. **Focal adhesion and actin dynamics: a place where kinases and proteases meet to promote invasion**. *Trends Cell Biol*. 14:241-249.

17. Conover, C.A., S.K. Durham, J. Zapf, F.R. Masiarz, and M.C. Kiefer. 1995. **Cleavage analysis of insulin-like growth factor (IGF)-dependent IGF-binding protein-4 proteolysis and expression of protease-resistant IGF-binding protein-4 mutants**. *J Biol Chem*. 270:4395-4400.

18. Chambers, A.F., A.C. Groom, and I.C. MacDonald. 2002. **Dissemination and growth of cancer cells in metastatic sites**. *Nat Rev Cancer*. 2:563-572.

19. Chandrasekar, N., S. Mohanam, M. Gujrati, W.C. Olivero, D.H. Dinh, and J.S. Rao. 2003. **Downregulation of uPA inhibits migration and PI3k/Akt signaling in glioblastoma cells**. *Oncogene*. 22:392-400.

20. Chang, C.C., G.S. Shieh, P. Wu, C.C. Lin, A.L. Shiau, and C.L. Wu. 2008. **Oct-3/4 expression reflects tumor progression and regulates motility of bladder cancer cells**. *Cancer Res*. 68:6281-6291.

21. Chang, J.H., S. Gill, J. Settleman, and S.J. Parsons. 1995. **c-Src regulates the simultaneous rearrangement of actin cytoskeleton, p190RhoGAP, and p120RasGAP following epidermal growth factor stimulation**. *J Cell Biol*. 130:355-368.

22. Chatterjee, S.J., and L. McCaffrey. 2014. **Emerging role of cell polarity proteins in breast cancer progression and metastasis**. *Breast Cancer (Dove Med Press)*. 6:15-27.

23. Chavez, K.J., S.V. Garimella, and S. Lipkowitz. 2010. **Triple negative breast cancer cell lines: one tool in the search for better treatment of triple negative breast cancer**. *Breast disease*. 32:35-48.

24. Chen, P.S., M.Y. Wang, S.N. Wu, J.L. Su, C.C. Hong, S.E. Chuang, M.W. Chen, K.T. Hua, Y.L. Wu, S.T. Cha, M.S. Babu, C.N. Chen, P.H. Lee, K.J. Chang, and M.L. Kuo. 2007. **CTGF enhances the motility of breast cancer cells via an integrin-{alpha}vbeta3-ERK1/2-dependent S100A4-upregulated pathway**. *J Cell Sci*. 120:2053-2065.

25. Chen, Y., and X.Y. Du. 2007. **Functional properties and intracellular signaling of CCN1/Cyr61**. *Journal of cellular biochemistry*. 100:1337-1345.

26. Chen, Y., L. Shi, L. Zhang, R. Li, J. Liang, W. Yu, L. Sun, X. Yang, Y. Wang, Y. Zhang, and Y. Shang. 2008. **The molecular mechanism governing the oncogenic potential of SOX2 in breast cancer**. *J Biol Chem*. 283:17969-17978.

27. Chu, I., A. Arnaout, S. Loiseau, J. Sun, A. Seth, C. McMahon, K. Chun, B. Hennessy, G.B. Mills, Z. Nawaz, and J.M. Slingerland. 2007. **Src promotes estrogen-dependent estrogen receptor alpha proteolysis in human breast cancer**. *J Clin Invest*. 117:2205-2215.

28. Chu, I., J. Sun, A. Arnaout, H. Kahn, W. Hanna, S. Narod, P. Sun, C.K. Tan, L. Hengst, and J. Slingerland. 2007. **p27 phosphorylation by Src regulates inhibition of cyclin E-Cdk2**. *Cell*. 128:281-294.

29. Desgrosellier, J.S., L.A. Barnes, D.J. Shields, M. Huang, S.K. Lau, N. Prevost, D. Tarin, S.J. Shattil, and D.A. Cheresh. 2009. **An integrin alpha(v)beta(3)-c-Src oncogenic unit promotes anchorage-independence and tumor progression**. *Nat Med*. 15:1163-1169.

30. Dimri, M., M. Naramura, L. Duan, J. Chen, C. Ortega-Cava, G. Chen, R. Goswami, N. Fernandes, Q. Gao, G.P. Dimri, V. Band, and H. Band. 2007. **Modeling breast cancer-associated c-Src and EGFR overexpression in human MECs: c-Src and EGFR cooperatively promote aberrant three-dimensional acinar structure and invasive behavior**. *Cancer Res*. 67:4164-4172.

31. Ditchfield, C., V.L. Johnson, A. Tighe, R. Ellston, C. Haworth, T. Johnson, A. Mortlock, N. Keen, and S.S. Taylor. 2003. **Aurora B couples chromosome alignment with anaphase by targeting BubR1, Mad2, and Cenp-E to kinetochores**. *J Cell Biol*. 161:267-280.

32. Durai, R., M. Davies, W. Yang, S.Y. Yang, A. Seifalian, G. Goldspink, and M. Winslet. 2006. **Biology of insulin-like growth factor binding protein-4 and its role in cancer (review)**. *International journal of oncology*. 28:1317-1325.

33. Durai, R., S.Y. Yang, K.M. Sales, A.M. Seifalian, G. Goldspink, and M.C. Winslet. 2007. **Insulin-like growth factor binding protein-4 gene therapy increases apoptosis by altering Bcl-2 and Bax proteins and decreases angiogenesis in colorectal cancer**. *International journal of oncology*. 30:883-888.

34. Escola, J.M., M.J. Kleijmeer, W. Stoorvogel, J.M. Griffith, O. Yoshie, and H.J. Geuze. 1998. **Selective enrichment of tetraspan proteins on the internal vesicles of multivesicular endosomes and on exosomes secreted by human B-lymphocytes**. *J Biol Chem*. 273:20121-20127.

35. Fincham, V.J., and M.C. Frame. 1998. **The catalytic activity of Src is dispensable for translocation to focal adhesions but controls the turnover of these structures during cell motility**. *EMBO J*. 17:81-92.
36. Finn, R.S. 2008. **Targeting Src in breast cancer**. *Ann Oncol*. 19:1379-1386.
37. Frame, M.C. 2002. **Src in cancer: deregulation and consequences for cell behaviour**. *Biochim Biophys Acta*. 1602:114-130.
38. Frame, M.C., V.J. Fincham, N.O. Carragher, and J.A. Wyke. 2002. **v-Src's hold over actin and cell adhesions**. *Nat Rev Mol Cell Biol*. 3:233-245.
39. Gidekel, S., G. Pizov, Y. Bergman, and E. Pikarsky. 2003. **Oct-3/4 is a dose-dependent oncogenic fate determinant**. *Cancer Cell*. 4:361-370.
40. Giet, R., C. Petretti, and C. Prigent. 2005. **Aurora kinases, aneuploidy and cancer, a coincidence or a real link?** *Trends Cell Biol*. 15:241-250.
41. Gonzalez, L., M.T. Agullo-Ortuno, J.M. Garcia-Martinez, A. Calcabrini, C. Gamallo, J. Palacios, A. Aranda, and J. Martin-Perez. 2006. **Role of c-Src in Human MCF7 Breast Cancer Cell Tumorigenesis**. *J. Biol. Chem.* 281:20851-20864.
42. Grande-Garcia, A., A. Echarri, J. de Rooij, N.B. Alderson, C.M. Waterman-Storer, J.M. Valdivielso, and M.A. del Pozo. 2007. **Caveolin-1 regulates cell polarization and directional migration through Src kinase and Rho GTPases**. *J Cell Biol*. 177:683-694.
43. Guarino, M. 2010. **Src signaling in cancer invasion**. *J Cell Physiol*. 223:14-26.
44. Guy, C.T., S.K. Muthuswamy, R.D. Cardiff, P. Soriano, and W.J. Muller. 1994. **Activation of the c-Src tyrosine kinase is required for the induction of mammary tumors in transgenic mice**. *Genes Dev*. 8:23-32.
45. Haydaroglu, A., and G. Ozyigit. 2013. **Principles and practice of modern radiotherapy techniques in breast cancer**. Springer, New York ; London. xv, 358 p. pp.
46. Hendrix, A., and A.N. Hume. 2011. **Exosome signaling in mammary gland development and cancer**. *The International journal of developmental biology*. 55:879-887.
47. Hinohara, K., S. Kobayashi, H. Kanauchi, S. Shimizu, K. Nishioka, E. Tsuji, K. Tada, K. Umezawa, M. Mori, T. Ogawa, J. Inoue, A. Tojo, and N. Gotoh. 2012. **ErbB receptor tyrosine kinase/NF-kappaB signaling controls mammosphere formation in human breast cancer**. *Proc Natl Acad Sci U S A*. 109:6584-6589.
48. Holliday, D.L., and V. Speirs. 2011. **Choosing the right cell line for breast cancer research**. *Breast Cancer Res*. 13:215.
49. Irby, R.B., and T.J. Yeatman. 2000. **Role of src expression and activation in human cancer**. *Oncogene*. 19:5636-5642.

50. Ishizawar, R.C., D.A. Tice, T. Karaoli, and S.J. Parsons. 2004. **The C terminus of c-Src inhibits breast tumor cell growth by a kinase-independent mechanism**. *J Biol Chem*. 279:23773-23781.

51. Jacobs, C., and H. Rubsamen. 1983. **Expression of pp60c-src protein kinase in adult and fetal human tissue: high activities in some sarcomas and mammary carcinomas**. *Cancer Res*. 43:1696-1702.

52. Jemal, A., F. Bray, M.M. Center, J. Ferlay, E. Ward, and D. Forman. 2011. **Global cancer statistics**. *CA Cancer J Clin*. 61:69-90.

53. Jenjaroenpun, P., Y. Kremenska, V.M. Nair, M. Kremenskoy, B. Joseph, and I.V. Kurochkin. 2013. **Characterization of RNA in exosomes secreted by human breast cancer cell lines using next-generation sequencing**. *PeerJ*. 1:e201.

54. Jeter, C.R., M. Badeaux, G. Choy, D. Chandra, L. Patrawala, C. Liu, T. Calhoun-Davis, H. Zaehres, G.Q. Daley, and D.G. Tang. 2009. **Functional evidence that the self-renewal gene NANOG regulates human tumor development**. *Stem Cells*. 27:993-1005.

55. Jin, W., C. Yun, J. Jeong, Y. Park, H.D. Lee, and S.J. Kim. 2008. **c-Src is required for tropomyosin receptor kinase C (TrkC)-induced activation of the phosphatidylinositol 3-kinase (PI3K)-AKT pathway**. *J Biol Chem*. 283:1391-1400.

56. Johnson, F.M., B. Saigal, M. Talpaz, and N.J. Donato. 2005. **Dasatinib (BMS-354825) tyrosine kinase inhibitor suppresses invasion and induces cell cycle arrest and apoptosis of head and neck squamous cell carcinoma and non-small cell lung cancer cells**. *Clin Cancer Res*. 11:6924-6932.

57. Joshi, B., S.S. Strugnell, J.G. Goetz, L.D. Kojic, M.E. Cox, O.L. Griffith, S.K. Chan, S.J. Jones, S.P. Leung, H. Masoudi, S. Leung, S.M. Wiseman, and I.R. Nabi. 2008. **Phosphorylated caveolin-1 regulates Rho/ROCK-dependent focal adhesion dynamics and tumor cell migration and invasion**. *Cancer Res*. 68:8210-8220.

58. Kennecke, H., R. Yerushalmi, R. Woods, M.C. Cheang, D. Voduc, C.H. Speers, T.O. Nielsen, and K. Gelmon. 2010. **Metastatic behavior of breast cancer subtypes**. *J Clin Oncol*. 28:3271-3277.

59. Kim, D., S. Kim, H. Koh, S.O. Yoon, A.S. Chung, K.S. Cho, and J. Chung. 2001. **Akt/PKB promotes cancer cell invasion via increased motility and metalloproteinase production**. *FASEB J*. 15:1953-1962.

60. Klinghoffer, R.A., C. Sachsenmaier, J.A. Cooper, and P. Soriano. 1999. **Src family kinases are required for integrin but not PDGFR signal transduction**. *EMBO J*. 18:2459-2471.

61. Kong, L., Z. Deng, H. Shen, and Y. Zhang. 2011. **Src family kinase inhibitor PP2 efficiently inhibits cervical cancer cell proliferation through down-regulating**

phospho-Src-Y416 and phospho-EGFR-Y1173. *Molecular and cellular biochemistry*. 348:11-19.

62. Lai, D., K.C. Ho, Y. Hao, and X. Yang. 2011. **Taxol resistance in breast cancer cells is mediated by the hippo pathway component TAZ and its downstream transcriptional targets Cyr61 and CTGF**. *Cancer Res*. 71:2728-2738.
63. Lannutti, B.J., N. Blake, M.J. Gandhi, J.A. Reems, and J.G. Drachman. 2005. **Induction of polyploidization in leukemic cell lines and primary bone marrow by Src kinase inhibitor SU6656**. *Blood*. 105:3875-3878.
64. Lawrence, J.B., C. Oxvig, M.T. Overgaard, L. Sottrup-Jensen, G.J. Gleich, L.G. Hays, J.R. Yates, 3rd, and C.A. Conover. 1999. **The insulin-like growth factor (IGF)-dependent IGF binding protein-4 protease secreted by human fibroblasts is pregnancy-associated plasma protein-A**. *Proc Natl Acad Sci U S A*. 96:3149-3153.
65. Lechner, A., N. Schutze, H. Siggelkow, J. Seufert, and F. Jakob. 2000. **The immediate early gene product hCYR61 localizes to the secretory pathway in human osteoblasts**. *Bone*. 27:53-60.
66. Lee, G.Y., P.A. Kenny, E.H. Lee, and M.J. Bissell. 2007. **Three-dimensional culture models of normal and malignant breast epithelial cells**. *Nat Methods*. 4:359-365.
67. Lehmann, B.D., J.A. Bauer, X. Chen, M.E. Sanders, A.B. Chakravarthy, Y. Shyr, and J.A. Pietenpol. 2011. **Identification of human triple-negative breast cancer subtypes and preclinical models for selection of targeted therapies**. *J Clin Invest*. 121:2750-2767.
68. Lin, B.R., C.C. Chang, L.R. Chen, M.H. Wu, M.Y. Wang, I.H. Kuo, C.Y. Chu, K.J. Chang, P.H. Lee, W.J. Chen, M.L. Kuo, and M.T. Lin. 2007. **Cysteine-rich 61 (CCN1) enhances chemotactic migration, transendothelial cell migration, and intravasation by concomitantly up-regulating chemokine receptor 1 and 2**. *Mol Cancer Res*. 5:1111-1123.
69. Lin, J., R. Huo, L. Wang, Z. Zhou, Y. Sun, B. Shen, R. Wang, and N. Li. 2011. **A novel anti-Cyr61 antibody inhibits breast cancer growth and metastasis in vivo**. *Cancer Immunol Immunother*. 61:677-687.
70. Ling, G.Q., D.B. Chen, B.Q. Wang, and L.S. Zhang. 2012. **Expression of the pluripotency markers Oct3/4, Nanog and Sox2 in human breast cancer cell lines**. *Oncology letters*. 4:1264-1268.
71. Lombardo, L.J., F.Y. Lee, P. Chen, D. Norris, J.C. Barrish, K. Behnia, S. Castaneda, L.A. Cornelius, J. Das, A.M. Doweyko, C. Fairchild, J.T. Hunt, I. Inigo, K. Johnston, A. Kamath, D. Kan, H. Klei, P. Marathe, S. Pang, R. Peterson, S. Pitt, G.L. Schieven, R.J. Schmidt, J. Tokarski, M.L. Wen, J. Wityak, and R.M. Borzilleri. 2004.

Discovery of N-(2-chloro-6-methyl- phenyl)-2-(6-(4-(2-hydroxyethyl)- piperazin-1-yl)-2-methylpyrimidin-4- ylamino)thiazole-5-carboxamide (BMS-354825), a dual Src/Abl kinase inhibitor with potent antitumor activity in preclinical assays. *J Med Chem*. 47:6658-6661.

72. Lu, K.V., S. Zhu, A. Cvrljevic, T.T. Huang, S. Sarkaria, D. Ahkavan, J. Dang, E.B. Dinca, S.B. Plaisier, I. Oderberg, Y. Lee, Z. Chen, J.S. Caldwell, Y. Xie, J.A. Loo, D. Seligson, A. Chakravari, F.Y. Lee, R. Weinmann, T.F. Cloughesy, S.F. Nelson, G. Bergers, T. Graeber, F.B. Furnari, C.D. James, W.K. Cavenee, T.G. Johns, and P.S. Mischel. 2009. **Fyn and SRC are effectors of oncogenic epidermal growth factor receptor signaling in glioblastoma patients**. *Cancer Res*. 69:6889-6898.
73. Lu, Y., Q. Yu, J.H. Liu, J. Zhang, H. Wang, D. Koul, J.S. McMurray, X. Fang, W.K. Yung, K.A. Siminovitch, and G.B. Mills. 2003. **Src family protein-tyrosine kinases alter the function of PTEN to regulate phosphatidylinositol 3-kinase/AKT cascades**. *J Biol Chem*. 278:40057-40066.
74. Luo, Y., F. Liang, and Z.Y. Zhang. 2009. **PRL1 promotes cell migration and invasion by increasing MMP2 and MMP9 expression through Src and ERK1/2 pathways**. *Biochemistry*. 48:1838-1846.
75. Ma, J.G., H. Huang, S.M. Chen, Y. Chen, X.L. Xin, L.P. Lin, J. Ding, H. Liu, and L.H. Meng. 2011. **PH006, a novel and selective Src kinase inhibitor, suppresses human breast cancer growth and metastasis in vitro and in vivo**. *Breast Cancer Res Treat*. 130:85-96.
76. Macias, H., and L. Hinck. 2012. **Mammary gland development**. *Wiley interdisciplinary reviews. Developmental biology*. 1:533-557.
77. Marcotte, R., H.W. Smith, V. Sanguin-Gendreau, R.V. McDonough, and W.J. Muller. 2012. **Mammary epithelial-specific disruption of c-Src impairs cell cycle progression and tumorigenesis**. *Proc Natl Acad Sci U S A*. 109:2808-28013.
78. Martin, G.S. 2001. **The hunting of the Src**. *Nat Rev Mol Cell Biol*. 2:467-475.
79. Martin, G.S. 2004. **The road to Src**. *Oncogene*. 23:7910-7917.
80. Mathivanan, S., and R.J. Simpson. 2009. **ExoCarta: A compendium of exosomal proteins and RNA**. *Proteomics*. 9:4997-5000.
81. Meng, Q., C. Xia, J. Fang, Y. Rojanasakul, and B.H. Jiang. 2006. **Role of PI3K and AKT specific isoforms in ovarian cancer cell migration, invasion and proliferation through the p70S6K1 pathway**. *Cell Signal*. 18:2262-2271.
82. Meng, X.N., Y. Jin, Y. Yu, J. Bai, G.Y. Liu, J. Zhu, Y.Z. Zhao, Z. Wang, F. Chen, K.Y. Lee, and S.B. Fu. 2009. **Characterisation of fibronectin-mediated FAK signalling pathways in lung cancer cell migration and invasion**. *Br J Cancer*. 101:327-334.

83. Mitra, S.K., S.T. Lim, A. Chi, and D.D. Schlaepfer. 2006. **Intrinsic focal adhesion kinase activity controls orthotopic breast carcinoma metastasis via the regulation of urokinase plasminogen activator expression in a syngeneic tumor model**. *Oncogene*. 25:4429-4440.

84. Monsky, W.L., T. Kelly, C.Y. Lin, Y. Yeh, W.G. Stetler-Stevenson, S.C. Mueller, and W.T. Chen. 1993. **Binding and localization of M(r) 72,000 matrix metalloproteinase at cell surface invadopodia**. *Cancer Res*. 53:3159-3164.

85. Morris, E. 2005. **The Normal Breast**. *In* Breast MRI. Springer New York. 23-44.

86. Mundy, G.R. 2002. **Metastasis to bone: causes, consequences and therapeutic opportunities**. *Nat Rev Cancer*. 2:584-593.

87. Myoui, A., R. Nishimura, P.J. Williams, T. Hiraga, D. Tamura, T. Michigami, G.R. Mundy, and T. Yoneda. 2003. **C-SRC tyrosine kinase activity is associated with tumor colonization in bone and lung in an animal model of human breast cancer metastasis**. *Cancer Res*. 63:5028-5033.

88. Nagata, Y., K.H. Lan, X. Zhou, M. Tan, F.J. Esteva, A.A. Sahin, K.S. Klos, P. Li, B.P. Monia, N.T. Nguyen, G.N. Hortobagyi, M.C. Hung, and D. Yu. 2004. **PTEN activation contributes to tumor inhibition by trastuzumab, and loss of PTEN predicts trastuzumab resistance in patients**. *Cancer Cell*. 6:117-127.

89. Nam, J.S., Y. Ino, M. Sakamoto, and S. Hirohashi. 2002. **Src family kinase inhibitor PP2 restores the E-cadherin/catenin cell adhesion system in human cancer cells and reduces cancer metastasis**. *Clin Cancer Res*. 8:2430-2436.

90. Nautiyal, J., P. Majumder, B.B. Patel, F.Y. Lee, and A.P. Majumdar. 2009. **Src inhibitor dasatinib inhibits growth of breast cancer cells by modulating EGFR signaling**. *Cancer Lett*. 283:143-151.

91. Neeft, M., M. Wieffer, A.S. de Jong, G. Negroiu, C.H. Metz, A. van Loon, J. Griffith, J. Krijgsveld, N. Wulffraat, H. Koch, A.J. Heck, N. Brose, M. Kleijmeer, and P. van der Sluijs. 2005. **Munc13-4 is an effector of rab27a and controls secretion of lysosomes in hematopoietic cells**. *Mol Biol Cell*. 16:731-741.

92. Nigg, E.A. 2001. **Mitotic kinases as regulators of cell division and its checkpoints**. *Nat Rev Mol Cell Biol*. 2:21-32.

93. Ostrowski, M., N.B. Carmo, S. Krumeich, I. Fanget, G. Raposo, A. Savina, C.F. Moita, K. Schauer, A.N. Hume, R.P. Freitas, B. Goud, P. Benaroch, N. Hacohen, M. Fukuda, C. Desnos, M.C. Seabra, F. Darchen, S. Amigorena, L.F. Moita, and C. Thery. 2010. **Rab27a and Rab27b control different steps of the exosome secretion pathway**. *Nat Cell Biol*. 12:19-30; sup pp 11-13.

94. Peinado, H., M. Aleckovic, S. Lavotshkin, I. Matei, B. Costa-Silva, G. Moreno-Bueno, M. Hergueta-Redondo, C. Williams, G. Garcia-Santos, C.M. Ghajar, A. Nitadori-Hoshino, C. Hoffman, K. Badal, B.A. Garcia, M.K. Callahan, J. Yuan, V.R.

Martins, J. Skog, R.N. Kaplan, M.S. Brady, J.D. Wolchok, P.B. Chapman, Y. Kang, J. Bromberg, and D. Lyden. 2012. **Melanoma exosomes educate bone marrow progenitor cells toward a pro-metastatic phenotype through MET**. *Nat Med*.

95. Peng, S.B., V. Peek, Y. Zhai, D.C. Paul, Q. Lou, X. Xia, T. Eessalu, W. Kohn, and S. Tang. 2005. **Akt activation, but not extracellular signal-regulated kinase activation, is required for SDF-1alpha/CXCR4-mediated migration of epitheloid carcinoma cells**. *Mol Cancer Res*. 3:227-236.

96. Perou, C.M., T. Sorlie, M.B. Eisen, M. van de Rijn, S.S. Jeffrey, C.A. Rees, J.R. Pollack, D.T. Ross, H. Johnsen, L.A. Akslen, O. Fluge, A. Pergamenschikov, C. Williams, S.X. Zhu, P.E. Lonning, A.L. Borresen-Dale, P.O. Brown, and D. Botstein. 2000. **Molecular portraits of human breast tumours**. *Nature*. 406:747-752.

97. Pichot, C.S., S.M. Hartig, L. Xia, C. Arvanitis, D. Monisvais, F.Y. Lee, J.A. Frost, and S.J. Corey. 2009. **Dasatinib synergizes with doxorubicin to block growth, migration, and invasion of breast cancer cells**. *Br J Cancer*. 101:38-47.

98. Pols, M.S., and J. Klumperman. 2009. **Trafficking and function of the tetraspanin CD63**. *Exp Cell Res*. 315:1584-1592.

99. Reissig, D., J. Clement, J. Sanger, A. Berndt, H. Kosmehl, and F.D. Bohmer. 2001. **Elevated activity and expression of Src-family kinases in human breast carcinoma tissue versus matched non-tumor tissue**. *J Cancer Res Clin Oncol*. 127:226-230.

100. Riffell, J.L., R.U. Janicke, and M. Roberge. 2011. **Caspase-3-Dependent Mitotic Checkpoint Inactivation by the Small-Molecule Inducers of Mitotic Slippage SU6656 and Geraldol**. *Mol Cancer Ther*. 10:839-849.

101. Rodriguez-Pinilla, S.M., D. Sarrio, G. Moreno-Bueno, Y. Rodriguez-Gil, M.A. Martinez, L. Hernandez, D. Hardisson, J.S. Reis-Filho, and J. Palacios. 2007. **Sox2: a possible driver of the basal-like phenotype in sporadic breast cancer**. *Mod Pathol*. 20:474-481.

102. Rucci, N., I. Recchia, A. Angelucci, M. Alamanou, A. Del Fattore, D. Fortunati, M. Susa, D. Fabbro, M. Bologna, and A. Teti. 2006. **Inhibition of protein kinase c-Src reduces the incidence of breast cancer metastases and increases survival in mice: implications for therapy**. *The Journal of pharmacology and experimental therapeutics*. 318:161-172.

103. Ryan, A.J., S. Napoletano, P.A. Fitzpatrick, C.A. Currid, N.C. O'Sullivan, and J.H. Harmey. 2009. **Expression of a protease-resistant insulin-like growth factor-binding protein-4 inhibits tumour growth in a murine model of breast cancer**. *Br J Cancer*. 101:278-286.

104. Saito, Y.D., A.R. Jensen, R. Salgia, and E.M. Posadas. 2010. **Fyn: a novel molecular target in cancer**. *Cancer*. 116:1629-1637.

105. Sandilands, E., C. Cans, V.J. Fincham, V.G. Brunton, H. Mellor, G.C. Prendergast, J.C. Norman, G. Superti-Furga, and M.C. Frame. 2004. **RhoB and Actin Polymerization Coordinate Src Activation with Endosome-Mediated Delivery to the Membrane**. *Developmental cell*. 7:855-869.

106. Sen, B., and F.M. Johnson. 2011. **Regulation of SRC family kinases in human cancers**. *Journal of signal transduction*. 2011:865819.

107. Shor, A.C., E.A. Keschman, F.Y. Lee, C. Muro-Cacho, G.D. Letson, J.C. Trent, W.J. Pledger, and R. Jove. 2007. **Dasatinib inhibits migration and invasion in diverse human sarcoma cell lines and induces apoptosis in bone sarcoma cells dependent on SRC kinase for survival**. *Cancer Res*. 67:2800-2808.

108. Soriano, P., C. Montgomery, R. Geske, and A. Bradley. 1991. **Targeted disruption of the c-src proto-oncogene leads to osteopetrosis in mice**. *Cell*. 64:693-702.

109. Sorlie, T., R. Tibshirani, J. Parker, T. Hastie, J.S. Marron, A. Nobel, S. Deng, H. Johnsen, R. Pesich, S. Geisler, J. Demeter, C.M. Perou, P.E. Lonning, P.O. Brown, A.L. Borresen-Dale, and D. Botstein. 2003. **Repeated observation of breast tumor subtypes in independent gene expression data sets**. *Proc Natl Acad Sci U S A*. 100:8418-8423.

110. Subramanian, A., P. Tamayo, V.K. Mootha, S. Mukherjee, B.L. Ebert, M.A. Gillette, A. Paulovich, S.L. Pomeroy, T.R. Golub, E.S. Lander, and J.P. Mesirov. 2005. **Gene set enrichment analysis: a knowledge-based approach for interpreting genome-wide expression profiles**. *Proc Natl Acad Sci U S A*. 102:15545-15550.

111. Summy, J.M., and G.E. Gallick. 2003. **Src family kinases in tumor progression and metastasis**. *Cancer Metastasis Rev*. 22:337-358.

112. Sun, X., C. Li, C. Zhuang, W.C. Gilmore, E. Cobos, Y. Tao, and Z. Dai. 2009. **Abl interactor 1 regulates Src-Id1-matrix metalloproteinase 9 axis and is required for invadopodia formation, extracellular matrix degradation and tumor growth of human breast cancer cells**. *Carcinogenesis*. 30:2109-2116.

113. Sun, Z.J., Y. Wang, Z. Cai, P.P. Chen, X.J. Tong, and D. Xie. 2008. **Involvement of Cyr61 in growth, migration, and metastasis of prostate cancer cells**. *Br J Cancer*. 99:1656-1667.

114. Tan, M., P. Li, M. Sun, G. Yin, and D. Yu. 2006. **Upregulation and activation of PKC alpha by ErbB2 through Src promotes breast cancer cell invasion that can be blocked by combined treatment with PKC alpha and Src inhibitors**. *Oncogene*. 25:3286-3295.

115. Tang, D.G. 2012. **Understanding cancer stem cell heterogeneity and plasticity**. *Cell research*. 22:457-472.

116. Tanji, M., T. Ishizaki, S. Ebrahimi, Y. Tsuboguchi, T. Sukezane, T. Akagi, M.C. Frame, N. Hashimoto, S. Miyamoto, and S. Narumiya. 2010. **mDia1 targets v-Src**

to the cell periphery and facilitates cell transformation, tumorigenesis, and invasion. *Mol Cell Biol*. 30:4604-4615.

117. Tardaguila, M., E. Gonzalez-Gugel, and A. Sanchez-Pacheco. 2011. **Aurora Kinase B Activity Is Modulated by Thyroid Hormone during Transcriptional Activation of Pituitary Genes**. *Mol Endocrinol*. 25:385-393.
118. Thery, C., S. Amigorena, G. Raposo, and A. Clayton. 2006. **Isolation and characterization of exosomes from cell culture supernatants and biological fluids**. *Current protocols in cell biology / editorial board, Juan S. Bonifacino ... [et al.]*. Chapter 3:Unit 3 22.
119. Thomas, S.M., and J.S. Brugge. 1997. **Cellular functions regulated by Src family kinases**. *Ann Rev Cell Dev Biol*. 13:513-609.
120. Tiede, B., and Y. Kang. 2011. **From milk to malignancy: the role of mammary stem cells in development, pregnancy and breast cancer**. *Cell research*. 21:245-257.
121. Timpson, P., G.E. Jones, M.C. Frame, and V.G. Brunton. 2001. **Coordination of cell polarization and migration by the Rho family GTPases requires Src tyrosine kinase activity**. *Current biology : CB*. 11:1836-1846.
122. Tryfonopoulos, D., S. Walsh, D.M. Collins, L. Flanagan, C. Quinn, B. Corkery, E.W. McDermott, D. Evoy, A. Pierce, N. O'Donovan, J. Crown, and M.J. Duffy. 2011. **Src: a potential target for the treatment of triple-negative breast cancer**. *Ann Oncol*. 22:2234-2240.
123. Tsai, M.S., D.F. Bogart, J.M. Castaneda, P. Li, and R. Lupu. 2002. **Cyr61 promotes breast tumorigenesis and cancer progression**. *Oncogene*. 21:8178-8185.
124. Vader, G., and S.M. Lens. 2008. **The Aurora kinase family in cell division and cancer**. *Biochim Biophys Acta*. 1786:60-72.
125. Vanharanta, S., and J. Massague. 2013. **Origins of metastatic traits**. *Cancer Cell*. 24:410-421.
126. Wang, C., R. Navab, V. Iakovlev, Y. Leng, J. Zhang, M.S. Tsao, K. Siminovitch, D.R. McCready, and S.J. Done. 2007. **Abelson interactor protein-1 positively regulates breast cancer cell proliferation, migration, and invasion**. *Mol Cancer Res*. 5:1031-1039.
127. Webb, D.J., K. Donais, L.A. Whitmore, S.M. Thomas, C.E. Turner, J.T. Parsons, and A.F. Horwitz. 2004. **FAK-Src signalling through paxillin, ERK and MLCK regulates adhesion disassembly**. *Nat Cell Biol*. 6:154-161.
128. Weis, S., J. Cui, L. Barnes, and D. Cheresh. 2004. **Endothelial barrier disruption by VEGF-mediated Src activity potentiates tumor cell extravasation and metastasis**. *J Cell Biol*. 167:223-229.

129. Williams, T.M., and M.P. Lisanti. 2005. **Caveolin-1 in oncogenic transformation, cancer, and metastasis**. *Am J Physiol Cell Physiol*. 288:C494-506.

130. Xie, D., C.W. Miller, J. O'Kelly, K. Nakachi, A. Sakashita, J.W. Said, J. Gornbein, and H.P. Koeffler. 2001. **Breast cancer. Cyr61 is overexpressed, estrogen-inducible, and associated with more advanced disease**. *J Biol Chem*. 276:14187-14194.

131. Xie, D., K. Nakachi, H. Wang, R. Elashoff, and H.P. Koeffler. 2001. **Elevated levels of connective tissue growth factor, WISP-1, and CYR61 in primary breast cancers associated with more advanced features**. *Cancer Res*. 61:8917-8923.

132. Xue, G., and B.A. Hemmings. 2013. **PKB/Akt-dependent regulation of cell motility**. *J Natl Cancer Inst*. 105:393-404.

133. Yeatman, T.J. 2004. **A renaissance for SRC**. *Nat Rev Cancer*. 4:470-480.

134. Zeng, Z.J., L.Y. Yang, X. Ding, and W. Wang. 2004. **Expressions of cysteine-rich61, connective tissue growth factor and Nov genes in hepatocellular carcinoma and their clinical significance**. *World journal of gastroenterology : WJG*. 10:3414-3418.

135. Zhang, Q., S.M. Thomas, S. Xi, T.E. Smithgall, J.M. Siegfried, J. Kamens, W.E. Gooding, and J.R. Grandis. 2004. **SRC family kinases mediate epidermal growth factor receptor ligand cleavage, proliferation, and invasion of head and neck cancer cells**. *Cancer Res*. 64:6166-6173.

136. Zhang, Q., J. Wu, Q. Cao, L. Xiao, L. Wang, D. He, G. Ouyang, J. Lin, B. Shen, Y. Shi, Y. Zhang, D. Li, and N. Li. 2009. **A critical role of Cyr61 in interleukin-17-dependent proliferation of fibroblast-like synoviocytes in rheumatoid arthritis**. *Arthritis Rheum*. 60:3602-3612.

137. Zhang, S., W.C. Huang, L. Zhang, C. Zhang, F.J. Lowery, Z. Ding, H. Guo, H. Wang, S. Huang, A.A. Sahin, K.D. Aldape, P.S. Steeg, and D. Yu. 2013. **SRC family kinases as novel therapeutic targets to treat breast cancer brain metastases**. *Cancer Res*. 73:5764-5774.

138. Zhang, X.H., Q. Wang, W. Gerald, C.A. Hudis, L. Norton, M. Smid, J.A. Foekens, and J. Massague. 2009. **Latent bone metastasis in breast cancer tied to SRC-dependent survival signals**. *Cancer Cell*. 16:67-78.

139. Zheng, X., R.J. Resnick, and D. Shalloway. 2008. **Apoptosis of estrogen-receptor negative breast cancer and colon cancer cell lines by PTP alpha and src RNAi**. *Int J Cancer*. 122:1999-2007.

APPENDIX

1.1. Supplementary information

Supplementary Video S1. Normal mitosis in control MDA-MB-231 cells. The video shows an example of cells (arrows) that undergo normal mitosis, followed by complete cell division. (Video available in the attached CD).

Supplementary Video S2. Blocked cell division in SU6656-treated MDA-MB-231 cells. The video shows aborted cell divisions (arrows) leading to the formation of cells displaying higher dimensions than no-dividing cells. (Video available in the attached CD).

PP2 vs. Control									
ID	Accession	Entrez Gene	Symbol	Description	Chr	PP2	DAS	SU	Amean
A_23_P372834	NM_198098	358	AQP1	aquaporin 1 (Colton blood group)	7	2,82	2,3	1,49	8,81
A_24_P403417	NM_004878	9536	PTGES	prostaglandin E synthase	9	2,3	1,51	-0,29	9,24
A_23_P207507	NM_003786	8714	ABCC3	ATP-binding cassette, sub-family C (CFTR/MRP), member 3	17	2,19	2,28	-0,13	8,85
A_23_P71880	NM_014471	27290	SPINK4	serine peptidase inhibitor, Kazal type 4	9	2,16	1,02	-0,62	11,5
A_33_P3301940	NM_018945	27115	PDE7B	phosphodiesterase 7B	6	1,97	0,7	-1,36	8,41
A_23_P74278	NM_001037341	5142	PDE4B	phosphodiesterase 4B, cAMP-specific	1	1,91	1,66	-0,64	9,89
A_33_P3366540	NM_001130518	55790	CSGALNACT1	chondroitin sulfate N-acetylgalactosaminyltransferase 1	8	1,88	2,1	-0,93	7,11
A_33_P3399208	AF436092	3106	HLA-B	major histocompatibility complex, class I, B	6	1,87	1,37	0,65	12,12
A_23_P102611	NM_003881	8839	WISP2	WNT1 inducible signaling pathway protein 2	20	1,56	0,81	0,33	6,11
A_23_P121144	NM_144634	131375	LYZL4	lysozyme-like 4	3	1,52	1,85	-1,3	7,4
A_23_P120594	NM_032501	84532	ACSS1	acyl-CoA synthetase short-chain family member 1	20	1,44	0,67	0,02	9,75
A_33_P3298024	NM_001144070	8714	ABCC3	ATP-binding cassette, sub-family C (CFTR/MRP), member 3	17	1,42	1,42	-0,81	8,77
A_23_P79803	NM_080607	128434	VSTM2L	V-set and transmembrane domain containing 2 like	20	1,38	1,4	-0,4	10,79
A_33_P3212764	AK097358	647662	FLJ40039	hypothetical LOC647662	12	-1,71	-2,12	0,98	6,07
A_23_P28815	NM_000782	1591	CYP24A1	cytochrome P450, family 24, subfamily A, polypeptide 1	20	-1,77	-1,85	-0,94	5,59
A_23_P93499	NM_016020	51106	TFB1M	transcription factor B1, mitochondrial	6	-2,26	-0,14	0	10,47

Supplementary Table 1. List of genes differentially expressed (P*adjust*≤0.05) after each treatment. For each gene we provide the $\log_2$ of fold change in the DAS, PP2 and SU6656 groups. The sign indicates the direction of the change, positive values refer to greater transcript abundance after treatment compared to the control, whereas negative values indicate less abundance. Amean: mean of the $\log_2$ intensity values over all samples as a measure of the average expression level. Chr: chromosomal localization of genes.

(* Due to the size of the "**Supplementary Table 1**.", the list of differentially expressed genes for Dasatinib vs. Control is available only in the electronic form in the attached CD).

SU6656 vs. Control									
ID	Accession	Entrez Gene	Symbol	Description	Chr	SU	DAS	PP2	Amean
A_23_P43197	NM_004929	793	CALB1	calbindin 1, 28kDa	8	3,32	-0,23	0,23	5,28
A_23_P321501	NM_182908	10202	DHRS2	dehydrogenase/reductase (SDR family) member 2	14	2,5	-1,64	-1,71	7,47
A_23_P130974	NM_025249	80726	KIAA1683	KIAA1683	19	2,41	1,06	0,35	7,17
A_32_P74409	NM_001145033	387763	C11orf96	chromosome 11 open reading frame 96	11	2,18	0,49	-0,36	8,27
A_23_P26457	NM_000517	3040	HBA2	hemoglobin, alpha 2	16	2,09	-0,35	-0,39	5,56
A_23_P39955	NM_001615	72	ACTG2	actin, gamma 2, smooth muscle, enteric	2	1,92	-0,09	0,37	5,89
A_24_P101800	BC065483	284804	LOC284804	hypothetical protein LOC284804	20	1,9	0,07	0,14	4,93
A_23_P161727	NM_001541	3316	HSPB2	heat shock 27kDa protein 2	11	1,7	0,07	0,35	4,88
A_23_P53137	NM_000559	3047	HBG1	hemoglobin, gamma A	11	1,65	-0,15	-0,12	5,08
A_23_P149545	NM_003528	8349	HIST2H2BE	histone cluster 2, H2be	1	1,39	0,92	0,08	5,47
A_23_P307328	NM_007331	7468	WHSC1	Wolf-Hirschhorn syndrome candidate 1	4	-1,44	-2,05	-0,66	10,03
A_23_P121253	NM_003810	8743	TNFSF10	tumor necrosis factor (ligand) superfamily, member 10	3	-1,56	0,46	0,52	9,83
A_33_P3295550	NM_030625	80312	TET1	tet oncogene 1	10	-1,93	1,13	0,64	9,32
A_23_P209625	NM_000104	1545	CYP1B1	cytochrome P450, family 1, subfamily B, polypeptide 1	2	-2,14	1,8	1,1	12,16
A_24_P105933	NM_004624	7433	VIPR1	vasoactive intestinal peptide receptor 1	3	-2,39	2,04	1,48	11,34

Supplementary Table 1. List of genes differentially expressed (P*adjust* ≤ 0.05) after each treatment.(Continuation).

Common pathways for Dasatinib, PP2 and SU6656		
Pathway name	**Source of annotation**	**Gene set size**
DNA_REPLICATION	KEGG	34
CELL CYCLE, MITOTIC	REACTOME	288
G1/S TRANSITION	REACTOME	96
DNA REPAIR	REACTOME	95
G2/M CHECKPOINTS	REACTOME	42
ACTIVATION OF THE PRE-REPLICATIVE COMPLEX	REACTOME	29
EXTENSION OF TELOMERES	REACTOME	23
LAGGING STRAND SYNTHESIS	REACTOME	19
NUCLEOTIDE EXCISION REPAIR	REACTOME	48
PURINE_METABOLISM	KEGG	146
METABOLISM OF LIPIDS AND LIPOPROTEINS	REACTOME	143
DNA REPLICATION	REACTOME	92
E2F MEDIATED REGULATION OF DNA REPLICATION	REACTOME	28
CELL_CYCLE	KEGG	112

Supplementary Table 2. Gene set enrichment analysis was applied for each cell treatment using annotations from Biocarta, KEGG and Reactome pathway databases. Common pathways for each treatment with FDR ≤0.05 are shown. NES=Normalized Enrichment Score, FDR= False Discovery Rate.

(*Complete list of specific pathways for each treatment and the list of common pathways for two of the three inhibitors are available only in the electronic form in the attached CD).

Pathway name	**Source of annotation**	**Gene set size**	**NES**	**FDR q-val**	**Sense**
SRC_GENES	Custom	42	-1,19	**0,19**	DOWN in DAS
SRC_GENES	Custom	42	-1,35	**0,083**	DOWN in PP2
SRC_GENES	Custom	42	-1,51	**0,024**	DOWN in SU

Supplementary Table 3. Ranked list of Src genes set for Dasatinib, PP2 and SU6656 treated cells determined by GSEA. SU6656 treatment caused a significant down-regulation of Src pathway (FDR=0.024), while PP2 and DAS showed this trend but do not pass the significance threshold (FDR<0.05). NES=Normalized Enrichment Score, FDR= False Discovery Rate, Src gene set size = 42.

(*Complete ranked list of genes from Src pathway for each treatment is available only in the electronic form in the attached CD).

1.2. Publications

Sánchez-Bailón, MP, Calcabrini, A, Gómez-Domínguez, D, Morte, B, Martín-Forero, E, Gómez-López, G, Molinari, A, Wagner, KU, Martín-Pérez, J. (2012). **Src kinases catalytic activity regulates proliferation, migration and invasiveness of MDA-MB-231 breast cancer cells**. Cell. Signal. 24(6): 1276-1286.

Additional publications:

Gómez-Casares, MT, García-Alegria, E, López-Jorge, CE, Ferrándiz, N, Blanco, R, Alvarez, S, Vaqué, JP, Bretones, G, Caraballo, JM, Sánchez-Bailón, P, Delgado, MD, Martín-Perez, J, Cigudosa, JC, León, J. (2013). **MYC antagonizes the differentiation induced by imatinib in chronic myeloid leukemia cells through down-regulation of p27(KIP1)**. Oncogene. 32(17): 2239-2246.

Maria Diakonova (Ed.) (2014). **Recent Advances in Prolactin Research**. Martín-Pérez, J, García-Martínez, JM, Sánchez-Bailón, MP, Mayoral-Varo, V, Calcabrini, A. Role of Src family kinases in prolactin signaling. Springer. In press.

Cellular Signalling 24 (2012) 1276–1286

Contents lists available at SciVerse ScienceDirect

Cellular Signalling

journal homepage: www.elsevier.com/locate/cellsig

Src kinases catalytic activity regulates proliferation, migration and invasiveness of MDA-MB-231 breast cancer cells

María Pilar Sánchez-Bailón [a,1], Annarica Calcabrini [a,b,1], Daniel Gómez-Domínguez [a], Beatriz Morte [c], Esther Martín-Forero [a], Gonzalo Gómez-López [d], Agnese Molinari [b], Kay-Uwe Wagner [e], Jorge Martín-Pérez [a,*]

[a] Dpto. Biología del Cáncer, Instituto de Investigaciones Biomédicas A. Sols (CSIC/UAM), Arturo Duperier 4, 28029 Madrid, Spain
[b] Dipartimento Tecnologie e Salute, Istituto Superiore di Sanità, Viale Regina Elena 299, 00161 Roma, Italy
[c] Centro de Investigación Biomédica en Red de Enfermedades Raras (CIBERER), Madrid, Spain
[d] Bioinformatics Unit (UBio), Structural Biology and Biocomputing Programme, Spanish National Cancer Research Centre (CNIO), Madrid, Spain
[e] Eppley Institute for Research in Cancer and Allied Diseases, University of Nebraska Medical Center, 986805 Nebraska Medical Center, Rm. 8009, Omaha, NE 68198-6805, USA

ARTICLE INFO

Article history:
Received 13 January 2012
Received in revised form 15 February 2012
Accepted 15 February 2012
Available online 27 February 2012

Keywords:
SFKs
Dasatinib
PP2
SU6656
Aurora B kinase
MDA-MB-231

ABSTRACT

SFKs are frequently deregulated in cancer where they control cellular proliferation, migration, survival and metastasis. Here we study the role of SFKs catalytic activity in triple-negative/basal-like and metastatic human breast cancer MDA-MB-231 cells employing three well-established inhibitors: Dasatinib, PP2 and SU6656. These compounds inhibited migration and invasion. Concomitantly, they reduced Fak, paxillin, p130CAS, caveolin-1 phosphorylation and altered cytoskeletal structures. They also inhibited cell proliferation, but in different manners. Dasatinib and PP2 increased $p27^{Kip1}$ expression and reduced c-Myc levels, restraining G1–S transition. In contrast, SU6656 did not modify $p27^{Kip1}$ expression, slightly altered c-Myc levels and generated polyploid multinucleated cells, indicating inhibition of cytokinesis. These later effects were also observed in SYF fibroblasts, suggesting a SFKs-independent action. ZM447439, an Aurora B kinase inhibitor, produced similar cell cycle and morphological alterations in MDA-MB-231 cells, indicating that SU6656 blocked Aurora B kinase. This was confirmed by inhibition of histone H3 phosphorylation, the canonical Aurora B kinase substrate. Furthermore, hierarchical clustering analysis of gene expression profiles showed that SU6656 defined a set of genes that differed from Dasatinib and PP2. Additionally, Gene Set Enrichment Analyses revealed that SU6656 significantly reduces the Src pathway. Together, these results show the importance of SFKs catalytic activity for MDA-MB-231 proliferation, migration and invasiveness. They also illustrate that SU6656 acts as dual SFKs and Aurora B kinase inhibitor, suggesting its possible use as a therapeutic agent in breast cancer.

1. Introduction

SFKs regulate intracellular signaling pathways originated by activated transmembrane growth factors and cytokines receptors, including EGF-R, PDGF-R, IGF-1R, VEGF-R, FGF-R, HER2, PRL-R, and E-R [1–3]. Consequently, SFKs modulate signaling cascades leading to cell proliferation, survival, differentiation, adhesion, migration, invasion, etc., in several biological models [1,4].

Functional deregulation or altered expression of SFKs is associated with human cancers [3,4]. Studies in human samples and animal models support the role of SFKs catalytic activity in tumorigenesis of breast, colorectal, pancreatic, prostatic, melanoma, gastric and ovarian cancers [5]. In breast cancer, increased tyrosine kinase activity of c-Src is associated with induction, progression and metastasis [3,6].

SFKs include nine members (c-Src, Blk, Fyn, Fgr, Hck, Lck, Lyn, Yes and Yrk). They have a modular structure with a membrane-targeting signal, Src homology domains SH2 and SH3 involved in protein–protein interactions. The kinase domain contains the ATP binding site K298 and the autophosphorylation Y418 residue. Phosphorylation of Y530 at carboxyl tail by CSK regulates kinase activity, as it favors intramolecular interactions, which unable SH2, SH3 and catalytic domains functionality [1,4].

Abbreviations: SFKs, Src family tyrosine kinases; EGF-R, epidermal growth factor receptor; PDGF-R, platelet-derived growth factor receptor; IGF-1R, insulin-like growth factor-1 receptor; VEGF-R, vascular endothelial growth factor receptor; FGF-R, fibroblast growth factor receptor; E-R, estrogen receptor; PRL-R, prolactin receptor; DAPI, 4',6-diamidino-2-phenylindole; MTT, 3-(4,5-dimethylthiazol-2-yl)-2,5-diphenyltetrazolium bromide; BrdU, bromodeoxyuridine; PI, propidium iodide; PARP, poly-ADP ribose polymerase; CSK, C-terminal Src kinase; GSEA, Gene Set Enrichment Analysis.

* Corresponding author. Tel.: +34 91 585 4416; fax: +34 91 585 4401.
E-mail address: jmartin@iib.uam.es (J. Martín-Pérez).

[1] Equally contributed to this work.

0898-6568/$ – see front matter © 2012 Elsevier Inc. All rights reserved.
doi:10.1016/j.cellsig.2012.02.011

SFKs phosphorylate proteins involved in focal adhesion complexes [1,4]. Upon interaction of Src-SH2 domain with auto-phosphorylated Y397-Fak, Src becomes activated and phosphorylates Fak at multiple sites including Y925 [7]. Src-Fak complex controls pathways leading to proliferation, survival, focal adhesion and cytoskeleton remodeling that have also implications in migration and invasiveness [4]. Likewise, Src-Fak complex phosphorylates proteins implicated in focal adhesion, such as paxillin and p130CAS [1,4]. Src also phosphorylates Y14-caveolin-1, which in turns acts as an effector of Rho/ROCK signaling involved in migration and invasion of tumor cells by modulating focal adhesion turnover [8,9]. Furthermore, SFKs catalytic activity is also involved in cell cycle progression. Phosphorylated Y925-Fak by Src serves as docking site for binding of P85-PI3K SH2 domain, leading to stimulation of PI3K/Akt pathway. Also, Src-Fak complex modulates Mek1-2/Erk1-2 pathway [1,2,4].

We previously observed that SFKs catalytic activity regulates the G1–S transition by controlling expression of c-Myc and $p27^{Kip1}$ in MCF7 and T47D non-metastatic human breast cancer cells [2,10] and in lymphoid cells [11,12]. Src phosphorylates $p27^{Kip1}$ on Y74/Y88 facilitating its degradation and, as a result, facilitates G1–S transition [13]. In addition, Src promotes proliferation and survival by activating PI3K/Akt-dependent pathways [12,14].

Together, these data suggest that the SFKs catalytic activity is a potential therapeutic target in several cancers. Thus, targeting the catalytic domain has developed numerous kinase inhibitors, as ATP-competitors. Because structural similarities of ATP pocket among kinases, these compounds are not fully specific for SFKs, instead they are considered as selective inhibitors [15]; such is the case of Dasatinib, PP2 and SU6656. Dasatinib is BCR/Abl and SFKs inhibitor that has additional targets such as c-Kit, Eph kinases [16,17]; it is used in chronic myelogenous leukemia (CML) and is under evaluation for solid tumors including advanced prostate and breast cancer. PP2 shows also weak inhibition to other kinases including EGFR, CK1δ and CSK [18]. SU6656 has some other targets identified in vitro: PDGFR, BRSK2, AMPK, Aurora B kinase, and CaMKKβ [18]. The lack of specificity of these inhibitors can be responsible for site-target effects when a single compound is used. To minimize this possible misunderstanding, we carried out studies on the role of SFKs catalytic activity in human triple-negative/basal like MDA-MB-231 breast cancer cells by employing Dasatinib, PP2 and SU6656.

We show that these three selective inhibitors of SFKs significantly reduced proliferation, migration and invasiveness. Particularly, SU6656 blocked Aurora B kinase and induced polyploidy multinucleated cells blocking cytokinesis. Hierarchical clustering analyses of gene expression profiles show that SU6656 defined an individual set of genes that differed from Dasatinib and PP2. In contrast to them, Gene Set Enrichment Analyses (GSEA) showed that SU6656 significantly reduced Src pathway.

2. Materials and methods

2.1. Reagents

Anti-c-Src 327 was from Calbiochem (Merck4Biosciences, Germany). Anti-Fak (A17), anti-p120-catenin (S-19) and anti-c-Myc (N2E6.2) were from Santa Cruz Biotechnology (Santa Cruz, USA). Anti-pY418-Src, secondary horseradish peroxidase-conjugated antibodies, goat-anti-mouse IgG Alexa-Fluor 488, goat-anti-rabbit IgG Alexa-Fluor 488 or 546 and ProLong antifade-reagent were from Invitrogen (Camarillo, USA). Anti-pY925-Fak, and anti-pY118-paxillin were from Cell Signaling Technologies (Danvers, USA). Anti-paxillin, anti-p130CAS, anti-caveolin, anti-pY14-caveolin, anti-β-catenin, anti-$p27^{Kip1}$, anti-BrdU FITC-conjugated and Matrigel™ were from BD-Biosciences (Bedford, USA). Anti-pS10-histone H3 and anti-phosphotyrosine 4G10 were from Millipore (Billerica, USA). Anti-Aurora B and anti-histone H3 were from ABCAM (Cambridge, UK). Anti-α-tubulin, anti-β-actin, TRITC-labeled phalloidin, DAPI, MTT, BrdU, trypan blue, propidium iodide (PI) and SU6656 were from Sigma-Aldrich (St. Louis, USA). Purified histone H3 was from Roche Applied Science (Indianapolis, USA). Acrylamide/Bis-acrylamide (29:1), SDS and ammonium persulfate were from Bio-Rad Laboratories (Hercules, USA). ECL was from GE Healthcare Biosciences (Pittsburgh, USA). BCA protein assay was from Thermo Scientific (Rockford, USA). PP2 was from Tocris (Ellisville, USA), and Dasatinib was from LC-Laboratories (Woburn, USA).

2.2. Cell cultures

MDA-MB-231 cells from ATCC were propagated in DMEM supplemented with 5% FCS, 2 mM glutamine, 100 IU/ml penicillin and 100 μg/ml streptomycin.

2.3. Metabolic activity and cell viability studies

For MTT assay, cells were 72 h-treated with DMSO (1:1000, Control), Dasatinib (10, 100, 500, 1000 nM), PP2 or SU6656 (1, 5, 25, 50 μM). Then, 10 μl of MTT reagent was added to each well (final concentration 0.5 mg/ml) and plates were incubated at 37 °C for 4 h. After solubilization of formazan crystals (2–3 h at 37 °C with 10% SDS/10 mM HCl), absorbance was measured at 570 nm in a VersaMax Elisa Microplate Reader (Molecular Devices, USA). Cell viability was determined by counting cells with trypan blue. Cells were 72 h-treated with DMSO (Control), Dasatinib (100 nM), PP2 (5 μM) or SU6656 (5 μM), then detached, mixed with a 0.4% trypan blue/PBS solution (1:1), loaded on a hemocytometer and counted.

2.4. Cell cycle analysis

Cell cycle studies were performed by double labeling with BrdU and PI. Cells were pretreated with inhibitors (at concentrations described above) for 2 h and pulsed for 30 min with BrdU (30 μM). Cultures were washed with fresh medium and incubated in the presence or absence of inhibitors for 3, 9, 24 and 36 h. Samples were prepared as previously described [10].

For cell cycle studies with PI of 24 h- and 72 h-treated cells (DMSO, 100 nM Dasatinib, 5 μM PP2, 5 μM SU6656 or 5 μM ZM447439), samples were prepared as previously described [10]. Cell acquisition was performed with a FACScan flow cytometer (BD). At least 10,000 events/sample were acquired in linear (for PI) and log (for FITC) mode. The proportion of cells in subG1, G1, S, G2/M, and >4N phases was calculated with CellQuest software (BD).

2.5. Cell migration (wound healing assay)

Cells were seeded in complete medium (8×10^5 cells/60 mm plate) and grown to confluence. The monolayer was scratched with a 200 μl micropipette tip and washed with fresh medium to remove floating cells. Complete medium containing DMSO or inhibitors (concentrations as above) was added to cultures. Photomicrographs were taken at 0 h and 20 h with a Nikon Eclipse TS100 inverted microscope (Nikon, England), equipped with Olympus DP20 digital camera (Olympus, Germany). Representative fields were photographed. Assays were repeated 3 times. Magnification, ×100.

2.6. Invasion assay

Invasiveness was determined using cell culture inserts for 24-well plate (8 μm-pore PET membranes) (BD). Filters were coated with 100 μl of ice-cold Matrigel diluted in DMEM basal medium and incubated overnight at 37 °C. Cells were seeded on the upper chamber (5×10^4/well/200 μl) in serum-free medium containing DMSO or inhibitors (see migration assay). The lower chamber was filled with

300 μl of 10% FBS-supplemented medium and DMSO or inhibitors; 24 h later, cells on the top of the inserts were removed and those on the lower surface fixed in methanol, stained with 10 μg/ml DAPI/PBS and mounted on slides with ProLong antifade-reagent. Filters were observed with a Plan 20×/0.50 objective using an Axiophot fluorescence microscope (Zeiss, Germany) equipped with an Olympus DP70 digital camera. DAPI-stained nuclei were counted. Assays were performed in triplicate and repeated 4 times.

2.7. Immunofluorescence and confocal microscopy

Cells seeded on sterile coverslips were 24 h-treated with DMSO or inhibitors (see above), fixed with 3.7% paraformaldehyde/PBS (10 min, room temperature), permeabilized with 0.1% Triton X-100/PBS (5 min, room temperature) and blocked 30 min with 1% BSA/PBS. Coverslips were incubated 1 h at 37 °C with 1:200 TRITC-labeled phalloidin (1:200 in PBS-1% BSA) or with anti-α-tubulin (1:50), anti-phospho-histone H3 (1:200), then with goat-anti-mouse IgG Alexa-Fluor 488 or goat-anti-rabbit IgG Alexa-Fluor 546 (1:200) for 1 h at 37 °C. After washing with PBS, cells were counterstained with 10 μg/ml DAPI/PBS for 10 min at 37 °C and coverslips were mounted on slides with ProLong reagent. Samples were observed and photographed with a Plan Apochromat 60×/1.40 objective using a Nikon Eclipse 90i fluorescence microscope equipped with Digital Sight DS-Qi1 camera and Nis-Elements BR imaging software (Nikon).

For confocal microscopy experiments, cells were fixed and permeabilized as above, saturated with 5% goat serum/PBS, and washed with PBS-1% BSA. Samples were incubated with anti-pY118-Paxillin (1:50), anti-pY925-Fak (1:50), anti-β-catenin (1:100), anti-p120-catenin (1:100) and with the secondary antibody for 1 h at 37 °C. Confocal images were acquired using an inverted Zeiss LSM 710 laser-scanning microscope with a Plan Apochromat 60×/1.40 objective. Sequential scanning mode was used to avoid crosstalk between channels. Z-optical stacks with 0.6 μm intervals through the cell Z-axis were recorded. Images were processed with ZEN 2009 software (Zeiss) and Adobe Photoshop CS.

2.8. Time-lapse video microscopy

Live cell imaging was performed with Microscope Cell Observer Z1 system (Carl Zeiss MicroImaging GmbH, Jena, Germany) equipped with a controlled environment chamber (37 °C constant temperature, 5% CO_2 atmosphere) and Camera Cascade 1k. MDA-MB-231 cells were seeded in complete medium in 35 mm μ-dishes for live cell imaging (10^5 cells/dish) (Ibidi GmbH, Martinsried, Germany). After 24 h, cells were treated with DMSO (control) or SU6656 (5 μM). Images were collected every 15 min with a 20× Plan Apochromat objective, starting 3 h after inhibitor addition until 20 h of treatment. Time-lapse movies were formatted using imaging software AxioVision 4.8 (Zeiss) and exported in QuickTime (Apple).

2.9. 3D cell culture assay

Three-dimensional (3D) analysis of morphology was performed as previously described (G.Y. Lee, P.A. Kenny, E.H. Lee, M.J. Bissell, Nature Methods, # 4923). Cell culture dishes (24-well plates) were pre-coated with 50 μl of undiluted Matrigel (10 mg/ml) and incubated for 30 min at 37 °C to allow Matrigel to gel. Cells were prepared by trypsinization from tissue culture plastic and resuspension in complete medium (see "Cell cultures" section) for counting. To analyze the effects of SFK selective inhibitors on 3D cell growth, 10^4 cells (per well of a 24-well plate) were resuspended in 300 μl of a mixture of complete medium/Matrigel (1:3) containing DMSO (control), Dasatinib (100 nM), PP2 (5 μM) or SU6656 (5 μM). Then, they were seeded over the gelified coat Matrigel and incubated for at least 30 min at 37 °C. 500 μl of complete medium containing DMSO or SFK selective inhibitors was added to the cultures and changed every 2–3 days until 21 days. To assess the effects of the inhibitors on MDA-MB-231 spheres already formed, drugs were added after a 21-day period of growth and maintained for additional 7 days. Treatments were performed in triplicate and assays were repeated 2 times. Cultures were observed at 10× magnification under a Nikon Eclipse TS100 inverted microscope (Nikon Instruments Europe B.V., Kingston, Surrey, England), equipped with Olympus DP20 digital camera (Olympus Europe GmbH, Hamburg, Germany), and representative fields were photographed.

2.10. Western blotting

Cells were washed in ice-cold PBS and lysed, and Western blot (WB) analyses of phospho-proteins/proteins were carried out as previously described [10].

2.11. Aurora B kinase activity assay

Exponentially growing cultures were lysed at 4 °C in lysis buffer (50 mM Hepes, pH 8, 600 mM KCl, 0.5% Nonidet P40, 1 mM Na_3VO_4, 1 mM DTT, 0.1 mM protease inhibitors). Aurora B kinase was immunoprecipitated from total cell extracts [19]. Immune-complexes were incubated with histone H3 (1 μg) for 30 min at 37 °C in kinase assay buffer (20 mM Hepes, pH 7.4, 150 mM KCl, 5 mM $MnCl_2$, 5 mM NaF, 1 mM DTT, 30 μM cold ATP) in the presence or absence of 1 μM SU6656. pS10-H3, H3 and Aurora B kinase expression were determined by WB.

2.12. Gene expression analyses

Cell cultures (70% confluent) were treated with 100 nM Dasatinib, 5 μM PP2 or SU6656 for 72 h. RNA was isolated using RNeasy kit from Qiagen (Valencia, USA) from three independent experiments carried out in triplicate. After testing for RNA integrity, triplicate RNAs from each treatment/experiment were pooled. Total RNA (10 μg) was used to prepare probes, and then targets were hybridized to "Agilent SurePrint G3 Human GE 8x60k Microarray" (Santa Clara, USA) following manufacture instructions.

Analysis for differential expression was performed using the Rplatform for statistical analysis (R Foundation for Statistical Computing, Vienna) and several packages from the Bioconductor project (http://www.bioconductor.org/). The raw data were imported into R and preprocessed using the half method for background correction and the quantile method for normalization. Probes with expression level below the detection control probe in all samples were removed. To identify differentially expressed genes, we used the limma package. Correction for multiple testing was accomplished by controlling the false discovery rate using the method from Benjamini and Hochberg [20]. Genes were selected as differentially expressed with $P_{adjust} \leq 0.05$. Hierarchical clustering analysis of gene expression profiles was carried out using the complete linkage method.

2.13. Gene Set Enrichment Analysis (GSEA)

Gene Set Enrichment Analysis [21] was applied using annotations from BioCarta, KEGG and Reactome pathway databases together with Src gene set previously reported [22]. Genes were ranked based on limma moderated t statistic. After Kolmogorov–Smirnov testing, those gene sets showing FDR ≤0.05, were considered significantly enriched among compared treatments.

3. Results

3.1. Effect of Dasatinib, PP2 and SU6656 on cell viability, SFKs kinase activity, migration and invasiveness of MDA-MB-231 cells

To determine the concentrations of inhibitors to be used in our study, we tested the effects of 72 h-treatment with different concentrations by MTT assay. As observed in Fig. 1A, at 100 nM Dasatinib (Das) and at 5 μM PP2 and SU6656 (SU) the mitochondrial metabolic activity was reduced to about 55% with respect to control cells (DMSO, vehicle). Viability studies using trypan blue exclusion test indicated that all three compounds inhibited cell proliferation, as shown by the reduced number of viable cells counted after 72 h-treatment (Fig. 1A). Furthermore, the percentage of trypan blue-positive cells was lower than 5% in all treatments (data not shown), suggesting that, under these experimental conditions, inhibitors were not cytotoxic. Consequently, these concentrations were employed in the following experiments. Furthermore, we determined

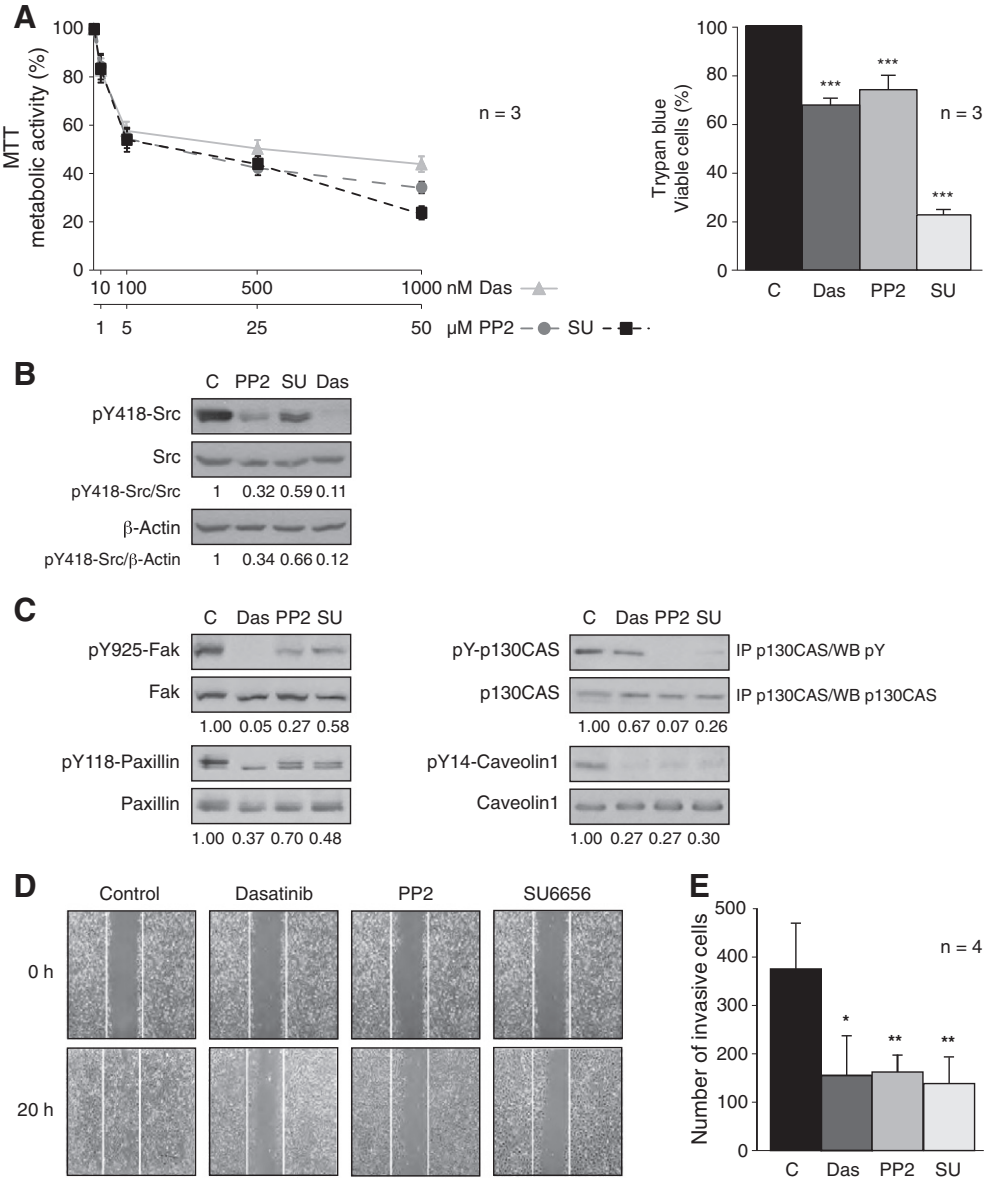

Fig. 1. Effect of Dasatinib, PP2 and SU6656 on MDA-MB-231 viability, SFKs catalytic activity, migration and invasion. A) Cells seeded in 96-well plates (1.8×10^4 cells/well) were incubated for 72 h with Dasatinib (Das), PP2 or SU6656 (SU). Metabolic activity (%) was calculated considering the value of control (DMSO-treated) at 72 h as 100%. For trypan blue assay, cells plated in 35 mm-dishes were treated with DMSO (C, control), Das (100 nM), PP2 (5 μM) or SU (5 μM) for 72 h and then counted in the hemocytometer with 0.4% trypan blue solution. The percentage of viable cells was calculated considering the value from control sample as 100%. Results represent the average and standard deviations (SD, bars) of three independent experiments carried out in triplicate; asterisks indicate significant differences between treated and control cells (***$P\leq0.001$). B) Extracts from cells incubated with DMSO (1:1000), PP2 (5 μM), SU (5 μM) or Das (100 nM) for 16 h were blotted with anti-pY418-Src, anti-c-Src (327) and anti-β-actin for loading control. Results are representative of three independent experiments. Ratios of pY418-Src/Src and pY418-Src/β-actin were determined by densitometry and values normalized versus control cells. C) Cell lysates from cultures treated for 24 h with either DMSO (C), Das, PP2 or SU (as above) were probed for pY925-Fak, pY118-Paxillin, pY14-Caveolin-1; p130CAS was immunoprecipitated from total cell extracts and immuno-complexes analyzed by WB with anti-pY (4G10). Membranes were reblotted with anti-total-protein as loading control. Results are representative of three independent experiments. Ratios of phosphorylated/total-protein were normalized versus control cells. D) Cell migration by wound healing assay after treatment with DMSO, Dasatinib, PP2 or SU6656 (as above) for 20 h. Fields are representative of three independent experiments performed in triplicate. Magnification, ×100. E) For invasiveness, cells (5×10^4) were seeded on modified Boyden chamber coated with Matrigel in serum-free media containing DMSO (C), Das, PP2 or SU (as above). After 24 h, cells on the lower surface of the filters were DAPI-stained and counted (see Materials and methods). Four independent experiments were made in triplicate. *$P<0.05$, **$P<0.01$ (Student t-test).

the effects of inhibitors on three-dimensional growth of MDA-MB-231. When cultures were treated from the beginning, SU6656 inhibited sphere formation (cells were not able to divide and showed enlarged size), while Dasatinib and PP2 reduced sphere size. If inhibitors were added after sphere formation (21 days), control samples showed continuously growing spheres (21 + 7 days-DMSO), while in the presence of the inhibitors sphere size remained unaltered (21 + 7 days-PP2 or SU6656) or it clearly appeared reduced (21 + 7 days-Dasatinib) (Suppl. Fig. 1). DAPI stain of fixed spheres seemed to exclude necrotic/apoptotic cells in treated 3D cultures (data not shown).

Next, we verified if inhibitor concentrations that reduced cell viability and proliferation were able to efficiently inhibit SFKs catalytic activity. To this aim, exponentially growing cultures were treated for 16 h with DMSO (vehicle), PP2, SU6656 or Dasatinib. Western blot analyses of lysed cell with anti-phospho-Y418-Src showed that all three compounds clearly reduced phosphorylation of Y418-Src (Fig. 1B).

The oncogenic potential of increased SFKs catalytic activity in tumor cells is pleiotropic and controls cytoskeletal-linked events, such as extracellular matrix-adhesion, migration, and invasion, which are associated to SFKs substrates including Fak, p130CAS and paxillin involved in integrin signaling and in adhesion dynamics [1,4]. We have then analyzed whether SFKs inhibitors affected the phosphorylation of these proteins. Phosphorylation of Y925-Fak by Src observed in DMSO-treated cells was inhibited upon 24 h treatment with Dasatinib, PP2 or SU6656 (Fig. 1C).

Activated Src-Fak complex engages and phosphorylates other proteins of focal adhesion complex, including paxillin and p130CAS [10]. Dasatinib, PP2 or SU6656, employed as above, strongly reduced Y118-paxillin phosphorylation as compared to DMSO-treated cells. Likewise, the amount of tyrosine-phosphorylated p130CAS was also diminished (Fig. 1C, IP p130CAS/WB pY).

Caveolin-1, a multifunctional membrane protein responsible for caveolae formation, is phosphorylated by SFKs at Y14 and mediates tumor migration and invasion through Rho/ROCK [9]. As observed here, these inhibitors clearly reduced pY14-caveolin as compared to control cells (Fig. 1C). Furthermore, we tested by confocal microscopy the expression and distribution of pY118-paxillin and pY925-Fak and their relationship with actin cytoskeleton (phalloidin-TRITC labeling). In control cells pY118-paxillin and pY925-Fak accumulated in focal adhesion area; after inhibitor treatments a consistent reduction of pY118-paxillin and pY925-Fak was observed (Suppl. Figs. 2 and 3). Actin cytoskeleton, characterized by stress fibers in untreated samples, showed a thickness of these structures at the cell edge after PP2 treatment. Dasatinib caused alterations of cytoskeleton structure with collapse of actin microfilaments. SU6656-treated cells maintained actin stress fibers, although in some cells, a thickening of these filaments was observed at the edges (Suppl. Figs. 2 and 3).

Since these inhibitors altered focal adhesion molecules and actin structures, we analyzed subcellular localization of β-catenin and p120 catenin. Treatments increased membrane-localized β-catenin and p120 catenin (Suppl. Figs. 4 and 5), while the total levels of both proteins remained unchanged, as observed by Western blot (data not shown).

Inhibition of focal adhesion protein phosphorylation and altered cellular distribution of catenins should lead to a reduction in adhesion dynamics and to inhibition of migration and invasion. To test this hypothesis, we determined the migration and invasion capability of MDA-MB-231 cells upon treatment with SFKs inhibitors. Migration assayed by wound healing repair showed that control cells migrated to heal the wound. Treatments with Dasatinib, PP2 and SU6656 clearly reduced cell migration (Fig. 1D). For invasion assay, cells treated with DMSO, Dasatinib, PP2 or SU6656 were loaded on the top of Matrigel in a Boyden chamber; those able to move throughout this extracellular matrix were then counted as a measurement of invasion (see Materials and methods). All three inhibitors significantly reduced cell invasion (Fig. 1E), suggesting that SFKs catalytic activity is involved in MDA-MB-231 cell migration and invasion processes.

3.2. Effects of SFKs inhibitors on cell cycle progression and morphology of MDA-MB-231 cells and SYF fibroblasts

Inhibition of cell proliferation induced by SFKs inhibitors could be ascribed to alteration of cell cycle progression. Studies performed by double labeling with BrdU and PI showed that treatment with Dasatinib or with PP2 induced G1 accumulation and reduced the number of cells in S or G2/M compartments as compared to control cells (Fig. 2A). Surprisingly, SU6656 caused an aberrant cell cycle; G1 and S phases decreased with time, and the G2/M started to decline after 24 h. A new set of cells that accumulated DNA (>4N) increased constantly (Fig. 2A). Thus, Dasatinib and PP2 appeared to affect G1–S transition, while SU6656 generated polyploidy.

To confirm these results, cell cycle was analyzed at longer time (72 h) by PI labeling. Dasatinib and PP2 caused accumulation of cells in G1 and reduced the number of cells in S and G2/M phases. The >4N compartment was minimal as in control cells (Fig. 2B). SU6656 reduced cells in G1 and S compartments, increased cells in G2/M and provoked a 60% increase of polyploid cells (Fig. 2B). Consistently, this compound did not inhibit DNA duplication, but it probably blocked completion of cell cycle, which is reliable with the strong reduction of cell number determined by trypan blue (Fig. 1A). It should be noticed that, besides the absence of cells in Sub-G1, no PARP degradation was detected (data not shown), suggesting that these compounds, under these experimental conditions, did not induce apoptosis.

In agreement with accumulation of cells in G1 upon treatment with Dasatinib and PP2, $p27^{Kip1}$ expression increased and c-Myc levels decreased as compared to control growing cells (Fig. 2C). Since SU6656 did not alter G1–S transition, expression of $p27^{Kip1}$ and c-Myc were similar to control cultures (Fig. 2C).

The differential effects induced by SU6656 as compared to Dasatinib and PP2 on viability, proliferation and cell cycle progression may be reflected on cell morphology. Then, we carried out double immunofluorescence labeling of nuclei and microtubules (see Materials and methods). Dasatinib-treated cells showed partially collapsed microtubule structure defining a pseudo-spherical shape (Fig. 2D). Tubulin staining pattern induced by PP2 was relatively similar to control cells, although cells adopted an elongated morphology (Fig. 2D). In SU6656-treated cells, microtubule cytoskeleton was also maintained. However, cell size clearly increased and multinucleation was induced (arrows indicated an example of several nuclei within a cell) (Fig. 2D), supporting the hypothesis that SU6656 blocked cell division.

To confirm this blockage, we carried out a 24 h videomicroscopy of cells treated with DMSO or with SU6656. While control cells divided along the time course of the experiment, SU6656-treated cells detached from the culture plate and before completing cell division re-attached giving rise to bigger multinucleated cells (Suppl. Videos 1 and 2).

These findings suggest that SU6656, in addition to inhibit SFKs, was affecting other targets that, in turn, could account for this unusual response as compared to Dasatinib and PP2. To support this hypothesis, we investigated whether SU6656 provoked similar cell cycle and morphological alterations in cells that do not express SFKs, such as mouse SYF fibroblast derived from triple deletion of *c-src*, *yes* and *fyn* [23]. Cell cycle analyses after PI labeling showed that 24 h treatment with Dasatinib or PP2 had no effects as compared with DMSO-treated cells (Fig. 3A), which is consistent with the fact that SYF fibroblasts do not express SFKs. SU6656 strongly reduced cells in G1 and S phases and increased the number of cells in G2/M and >4N compartments (Fig. 3A). Consistently, Dasatinib or PP2 did

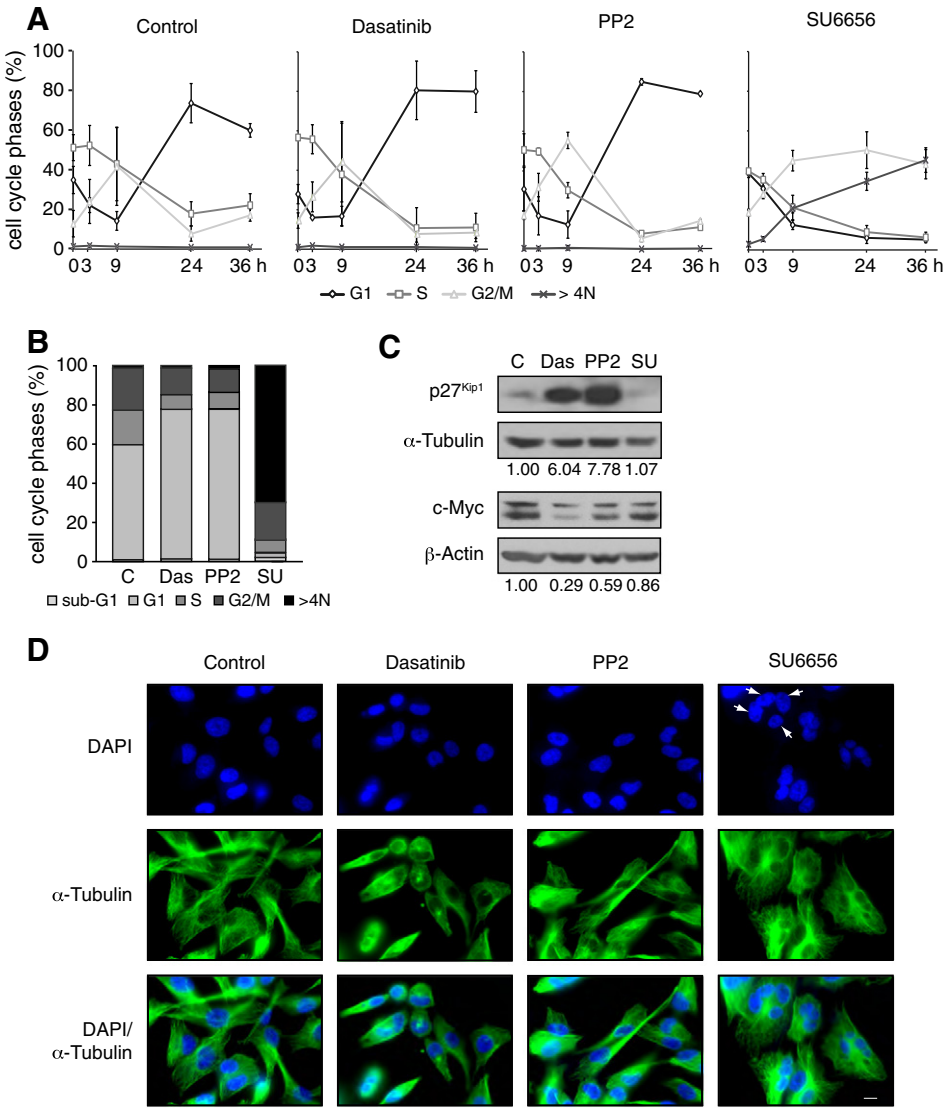

Fig. 2. Effects of Dasatinib, PP2 and SU6656 on MDA-MB-231 cell cycle progression, p27^{Kip1} and c-Myc expression, morphological features. A) Cell cycle analysis by pulse/chase BrdU and PI labeling of cells treated with DMSO (Control), Dasatinib (100 nM), PP2 (5 μM) or SU6656 (5 μM). Cells were collected at indicated times and analyzed by flow cytometry. Results are expressed as percentage of BrdU-labeled cells in the G1, S, and G2/M phases, as defined by PI label. Results represent the average ± SD of four independent experiments. B) Cell cycle analysis by PI labeling of MDA-MB-231 after treatments with DMSO (C), Das, PP2, SU (as above) for 72 h. Cell percentages in cell cycle phases (sub-G1, G1, S, G2/M, >4N) were calculated from DNA histograms by CellQuest software. C) Lysates from cells treated for 24 h with DMSO (C), Das, PP2 or SU (as above) were analyzed by WB for p27^{Kip1} and c-Myc. Membranes were reblotted either with anti-α-tubulin or β-actin for loading control. Results are representative of three independent experiments. D) Immunofluorescence of cultures treated with DMSO (Control), Dasatinib, PP2 and SU6656 (as above) for 24 h. Cells were labeled for DNA (DAPI, blue) and for microtubules (anti-α-tubulin, green). Representative images captured with a Nikon Eclipse 90i fluorescence microscope. Bar = 10 μm. Arrows show a multinucleated cell.

not significantly alter cell morphology as compared to control cultures (Fig. 3B). In contrast, SU6656 produced enlarged multinucleated cells (arrows indicated several nuclei within a cell) (Fig. 3B). Together, these results resemble those induced by SU6656 in MDA-MB-231 cells (Fig. 2B and D). It should be noted that SU6656 caused similar alterations in MCF7 and SUM159 human breast cancer cell lines (data not shown), suggesting that SU6656-mediated cell cycle alteration is a common effect in breast cancer cells.

3.3. Differential effects of SU6656 versus Dasatinib and PP2: inhibition of Aurora B kinase

Blockage of cell division by SU6656 suggests that a kinase involved in regulation of mitosis and cell division could also be affected. Among these enzymes, Aurora B kinase, which inhibition causes polyploidy in a variety of human tumor cell lines [24], is inhibited in vitro by SU6656 [18,25]. Therefore, we compared the effects of SU6656 (5 μM) and ZM447439 (5 μM), a selective inhibitor of Aurora B kinase [19,26], on cell cycle progression and morphology of MDA-MB-231 cells. After 24 h treatment, cell cycle analyses by PI labeling showed that both inhibitors reduced cells in G1 and S phases and robustly increased cells in G2/M and >4N compartments (Fig. 4A). Immunofluorescence analyses showed that both SU6656 and ZM447439 induced multinucleated cells (arrows indicated several nuclei within a cell) (Fig. 4B). Since serine-10 of histone H3 is a canonical substrate for Aurora B kinase [19,24,26,27], we investigated whether SU6656 blocked this phosphorylation, using ZM443979-treated cells as a positive control. Exponentially growing cultures treated 24 h with SU6656 or with ZM443979 showed strong reduction of pS10-H3 as compared to control cultures (Fig. 4C). We then immunoprecipitated Aurora B kinase from cultures treated for 24 h with DMSO or with SU6656 and

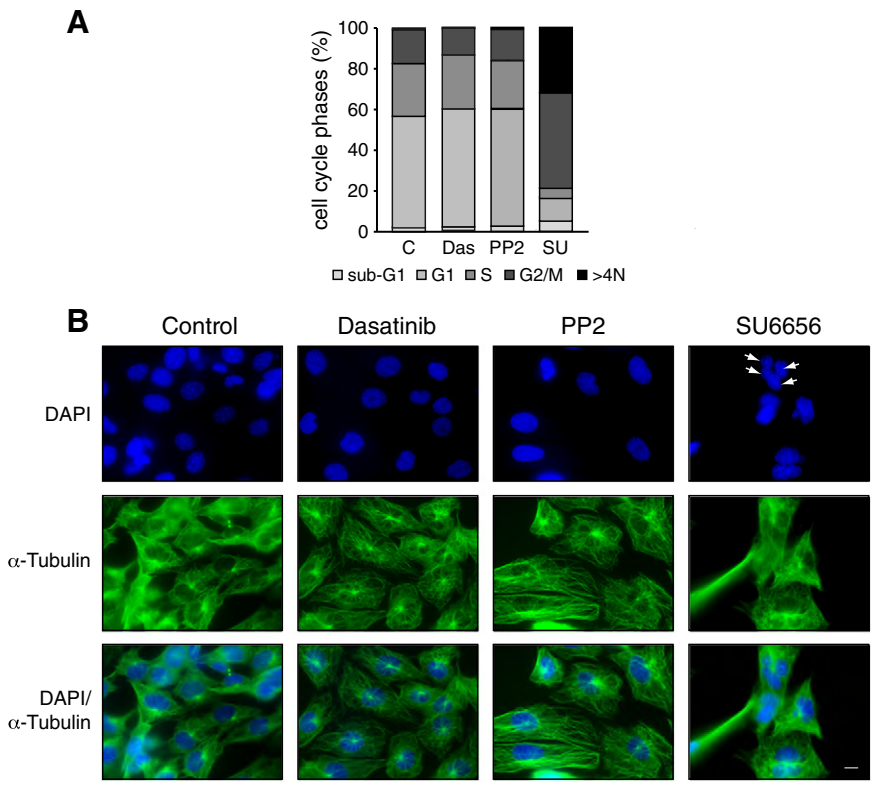

Fig. 3. Effects of Dasatinib, PP2 and SU6656 in SYF fibroblasts. A) Cell cycle analyses of SYF cells treated with DMSO (C), Das (100 nM), PP2 (5 μM) and SU (5 μM) for 24 h. PI labeling was carried out as in Fig. 2B. B) Cultures treated as above were labeled with DAPI and with anti-α-tubulin and analyzed by immunofluorescence as in Fig. 2D. Arrows indicate a multinucleated cell. Bar = 10 μm.

carried out in vitro kinase assay using purified histone H3 as a substrate (see Materials and methods). The level of pS10-H3 detected in immuno-complexes from SU6656 treated cells was strongly diminished as compared to those from control cells (Fig. 4D). As the amounts of H3 and Aurora B kinase in the immuno-complex reactions were similar, it can be argued that SU6656 inhibited Aurora B kinase activity in MDA-MB-231 cells. Fluorescence microscopy of mitotic cells stained with DAPI, α-tubulin and pS10-H3 confirmed these results. As compared to control cells, 24 h treatment with SU6656 or with ZM443979 induced the appearance of cells with multiple spindle poles and drastic reduction of pS10-H3 staining (Fig. 4E), a characteristic phenotype of Aurora B kinase-inhibited cells [28]. Together these data showed that SU6656 mimicked the effects of ZM443979 in cell cycle, morphology and histone H3 phosphorylation and suggest that SU6656 inhibited cell division of MDA-MB-231 cells by blocking the functionality of Aurora B kinase.

3.4. Differential gene expression induced by Dasatinib, PP2 and SU6656

In view of the differential responses of SU6656 versus Dasatinib and PP2 for cell cycle regulation, we engaged analyses of gene expression profiles induced by these compounds. All studies were carried out in triplicate and RNA was used to hybridize Agilent microarrays. One of SU6656 triplicate was discarded because it did not pass quality control standards. All treatments resulted in gene expression changes. Using a statistical cut-off of P*adjust* ≤0.05, we obtained 1866 differentially expressed probes (1641 annotated sequences) after Dasatinib treatment, 21 after SU6656 (15 annotated sequences) and 16 probes after PP2 treatment. The complete list of genes is provided in Suppl. Table 1. The hierarchical clustering of all individual data representing all selected differentially expressed sequences is shown in Fig. 5A. The columns contain data for individual samples, which clustered in four groups as a function of treatment, and indicated that replicates were fairly homogeneous. The rows show relative intensities of the probes and defined two main clusters of differentially expressed genes, having higher or lower expression after treatments. The results revealed that the effects of Dasatinib were more pronounced than those of PP2, although in most cases there was also an effect, but of lower intensity. This gene expression pattern did not correspond to that observed for SU6656 treatment, which is more similar to DMSO-treated cells (Control). The comparisons of each individual treatment versus control using plot profile representations are shown in Fig. 5B. These plots show expression values along different samples for probes selected as differentially expressed in the three treatment groups. The data indicated again that Dasatinib produced large changes of gene expression that diverged to control and SU6656 samples and to lower degree to PP2. Although only a reduced number of genes passed the statistical analysis after PP2 treatment, the plots showed that there was a great agreement between PP2 and Dasatinib. The PP2 versus Control analysis showed two main clusters, PP2-Dasatinib, and SU6656-Control. Instead, in the evaluation of SU6656 versus Control, a set of genes defined in an individual group that differed from the rest of treatments. In addition, almost all genes selected in PP2 and Dasatinib groups did not alter their expression after SU6656 treatment.

Furthermore, to study pathways of gene expression related to biological functions analyzed above upon different treatments, GSEA [21] was applied using annotations from BioCarta, KEGG and Reactome pathway databases together with Src gene set previously reported [22]. The analyses (Suppl. Table 2) showed that most of the pathways detected were down regulated in each treatment. Exceptionally, glycolysis was upregulated in Dasatinib-treated cells, while asthma and autoimmune thyroid disease were increased in

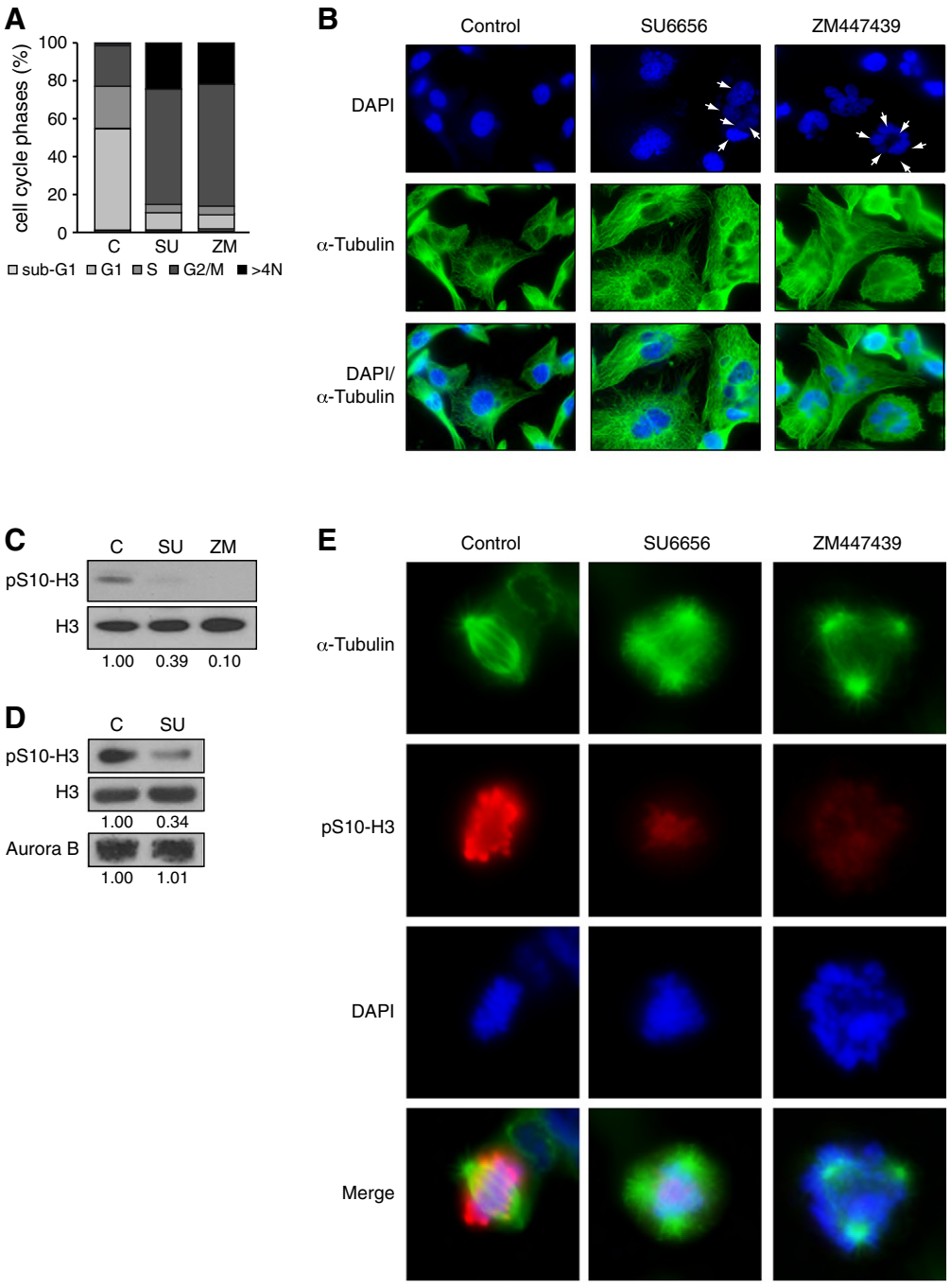

Fig. 4. Comparative effects of SU6656 and ZM447439 in MDA-MB-231 cells. A) Cell cycle analyses by PI labeling of cultures treated with DMSO (C), SU (5 μM) or ZM447439 (ZM, 5 μM) for 24 h were performed as in Fig. 2B. B) Immunofluorescence of cells labeled with DAPI and with anti-α-tubulin performed as in Fig. 2D. Arrows show multinucleated cells. Bar = 10 μm. C) Histone H3 phosphorylation (pS10-H3) determined by WB in extracts of cell treated with DMSO (C), SU or ZM (as above) for 24 h. Membranes were blotted against anti-histone H3 (H3) for loading control. Results are representative of three independent experiments. D) Aurora B kinase was immunoprecipitated from cultures treated with DMSO (C) or SU (5 μM) for 24 h. Immune-complexes were incubated with histone H3 in the presence or absence of SU6656 (1 μM) and ATP; the extent of S10-H3 phosphorylation determined by WB. Membranes were reblotted with anti-histone H3 and anti-Aurora B kinase for loading control. Results are representative of three independent experiments. E) Immunofluorescence micrographs of mitotic MDA-MB-231 cells. Control and treated cells (SU6656 or ZM447439 at 5 μM, 24 h) were labeled for DNA (DAPI, blue), microtubules (anti-α-tubulin, green) and pS10-histone H3 (anti-pS10-H3, red). Representative images of mitotic figures show multiple spindle poles in inhibitor-treated cells.

PP2-treated cells. Some pathways were shared by Dasatinib, PP2 and SU6656, while others appears to be more specific. These pathways can be summarized in main categories. Common to all three treatments are pathways involved in different processes of cell cycle regulation, immune system and metabolism of lipids and lipoproteins. Dasatinib and PP2 shared pathways involved in signaling by EGFR in cancer, by GPCR and by NGF. In addition of cell cycle regulation, metabolism of carbohydrates was common in PP2 and SU6656, while pathways involved in renal cell carcinoma, pancreatic, bladder and colorectal cancer and WNT signaling appeared to be specific for SU6656. Interestingly, GSEA analyses of Src gene pathway (Suppl. Table 3) showed a significant reduction upon SU6656 treatment (FDR = 0.024), while PP2 and Dasatinib treatments had FDR > 0.05 (0.083 and 0.193, respectively).

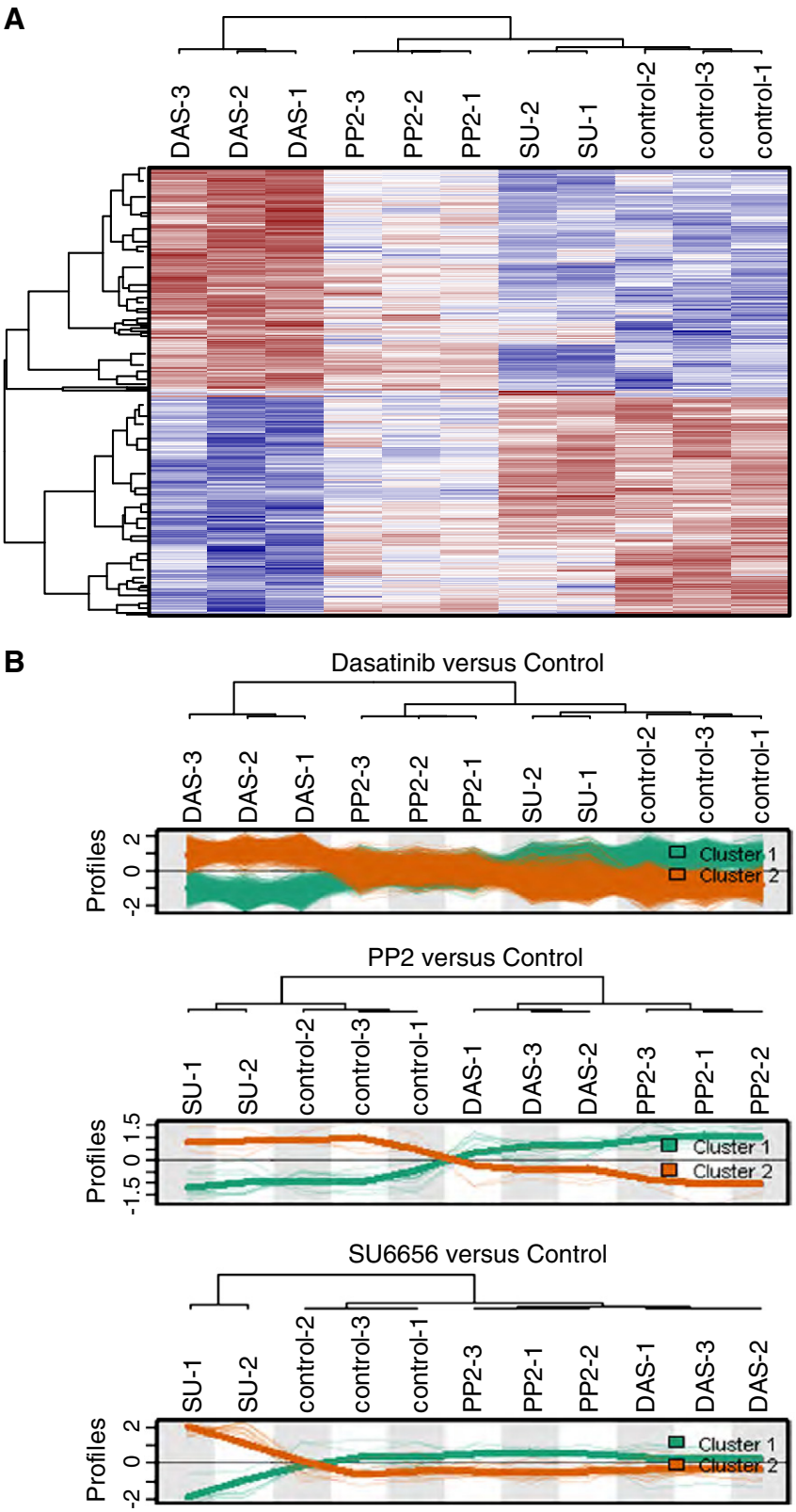

Fig. 5. Gene expression profiles regulated by Dasatinib, PP2 and SU6656. A) Hierarchical clustering (heat map) of all individual data representing the differentially expressed sequences after the three treatments at P*adjust* ≤0.05. Columns correspond to samples; row corresponds to individual probe sets. Intensities were normalized across the rows. Normalized log intensity values of probes were centered to the median value of each probe set and colored on a range of +2 (red) and −2 (blue); white indicates intermediate value. B) Comparisons between effects of Dasatinib, PP2 and SU6656 treatments are shown in plot profiles. Signal intensities are normalized as in the heat map and expression values are colored based on the overall pattern. For each pattern, a loess (locally weighted polynomial regression) fit line describes the overall profile of the corresponding group. This tendency profile is plotted up-regulated sequences (Cluster 1, green) and down-regulated sequences (Cluster 2, orange).

4. Discussion

SFKs regulate signaling pathways engaged in the control of many cellular processes. As they are frequently deregulated in numerous tumors including breast cancer [3–6], their catalytic activity has been considered as a target for cancer therapy. Since there are not fully specific inhibitors of SFKs, here, we studied the role of SFKs catalytic activity in human triple-negative/basal-like MDA-MB-231 breast cancer cells employing Dasatinib, PP2 and SU6656 selective inhibitors. Interestingly, while these compounds inhibited pY418-Src, GSEA analysis showed that Src gene set expression was significantly reduced by SU6656. All three compounds significantly reduced cellular proliferation, migration and invasion.

SFKs, directly or through a complex with Fak, control pathways involved in the dynamics of focal adhesions, which are engaged in the regulation of cellular migration and invasiveness [1,4]. Thus, Src/Fak phosphorylates proteins of the focal adhesion complex including paxillin, p130CAS, as well as caveolin-1. Consistent with inhibition of SFKs catalytic activity by Dasatinib, PP2 and SU6656, tyrosine phosphorylation of paxillin, p130CAS and caveolin-1 was reduced, cytoskeleton architecture was altered and cellular migration and invasiveness were also inhibited. In this context, we previously showed that the functionality of SFKs was essential for cellular migration, spreading and adhesion of MCF7 cells [10]. Here, we observed that migration of SYF fibroblasts, which lack SFKs, was not altered by Dasatinib, PP2 or SU6656 treatments (data not shown). Together, these data suggest that reduction caused in MDA-MB-231 cells by these compounds could be ascribed to inhibition of SFKs catalytic activity.

Concomitantly, GSEA analysis of the gene expression patterns showed that these inhibitors also down-regulated several pathways associated with migration, cell motility and cytoskeleton reorganization, which in turn could affect cell invasion.

Studies in different tumor cells support these results. Dasatinib reduced migration and invasion in head and neck squamous cell carcinoma, non-small cell lung cancer [29] and in breast cancer cell lines [30,31]. Interestingly, basal-like/triple-negative breast cancer cell lines with high levels of caveolin-1 expression, like MDA-MB-231 cells, are characterized by sensitivity to Dasatinib, while low expression of caveolin-1 correlates with resistance [32]. In MDA-MB-231 and BT-549, inhibition of SFKs by SU6656 suppresses invadopodia formation while enhances tubulin-based microtentacle, effects associated with reduced cellular invasion [33]. PP2 also inhibits invasion in MDA-MB-231 [34] and ovarian cancer cells [35].

Dasatinib, PP2 and SU6656 significantly reduced cell proliferation and specifically altered cellular morphology. Dasatinib generated pseudo-spherical cells, PP2 caused elongated spindle morphology and SU6656 produced flattened enlarged cells, indicating that they affected additional targets. SU6656 similarly altered morphology of SYF fibroblasts, while Dasatinib and PP2 did not. Therefore, the changes induced by SU6656 in MDA-MB-231 seem to be independent on SFKs catalytic activity. Our results concerning effects of Dasatinib on cell proliferation are similar to those previously described [30]. Others have reported that Dasatinib induces cell death and apoptosis in tumor cell lines including MDA-MB-468 [36], head and neck squamous cell carcinoma, non-small cell lung cancer cells and in osteosarcoma and Ewing's subset of bone sarcomas [29,37]. In contrast, in our study Dasatinib, PP2 and SU6656 did not induce cytotoxic effects.

Concomitant with inhibition of cell proliferation, Dasatinib and PP2 reduced c-Myc expression and increased $p27^{Kip1}$ levels, which are consistent with a blockage of cell cycle progression in G1. Dasatinib and PP2 produced similar results in studies conducted in MDA-MB-231, W53 lymphoid cells, MCF7 and in ovarian cancer cells [2,11,30,35]. Also, interfering SFKs functionality by conditional expression of SrcDN in MCF7 cells causes accumulation in G1 and increased $p27^{Kip1}$ expression [10].

Interestingly, SU6656 neither blocked G1 to S transition, nor induced $p27^{Kip1}$ expression, causing only a small reduction of c-Myc levels. Instead, SU6656 caused polyploidy. These findings could explain the quantitative differences observed between trypan blue and MTT proliferation assays. In trypan blue assays, SU6656 induced an inhibitory effect more evident (80%) than Dasatinib or PP2 (25–35%), while in MTT assays the inhibition was quite similar (approximately 45%). Analyzing cell cycle progression with BrdU/PI labeling at 24 h or with PI at 72 h solved discrepancy between these two methods. In both assays, Dasatinib and PP2 increased cell number in G1, suggesting that they blocked G1–S transition. Consistently, GSEA analysis showed that G1/S transition pathway (Reactome) is down regulated in Dasatinib and PP2-treated cells (FDR $\leq 1\times10^{-6}$). In contrast, SU6656 caused accumulation of large polyploid multinucleated cells, suggesting that it did not block cell cycle at a particular phase. Instead, cells seemed to enter and go out of mitosis but failed to divide. This implies that cell continued to be metabolically active in order to synthesize all components necessary for cycling, which explains higher values obtained with MTT than with trypan blue assay. Indeed, time-lapse video microscopy showed that SU6656 treated cells detached from the substrate just before cell division but, in contrast to dividing control cells, they re-attached and did not complete cytokinesis, generating enlarged cells. SU6656 also induced polyploidia and multinucleation of SUM159 and MCF7 human breast cancer cell lines (data not shown). Since MCF7 has a functional p53, while MDA-MB-231 and SUM159 have p53 mutated [38], these effects appear to be p53 independent.

Polyploidy has been also observed in B-lymphocytes, non-Hodgkin's lymphoma and megakaryocytic cells upon treatment with SU6656 [25,39]. SU6656 caused similar effects in SYF, indicating that SU6656 is targeting additional kinases involved in cell division. Indeed, SU6656 inhibits Aurora B kinase in vitro [18]. It is well established that Aurora B kinase, in addition to phosphorylate S10-H3, is a spindle checkpoint kinase required for cytokinesis and its inhibition eliminates mitotic checkpoint generating polyploid multinucleated cells [24]. We found that ZM447439, a known inhibitor of Aurora B kinase [19,26], produced similar effects as SU6656 in cell cycle progression, morphological alterations and inhibition of S10-H3 phosphorylation in MDA-MB-231 cells. Furthermore, SU6656 also inhibited Aurora B kinase in these cells. Similar results were observed in megakaryocytic [25] and MCF7 cells [27].

Since Aurora B kinase is required for completion of mitosis, chromosome segregation and cytokinesis, and is up-regulated in a variety of tumors, it is considered as relevant target in cancer therapy [40,41]. In this context, AZD1152, another Aurora B kinase inhibitor, blocks proliferation in human breast cancer cell lines and reduces lung metastasis of MDA-MB-231 in nude mouse [42].

In conclusion, our results in human metastatic breast cancer cells indicate that SFKs catalytic activity is required for proliferation, migration and invasiveness, through the regulation of molecular pathways involved in these cellular processes. Of particular interest is SU6656 that being a dual SFKs/Aurora B kinase inhibitor could have a potential use as a therapeutic agent in metastatic breast cancer.

Supplementary materials related to this article can be found online at doi:10.1016/j.cellsig.2012.02.011.

Authorship

M.P. Sánchez-Bailón, A. Calcabrini, D. Gómez-Domínguez, E. Martín-Forero and J. Martín-Pérez performed the experiments, analyzed the data, made figures and reviewed the manuscript; B. Morte and G. Gómez-López analyzed the microarray data and

contributed to write the manuscript; A. Molinari and K-U. Wagner discussed the experimental data and contributed to write the manuscript; J. Martín-Pérez conceived and designed the experiments, analyzed the data, and wrote the manuscript.

Acknowledgments

Authors are thankful to J. León, A. Sánchez-Pacheco, A. Muñoz, A. Zambrano, A. Aranda for comments and suggestions and L. Naranjo-Valencia and N. Guillén Díaz-Maroto for assistance. This work was supported by grants from Ministerio de Ciencia e Innovación [SAF2009-09254] and Fundación de Investigación Médica Mutua Madrileña. M.P. S-B. was supported by a FPI fellowship from Ministerio de Ciencia e Innovación, and A.C. was partially supported by a grant from Fundación de Investigación Médica Mutua Madrileña. J. M-P. is a member of GEICAM.

References

[1] S.M. Thomas, J.S. Brugge, Annual Review of Cell and Developmental Biology 13 (1997) 513–609.
[2] J.J. Acosta, R.M. Munoz, L. Gonzalez, A. Subtil-Rodriguez, M.A. Dominguez-Caceres, J.M. Garcia-Martinez, A. Calcabrini, I. Lazaro-Trueba, J. Martín-Pérez, Molecular Endocrinology 17 (2003) 2268–2282.
[3] E.L. Mayer, I.E. Krop, Clinical Cancer Research 16 (2010) 3526–3532.
[4] M. Guarino, Journal of Cellular Physiology 223 (2010) 14–26.
[5] J.M. Summy, G.E. Gallick, Cancer Metastasis Reviews 22 (2003) 337–358.
[6] X.H. Zhang, Q. Wang, W. Gerald, C.A. Hudis, L. Norton, M. Smid, J.A. Foekens, J. Massague, Cancer Cell 16 (2009) 67–78.
[7] V.G. Brunton, E. Avizienyte, V.J. Fincham, B. Serrels, C.A. Metcalf III, T.K. Sawyer, M.C. Frame, Cancer Research 65 (2005) 1335–1342.
[8] T.M. Williams, M.P. Lisanti, American Journal of Physiology Cell Physiology 288 (2005) C494–C506.
[9] B. Joshi, S.S. Strugnell, J.G. Goetz, L.D. Kojic, M.E. Cox, O.L. Griffith, S.K. Chan, S.J. Jones, S.P. Leung, H. Masoudi, S. Leung, S.M. Wiseman, I.R. Nabi, Cancer Research 68 (2008) 8210–8220.
[10] L. Gonzalez, M.T. Agullo-Ortuno, J.M. Garcia-Martinez, A. Calcabrini, C. Gamallo, J. Palacios, A. Aranda, J. Martin-Perez, Journal of Biological Chemistry 281 (2006) 20851–20864.
[11] J.A. Fresno Vara, M.A. Dominguez Caceres, A. Silva, J. Martín-Pérez, Molecular Biology of the Cell 12 (2001) 2171–2183.
[12] M.A. Dominguez-Caceres, J.M. Garcia-Martinez, A. Calcabrini, L. Gonzalez, P.G. Porque, J. Leon, J. Martin-Perez, Oncogene 23 (2004) 7378–7390.
[13] M. Grimmler, Y. Wang, T. Mund, Z. Cilensek, E.M. Keidel, M.B. Waddell, H. Jakel, M. Kullmann, R.W. Kriwacki, L. Hengst, Cell 128 (2007) 269–280.
[14] R.H. Medema, G.J. Kops, J.L. Bos, B.M. Burgering, Nature 404 (2000) 782–787.
[15] T. Chen, J.A. George, C.C. Taylor, Anti-Cancer Drugs 17 (2006) 123–131.
[16] L.J. Lombardo, F.Y. Lee, P. Chen, D. Norris, J.C. Barrish, K. Behnia, S. Castaneda, L.A. Cornelius, J. Das, A.M. Doweyko, C. Fairchild, J.T. Hunt, I. Inigo, K. Johnston, A. Kamath, D. Kan, H. Klei, P. Marathe, S. Pang, R. Peterson, S. Pitt, G.L. Schieven, R.J. Schmidt, J. Tokarski, M.L. Wen, J. Wityak, R.M. Borzilleri, Journal of Medicinal Chemistry 47 (2004) 6658–6661.
[17] J. Das, P. Chen, D. Norris, R. Padmanabha, J. Lin, R.V. Moquin, Z. Shen, L.S. Cook, A.M. Doweyko, S. Pitt, S. Pang, D.R. Shen, Q. Fang, H.F. de Fex, K.W. McIntyre, D.J. Shuster, K.M. Gillooly, K. Behnia, G.L. Schieven, J. Wityak, J.C. Barrish, Journal of Medicinal Chemistry 49 (2006) 6819–6832.
[18] J. Bain, L. Plater, M. Elliott, N. Shpiro, C.J. Hastie, H. McLauchlan, I. Klevernic, J.S. Arthur, D.R. Alessi, P. Cohen, Biochemical Journal 408 (2007) 297–315.
[19] M. Tardaguila, E. Gonzalez-Gugel, A. Sanchez-Pacheco, Molecular Endocrinology 25 (2011) 385–393.
[20] Y. Benjamini, Y. Hochberg, Journal of the Royal Statistical Society Series B 57 (1995) 289–300.
[21] A. Subramanian, P. Tamayo, V.K. Mootha, S. Mukherjee, B.L. Ebert, M.A. Gillette, A. Paulovich, S.L. Pomeroy, T.R. Golub, E.S. Lander, J.P. Mesirov, Proceedings of the National Academy of Sciences of the United States of America 102 (2005) 15545–15550.
[22] A.H. Bild, A. Potti, J.R. Nevins, Nature Reviews Cancer 6 (2006) 735–741.
[23] R.A. Klinghoffer, C. Sachsenmaier, J.A. Cooper, P. Soriano, EMBO Journal 18 (1999) 2459–2471.
[24] R. Giet, C. Petretti, C. Prigent, Trends in Cell Biology 15 (2005) 241–250.
[25] B.J. Lannutti, N. Blake, M.J. Gandhi, J.A. Reems, J.G. Drachman, Blood 105 (2005) 3875–3878.
[26] C. Ditchfield, V.L. Johnson, A. Tighe, R. Ellston, C. Haworth, T. Johnson, A. Mortlock, N. Keen, S.S. Taylor, The Journal of Cell Biology 161 (2003) 267–280.
[27] J.L. Riffell, R.U. Janicke, M. Roberge, Molecular Cancer Therapeutics 10 (2011) 839–849.
[28] Y. Tao, P. Zhang, F. Girdler, V. Frascogna, M. Castedo, J. Bourhis, G. Kroemer, E. Deutsch, Oncogene 27 (2008) 3244–3255.
[29] F.M. Johnson, B. Saigal, M. Talpaz, N.J. Donato, Clinical Cancer Research 11 (2005) 6924–6932.
[30] C.S. Pichot, S.M. Hartig, L. Xia, C. Arvanitis, D. Monisvais, F.Y. Lee, J.A. Frost, S.J. Corey, British Journal of Cancer 101 (2009) 38–47.
[31] Y.L. Choi, M. Bocanegra, M.J. Kwon, Y.K. Shin, S.J. Nam, J.H. Yang, J. Kao, A.K. Godwin, J.R. Pollack, Cancer Research 70 (2010) 2296–2306.
[32] F. Huang, K. Reeves, X. Han, C. Fairchild, S. Platero, T.W. Wong, F. Lee, P. Shaw, E. Clark, Cancer Research 67 (2007) 2226–2238.
[33] E.M. Balzer, R.A. Whipple, K. Thompson, A.E. Boggs, J. Slovic, E.H. Cho, M.A. Matrone, T. Yoneda, S.C. Mueller, S.S. Martin, Oncogene 29 (2010) 6402–6408.
[34] S. Mehrotra, L.R. Languino, C.M. Raskett, A.M. Mercurio, T. Dohi, D.C. Altieri, Cancer Cell 17 (2010) 53–64.
[35] M. Aponte, W. Jiang, M. Lakkis, M.J. Li, D. Edwards, L. Albitar, A. Vitonis, S.C. Mok, D.W. Cramer, B. Ye, Cancer Research 68 (2008) 5839–5848.
[36] J. Nautiyal, P. Majumder, B.B. Patel, F.Y. Lee, A.P. Majumdar, Cancer Letters 283 (2009) 143–151.
[37] A.C. Shor, E.A. Keschman, F.Y. Lee, C. Muro-Cacho, G.D. Letson, J.C. Trent, W.J. Pledger, R. Jove, Cancer Research 67 (2007) 2800–2808.
[38] M. Wasielewski, F. Elstrodt, J.G. Klijn, E.M. Berns, M. Schutte, Breast Cancer Research and Treatment 99 (2006) 97–101.
[39] N. Dussault, C. Simard, S. Neron, S. Cote, Blood Cells, Molecules & Diseases 39 (2007) 130–134.
[40] M.A. Hardwicke, C.A. Oleykowski, R. Plant, J. Wang, Q. Liao, K. Moss, K. Newlander, J.L. Adams, D. Dhanak, J. Yang, Z. Lai, D. Sutton, D. Patrick, Molecular Cancer Therapeutics 8 (2009) 1808–1817.
[41] N. Keen, S. Taylor, Cancer Metastasis Reviews 28 (2009) 185–195.
[42] C.P. Gully, F. Zhang, J. Chen, J.A. Yeung, G. Velazquez-Torres, E. Wang, S.C. Yeung, M.H. Lee, Molecular Cancer 9 (2010) 42.